2011

Transmission loss and psychoacoustics of magnesium panels for automotive dash panel applications

Michael Bowie

University of Windsor

TRANSMISSION LOSS AND PSYCHOACOUSTICS OF MAGNESIUM PANELS FOR AUTOMOTIVE DASH PANEL APPLICATIONS

By

Michael Bowie

A Thesis
Submitted to the Faculty of Graduate Studies
Through the Department of Mechanical, Automotive and Materials Engineering
In Partial Fulfillment of the Requirements for
The Degree of Master of Applied Science at the
University of Windsor

Windsor, Ontario, Canada
2011

Canada

DECLARATION OF ORIGINALITY

I hereby state that I am the sole author of this thesis, and that no part of this thesis has been published or submitted for publication.

I state that, to the best of my knowledge, my thesis does not infringe upon anyone's copyright nor violate any proprietary rights and that any ideas, quotations, or any other material from the published work of other people included in my thesis are fully acknowledged for accordance with the standard referencing practices. Furthermore, to the extent that I have included copyrighted material that violates the bounds of fair dealing within the meaning of the Canada Copyright Act, I state that I have obtained written permission from the copyright owner(s) to include such material in my thesis, and have included copies of such copyrighted clearances to my references.

I declare that this is a true copy of my thesis, including any final revisions, as approved by my thesis committee and the Graduate Studies office, and that this thesis has not been submitted for a higher degree to any other University or institution.

ABSTRACT

Many drivers are subjected to excessive noise from the powertrain during normal vehicle operation in everyday life. Currently, steel and aluminum are being exclusively used with an automotive underpad backing and plastic covering in many automobiles for the dash panel. Many automotive companies are now trying to produce light-weight vehicles to lower emissions and increase fuel efficiency. A proposed method currently being considered is to replace steel or aluminum with magnesium for the dash panel. One particular area of performance that needs to be evaluated before mass production of the dash panels is the acoustic properties of the materials. A particular aspect that is evaluated is transmission loss. This thesis discusses the impedance tube device and methods used to measure the transmission loss of materials, the importance of this property, as well as the evaluation of absorption coefficients of underpads and psychoacoustic parameters.

DEDICATION

This work is dedicated to my parents.

ACKNOWLEDGEMENTS

TABLE OF CONTENTS

LIST OF FIGURES

LIST OF TABLES

NOMENCLATURE

A	Incident Complex Sound Pressure before Material Sample
B	Reflected Complex Sound Pressure before Material Sample
C	Incident Complex Sound Pressure after Material Sample
D	Reflected Complex Sound Pressure after Material Sample
p_0	Complex Sound Pressure at Front of Sample Face
u_0	Complex Particle Velocity at Front of Sample Face
p_d	Complex Sound Pressure at Back of Sample Face
u_d	Complex Particle Velocity at Back of Sample Face
a	Anechoic Termination Condition
b	Blocked Termination Condition
o	Open Termination Condition
s	Arbitrary Termination Condition
$T_{11}, T_{12}, T_{21}, T_{22}$	Transfer Matrix Entries
d	Thickness of the Test Specimen
α	Transmission Loss Coefficient
τ	Transmission Coefficient
τ_{gap}	Sound Transmission Coefficient of the Test Specimen Materials
τ_{actual}	Actual Sound Transmission Coefficient
t	Transmission Coefficient
STL	Sound Transmission Loss
STL_{theory}	Theoretical Sound Transmission Loss
$STL_{measured}$	Measured Sound Transmission Loss
STL_{actual}	Actual Sound Transmission Loss
FTL	Field Transmission Loss
TL(dB)	Transmission Loss
TL	Transmission Loss
dB	Decibel
Π_t	Incident Sum of Acoustic Powers
Π_r	Reflected Sum of Acoustic Powers
I_i	Incident Sound Intensity
I_t	Transmitted Sound Intensity
Δf	Frequency Interval for Bark Band
f_t	Temporal Frequency
ρ	Density
c	Speed of Sound
m	Mass Density
f	Frequency
ARC	Acoustic Research Centre
B&K	Bruel & Kjaer
BEM	Boundary Element Method
BSR	Buzz, Squeak and Rattle
C-F-C-F	Constrained-Free-Constrained-Free
CF	Correlation Factor
CAFE	Corporate Average Fuel Economy

GM	General Motors
HVAC	Heating, Ventilating and Air Conditioning
Hz	Hertz
kHz	Kilohertz
kg	Kilograms
K	A Constant for Sharpness Calculation
IC	Internal Combustion Engine
MDF	Medium Density Fibreboard
MNR	Measured Noise Reduction
NVA	Noise, Vibration and Acoustics
NVH	Noise Vibration Harshness
PULSE	B&K Data Processing Software
rpm	Revolutions per Minute
mm	Millimetres
cm	Centimetres
A_{gap}	Area of the Gap
A	Total Surface Area
A_{sample}	Surface Area of Test Sample
$g(z)$	A Weighting Factor for Sharpness Calculation
k	Wavenumber
lb-s/in	Pound-Seconds Per Inch
N	Total Loudness
$n'(z)$	Specific Loudness
P	Phons
RUL	Rieter Ultra-Light
SPL	Sound Pressure Level
S	Sones
S	Sharpness
T	Temperature
W	Watts of Power
z	Bark band Frequency

Chapter 1: INTRODUCTION

When considering a vehicle purchase, most members of the public are unaware of the importance of preliminary Noise, Vibrations and Harshness (NVH) testing that is undertaken in the design process involving the material selection and thickness of the vehicle's dash panel. Without it, audible conditions inside the vehicle passenger cabin may be unbearable for passengers due to leaks around the perimeter of the dash panel, or faulty materials. Beneath the plastic layer that is visible and surrounds the radio and heating, ventilating and air-conditioning (HVAC) vents in the front seat of the passenger cabin, there are two main layers. These are an underpad or soft layer for the purpose of absorbing the powertrain noise, and the metal layer, for the purpose of acting as a firewall for the vehicle cabin from the engine or powertrain, as well as aiding in the blocking of powertrain noise. The dash panel structure requires strength to withstand the stresses from neighbouring components, for example door hinges and hood, and numerous other factors that affect the safety and comfort of passengers. A significant aspect involves NVH testing to ensure appropriate audible conditions within the interior of the vehicle cabin.

Among various factors considered in NVH testing of the vehicle dash panel, two particular properties involve transmission loss and psychoacoustics. Transmission loss is defined as the reduction in sound level transmitted through a material, two materials in this particular case. In NVH testing of the materials, transmission loss is a vital consideration. Both random incidence, tested by the Sound Transmission Loss (STL) Suite two-room method, and normal incidence, tested by the NVH laboratory impedance tube method, transmission loss must be evaluated. Psychoacoustics should also be

1

considered. Psychoacoustics is defined as the human perception of sound and sound quality. Specifically, the psychoacoustic aspects to be considered for the dash panel are the specific loudness of the powertrain noise in the frequency domain, as well as the total loudness and sharpness in the time domain, since this property has not yet been standardized for frequency domain analysis. This psychoacoustic evaluation of the dash panel is a new area that has not yet been explored; however using it will ultimately enhance the NVH performance of the finished dash panel. This evaluation can only be performed from recordings of the signals of the STL Suite two-room method, since no impedance tube method currently exists. The new material being proposed for light-weight industrial manufactured vehicles is AZ31B magnesium, to replace 6061-T6 aluminum or 1018 cold-rolled steel. The currently utilized 1018 cold-rolled steel in dash panels of most automobiles characteristically is a very heavy material and thus increases the overall weight of the vehicle. The density of this grade of steel is approximately 7800 kilograms per cubic metre. The 6061-T6 aluminum is light in comparison but heavy when compared to AZ31B magnesium. Specifically, 6061-T6 aluminum's density is approximately 2700 kilograms per cubic metre, while AZ31B magnesium's is only approximately 1800 kilograms per cubic metre. Aluminum also performs poorly in fatigue testing, is more expensive, and takes more energy to produce per kilogram than steel.

Research is required to evaluate the Transmission Loss (TL) and psychoacoustic performance of magnesium in comparison to the currently utilised steel and aluminum firewalls. Many different thicknesses of the metal layers in combination with two different thicknesses of the underpad layer were tested utilising two different

methodologies. Specifically, these are: 4.9 mm, 2 mm, and 1 mm for 1018 cold-rolled steel; 4 mm and 2 mm for AZ31B magnesium; and 4.7 mm, 2 mm and 1.27 mm for 6061-T6 aluminum. Conventionally, the currently most common thicknesses of 1018 cold-rolled steel and 6061-T6 aluminum used as dash panel firewalls are 1 mm and 1.27 mm, respectively. However, for comparison to the 4 mm and 2 mm thicknesses of AZ31B magnesium, the 4.9 mm and 2 mm thicknesses of 1018 cold-rolled steel, and the 4.7 mm and 2 mm thicknesses of 6061-T6 aluminum have been considered. Commercially, the 4 mm thicknesses of 1018 cold-rolled steel and 6061-T6 aluminum for comparison to the 4 mm thickness of AZ31B magnesium were not available, so the closest available thicknesses of 4.7 mm for the 6061-T6 aluminum and 4.9 mm for the 1018 cold-rolled steel were acceptable. One methodology of testing will involve the ASTM E2611 four-microphone impedance tube method, in which two different impedance tubes of 100 mm, for the 100 – 2000 Hz frequency range, and 29 mm, for the 2000 – 6400 Hz frequency range, inner diameters will be utilised. The other methodology will involve the J1400 SAE STL Suite two-room test method, in which eight metal layers, two magnesium, three steel and three aluminum, of the mentioned different thicknesses and uniform 60cmX60cm surface areas will be tested in combination with one of two 60cmX60cm surface area, 15 mm and 19 mm thick samples of Rieter Ultra-Light (RUL) automotive underpad. For psychoacoustics purposes, the dash panel material samples will be subjected to 10 second duration signals of random or uniform white noise, periodic random or scattered white or pseudorandom noise, diesel generator noise, and electric motor noise. For each signal, two microphones in the reverberation room, and two in the receiver semi-anechoic room will be employed for

average specific loudness, total loudness and sharpness evaluation. The averaged values of specific loudness, total loudness and sharpness from two microphones will be utilised to obtain more accurate data than one microphone could provide. For the Random Incidence Transmission Loss (TL_r) semi-anechoic room and reverberation room measurements, random or uniform white noise, periodic random or scattered white or pseudorandom noise, diesel generator noise and electric motor noise, each of 10 seconds signal durations will also be considered. The additional three signals to the random or uniform white noise signal will be included for a more 'real world' TL evaluation that goes beyond the theoretical J1400 standard, for practicality.

The goal of this research is to comparatively evaluate magnesium's TL performance relative to those of aluminum and steel, currently utilised in automotive dash panels. This will be accomplished by testing circular dash panel samples in an impedance tube, and comparing TL values of magnesium to those of the same thickness, or within 1 mm difference in thickness of aluminum and steel, each with an underpad. As well, the TL of larger, square, 60cmX60cm sheet samples of magnesium with underpad dash panel samples will be compared to those of aluminum and steel, each with the same underpad. These samples will be tested in an STL Suite consisting of a semi-anechoic room, with a reverberation room beneath and an opening for testing materials utilising a buck, and sealed flanking paths. Also, the psychoacoustic response of these materials will be compared in terms of specific loudness, total loudness and sharpness, in the STL Suite. The higher values obtained from two microphones averaged above the sample will be interpreted as inferior results in comparison to another dash panel sample of the same thickness, or within 1 mm. Once magnesium has been evaluated

comparatively to aluminum and steel, each with an underpad to simulate dash panel arrangements, it will be classified as either a worthy competitor for material selection for dash panels, or not a worthy competitor. The outcome will be dependent upon the relative performance of many values across the frequency range of 100 Hz – 10000 Hz. Also, the upper limit for loudness will be 22.5 Barks equal to 10.55 kHz, closest to 10000 Hz of J1400 as possible.

Chapter 2: LITERATURE SURVEY

The purpose of this chapter is to review the history of magnesium, including past automotive component applications. As well, psychoacoustics will be defined and thoroughly discussed, including the loudness, Zwicker loudness, masking, and sharpness metrics. Also, the history of psychoacoustics, including the Fletcher-Munson curves, will be presented. The results of psychoacoustic tests currently being conducted at the Michigan Technological University involving the comparison of magnesium to aluminum and steel in terms of buzz, squeak and rattle (BSR) for the automotive dash panel application will be discussed. Included is a discussion of the current benefits of using magnesium for many different automotive components.

The material properties of magnesium that make it superior to steel and aluminum for the dash panel application will be highlighted. In addition, the results of a test recently conducted by graduate students at Zhejiang University in China, involving the modal analysis of magnesium alloy AZ91D to aluminum alloy ADC12 will be reviewed. The purpose of using magnesium for the specific application of the automotive dash panel will be presented. As well, the purpose of using the SAE J1400 method over the other STL Suite two-room methods of ASTM E336 and ASTM E2249 for TL testing will be outlined. This outline will include ways to correct errors in TL measurements utilising an impedance tube due to differences in diameter between the test specimen and the tube. In closing, similarities of the three STL Suite two-room methods of SAE J1400, ASTM E336 and ASTM E2249 to the four-microphone impedance tube method of ASTM E2611 will be compared.

2.1 History

2.1.1 Discovery and Development

Magnesium was first discovered by Sir Humphrey Davy in the United Kingdom in 1808. He used potassium to reduce magnesium oxide, and in the process, discovered magnesium [6]. Magnesium was first utilised in industry for production in France in 1863. The first commercial production of magnesium took place at Greisheim Elektron, Germany in 1886 [31]. Resources from which magnesium can be recovered are virtually unlimited, and are globally widespread [26].

2.1.2 Past Applications

Since the 1930s, automotive industries have utilised magnesium in the production of a wide range of parts on the vehicle. These include oil pumps, mounts, brackets, pistons and engine housings. As well, wheels were one of the first automotive components to utilise magnesium [30]. Magnesium has also been utilised for under-the-hood components, such as cam covers [45].

2.1.3 Current Applications

Currently, dashboard panels made from a single magnesium casting are being prototyped for evaluation of their suitability in automobiles. European and U.S. automakers have different standards regarding the use of magnesium. In Europe, the main concern for magnesium use is weight reduction and to decrease emissions, thus increasing the fuel efficiency. In the U.S., the main concern is emissions reduction to address Corporate Average Fuel Economy (CAFE) requirements [30]. Thus, magnesium's unique properties allow the automotive industry to reduce the mass of the vehicle in order to satisfy the increasing CAFE requirements [3].

General Motors (GM) has tested commercial magnesium wrought alloys and has produced two prototype magnesium components. For the 2004 model year, the Federal Government set the CAFE standards at 20.7 miles per gallon for light trucks, including minivans and sport utility vehicles. Increasing the CAFE standards could result in the increased use of magnesium for fuel economy. The GM "Plastic" NAO 2004 model year Epsilon had a magnesium instrument panel. The 2005 Pontiac Grand AM mid-size car also had a magnesium instrument panel. In general, the GM Savana and Chevrolet Express G-vans possess one of the largest magnesium die-castings; the instrument panel has a mass of 12 kg as opposed to 18 kg if it were made of steel [5].

The current most common applications of magnesium alloys for automotive components are for the drivetrain and the interior [39]. Magnesium use for dash panel firewalls has been increasing recently, but has had limitations due to die castings of structural products, since the higher cost of the metal is offset by the low cost of die-casting automotive parts. So, magnesium has a very good manufacturability, but the high-volume production necessary requires a lower material cost [12]. As well, magnesium has better elongation than other die-casting metals, a longer die life than aluminum die casting, and has the ability to produce thinner walls than aluminum die-casting [14].

Magnesium dash panel applications are currently for mid-to-high end passenger cars, since NVH is a critical factor for competition. The column mounting stiffness and the radio and HVAC stiffness are critical factors affecting the NVH performance [29].

2.2 Psychoacoustics

Psychoacoustics is often referred to as sound quality, and is defined as the quantification of a qualitative assessment of the resulting acoustic output of a source [48]. It involves a combination of psychology and physical science and engineering, which results in metrics that numerically assess the strength of various sensations evoked by a sound [16]. The application of psychoacoustics allows for more meaningful assessment into whether a noise will be acceptable to people than can be determined from Sound Pressure Level (SPL) [16].

2.2.1 The History of Psychoacoustics

Psychoacoustics is defined as the area of general acoustics that details the human perception of sound, its pleasantness and quality. Psychoacoustics regards the concern of the relationship between the objective, physical, and quantifiable properties of the stimulus of sound in the air environment and the subjective, psychological, and qualitative responses it arouses. In the early 1970s, the up-down method was the newly transformable, for jury testing and regular testing, evaluation method of psychoacoustics [28]. Fletcher and Munson were the acousticians who developed the famous equal loudness contours, a very important graph showing that the loudness concept of psychoacoustics is non-linear over the frequency range, as shown in the following figure [15].
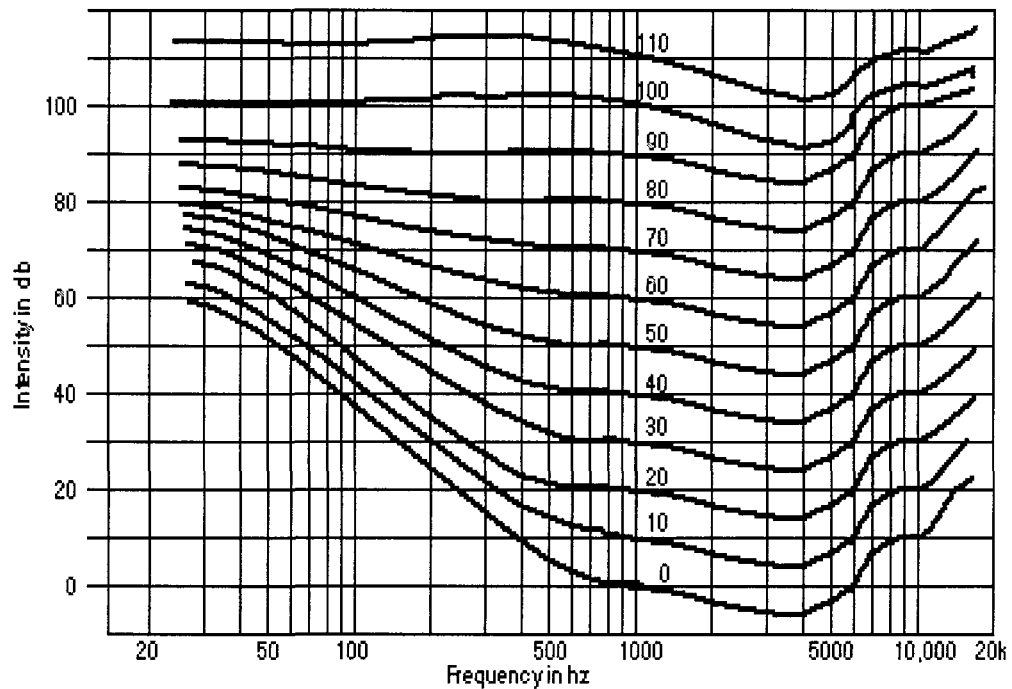
Figure 1: Equal Loudness Contours, or Fletcher-Munson Curves (Fletcher, H. C., & Munson, W. A., n.d.)

These contours were developed from data obtained by asking people to judge when two pure tones of different frequencies were the same loudness. These tests were conducted in the 1930s, and were very difficult judgements to make, and the curves are the averaged results from many subjects [15]. The main characteristic of the equal loudness curves is decreased sensitivity at low and high frequencies. Note that there is one curve for each value of loudness in sones. However, as the loudness level in sones increases, the curves flatten. For any level of loudness, the maximum sensitivity occurs at about 3 kHz, which is the resonant frequency of the ear canal.

An important point to note regarding the reverberation or echo in the vehicle passenger cabin is that the driver and passengers increase the absorption of the transmitted powertrain noises. This improves the comfort level inside the cabin. The NVH performance of the dash panel is also very important because a poor TL and/or

psychoacoustic metric of the magnesium with under-padding or automotive underlayment layers will affect speech intelligibility inside the vehicle cabin [15].

While loudness is a subjective quantity, plenty of research going back to as early as the 1920s was purposed for quantifying this sound quality metric [9]. Fletcher and Munson continued with the work started by Kingsbury in 1927, deriving loudness levels over the complete practical auditory range [17, 25] (Bell Laboratory Testing). This was not an ideal free-field environment, so calibration factors were obtained at each frequency to correct for the receiver playback. These calibration values were combined to form a calibration curve or transfer function utilized to adjust the results. This added correction could have led to a potential error source in the experiment. If Fletcher and Munson had access to free-field conditions in which to present the pure tones, the calibration factors would not have been necessary. Unfortunately, the technology for this was not available at the time of the experiment, but the results acquired were still an important foundation for future work [9].

The work by Fletcher and Munson was followed by others [9]. These included Churcher and King in 1937, and Zwicker and Feldtkeller in 1955 [23, 49]. Each of the data sets obtained presented experimental contours of equal loudness. However, Robinson and Dadson noticed that the previous investigations showed considerable discrepancies when compared to each other [9]. This resulted in a more extensive investigation being carried out in 1956 by Robinson and Dadson at the National Physical Laboratory. The results were later adopted as the first international standard for equal loudness contours [36].

The overall purpose of the project was to provide a comprehensive set of equal loudness contours which produced consistent results, correcting the previous discrepancies [9]. The new study included a threshold for loudness, and loudness values for SPLs up to 130 dB. The frequency range was also extended from 25 Hz up to 15 kHz [36]. The extensive nature of this investigation resulted in significant portions utilised directly in the formulation of the first standardised set of equal loudness contours given in ISO 226.196 [9].

Revisions of the ISO 226:1987 contours were considered to be necessary as knowledge in the acoustic community progressed. Based on their results, Fastl and Zwicker noted discrepancies between the contours of this standard and their own findings. These results were compared in a compilation study produced by Suzuki and Takeshima, indicating the research done to date concerning the equal loudness contours [9]. Looking at work from various investigations as well as their own, Suzuki and Takeshima's study confirmed that different trends were in fact present at frequencies below 800 Hz [42]. This new investigation showed that values of Robinson and Dadson's 1956 contours were lower, by as much as about 8 dB, at certain frequencies. Thus, Suzuki and Takeshima derived a new set of equal loudness contours [9].

In 1936, Stevens developed a new scale for describing loudness using sones instead of phons. This unit was and currently is the basis on which the majority of recent loudness metrics state their values [40]. Over a few decades, Stevens developed some of the fundamental concepts utilised for the prediction of loudness. These included the power law, and much later the development of the Mark VI loudness model in 1961. This is now known as Method A, one of the two separate loudness methods for the ISO

532 document, originally standardised in 1975 [41]. The other Method B is more commonly utilised in industry, referred to as ISO 532B [9]. This model was developed from the loudness model by Acousticians Paulus and Zwicker, and played an important role in the development of the loudness metrics in use today [35]. Zwicker's method attempts to better approximate the sensation of loudness by approximating the filtering process of the human auditory system with the use of critical bands [9].

The DIN 45631 German standard for stationary loudness was originally accepted in 1991 by the Deutsches Institut fur Normany (DIN – translating to the German Institute for Standardisation). This model was originally based on Zwicker's work for ISO 532B, and has come to be known in industry as the Modified Zwicker Method [9].

The ANSI S3.4 2007 model was based on the work of S. Stevens as in Method A of ISO 532:1975. However, in 1996 Glasberg and Moore developed a new method which would eventually replace the 1980 ANSI standard as an improved estimation of loudness [32]. Specifically, Glasberg and Moore's approach was another extension of Zwicker's 1972 model [9]. Their model utilises transfer function contours imitating the effects of the outer and middle ear. This was based on their earlier work as well [19].

2.2.2 Loudness

2.2.2.1 Masking

Loudness is a metric which measures the perceived intensity of a sound qualitatively [47]. Like most psychoacoustic metrics, loudness is a relative rather than absolute quantity. In detail, it gives the perceived loudness of a sound relative to a reference sound [20]. Loudness differs from A-weighted SPL by taking into account

masking. Masking is a term utilised to convey the concept of one sound covering up another sound. In more detail, masking can also be used to convey one frequency component of a sound covering up another frequency component of the same sound. For example, a given sound will prevent other sounds of lower SPL with similar frequency content from being audible. This is defined as frequency masking. A second type of masking happens when one sound follows another very closely in time. The second sound will either not be audible, or be audible at a reduced perceived intensity. This is defined as temporal or time masking [11].

2.2.2.2 Zwicker Loudness

Zwicker loudness is defined as a standardised metric that gives detail to the human perception of loudness [48]. This is a replacement of just the simply reported SPL. Zwicker declared that this quantity takes into account the temporal processing of sounds, as well as audiological masking effects [48]. His statement reads as 'Loudness comparisons can lead to more precise results than magnitude estimations. For this reason, the loudness level was created to characterize the loudness sensation of any sound' [48]. People often think that the perceived loudness will depend directly on the sound pressure, which results in the equal loudness contours, as long as the sound pressure remains constant. This is usually not correct, because sound possesses temporal and spectral masking, resulting in a difference between loudness and equal SPLs by a factor as high as 1:4 [48]. This results from the observation that broad band noises are perceived to be louder than narrow band noises that have the same SPL [10].

Specifically, Zwicker loudness is a method for estimating the total loudness. Zwicker loudness is based on the use of 1/3 octave band analysis of the sound signal.

The Zwicker loudness model takes into account masking effects. The following figure shows the masking curves [22].
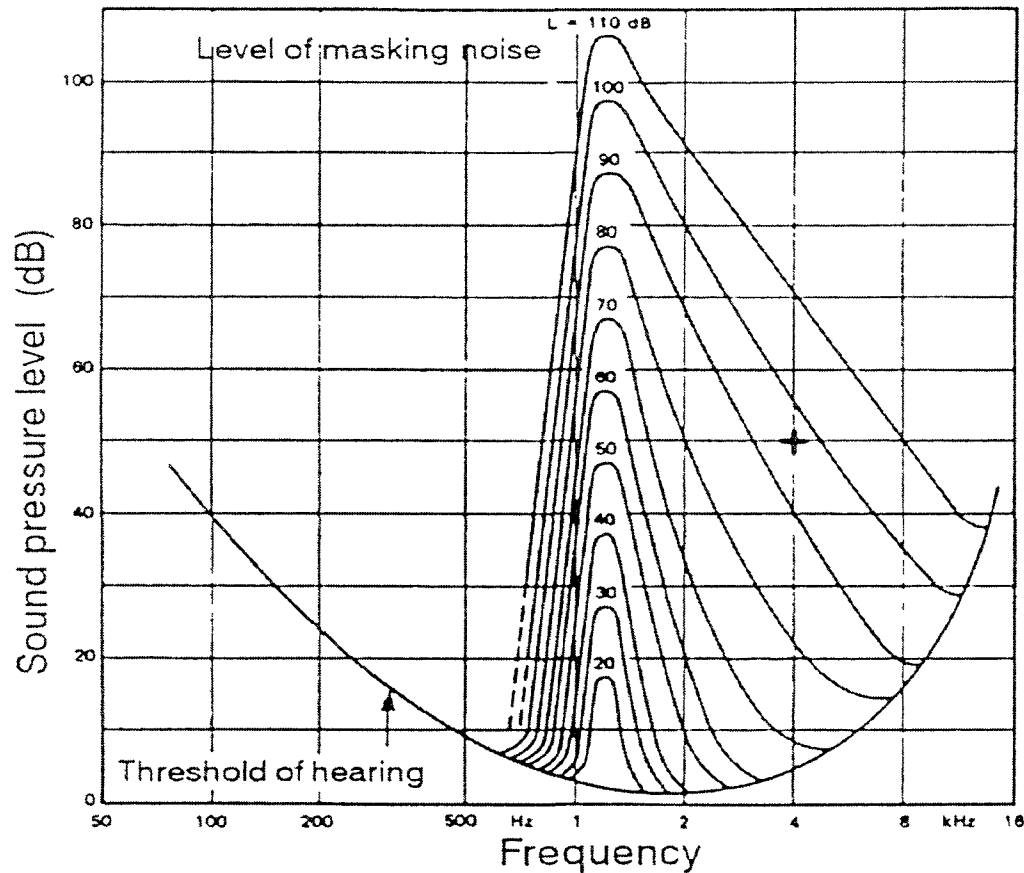
Figure 2: Zwicker Loudness Model Masking Curves (Human Factors Course, 2007).

When a horizontal line is drawn, the SPL of a peak at about 1 kHz may be masked by a higher SPL at a higher or lower frequency, of one of the higher successive peaks [22].

2.2.2.3 Measurement of Loudness

Any sound can have its loudness level measured, but it is most easily understood using pure tones. The unit of loudness is defined as the sone, as opposed to the dB for SPL. Figure 1 shows the equal loudness contours for pure tones in a free field environment. Note that sound intensity level is equal to SPL when rounded to the nearest dB. Zwicker used a pure tone at 1000 Hz as a reference to obtain the perceived loudness

at all other frequencies by experimental jury tests. Specifically, the loudness of the 1000 Hz tone with a SPL of 40 dB was arbitrarily chosen as the reference signal, and also corresponds to a loudness level of 40 phons. Note that loudness is usually measured in sones, where 40 phons equal 1 sone. The loudness level in sones increases exponentially or doubles each time the sound source is perceived to be twice as loud or 10 dB higher on the SPL scale. The relationship between the phon (P) and the sone (S) is given by the following equation [48].

$$S = 2^{\frac{(P-40)}{10}} \tag{1}$$

Phon curves provide information about the equivalence of sounds, but not about the absolute loudness level. For example, one cannot say how many times louder a 40 phon sound is with respect to a 20 phon sound. Therefore, Fletcher and Munson further tested with a rating scale that was named the sone. Specifically, one sone is defined as the absolute level of loudness of a 1000 Hz tone of 40 dB, or 40 phons [22].

Also loudness is usually declared across non-conventional bandwidths, instead of fractions of the octave. A special frequency scale is used to describe the critical band rate, and is declared by the unit "Bark", which has a range from 0 to 24 [48]. The upcoming Table 1 in Chapter 5: RESULTS AND DISCUSSION shows the 21 Bark band frequencies that were used for this study for specific loudness evaluation. Specific loudness is defined as the loudness level in sones per unit Bark, and is used to evaluate loudness across the frequency range. To get the total loudness, the specific loudness vs. frequency curve is integrated across the frequency range. The following equation shows the relationship between the 24 Bark bands and the equivalent 1/3 octave bands [48].

$$\Delta f = 25 + 75 * \left[1 + 1.4 * \left(\frac{ft}{1000}\right)^2\right]^{0.69} \tag{2}$$

Here Δf is the frequency bandwidth, and f_t is the one-third octave bandwidth centre frequency.

2.2.3 Sharpness

Sharpness is a quantity describing the high frequency annoyance of noise. It is calculated by applying a weighting factor to the higher frequency band content of loudness. This measured quantity is particularly useful for sounds such as broadband sources, wind or rushing air noise, and gear meshing noise. In the automobile engine, the high frequency content of intake noise is created by intake air travelling across the valve seat at high velocities. Also, wind noise is present during normal vehicle conditions, as well as high-frequency tire squeals. For these reasons, it is assumed that sharpness is an appropriate psychoacoustic metric for the evaluation of magnesium, aluminum, and steel dash panels. The unit used to measure sharpness is defined as the acum. This is Latin for sharp. The calculation of sharpness is taken from the loudness level in each frequency band, where more weighting is applied to the higher frequency bands. Zwicker defined the reference for 1 acum of sharpness as the following. 'The reference sound producing 1 acum is a narrow band noise, at a centre frequency of 1 kHz having a level of 60 dB' [48].

2.2.3.1 Calculation of Sharpness

The calculation of sharpness depends specifically on the specific loudness distribution of the sound. In more detail, sharpness is calculated by the interpretation of the specific loudness curve, multiplied by a weighting factor, and divided by the total loudness. The most common algorithm for sharpness calculation is the Von Bismarck equation, given by the following [38].

$$S = K * \frac{\int_0^{24\,Bark} n'(z)*z*g(z)*dz}{N} \qquad (3)$$

Here, n'(z) is the specific loudness, z is the Bark band frequency, g(z) is a weighting

factor, N is the total loudness, and K is a constant [38].

2.2.4 Psychoacoustics BSR Test Results

Relating to psychoacoustics, three annoying sounds from the powertrain among

many are buzz, squeak and rattle (BSR). Buzz is caused by structure-borne vibrations,

squeak is caused by two surfaces sliding against each other, and rattle is caused by an

impact between two hard surfaces. To produce BSR there must be relative motion or an

impact between two contacting surfaces. Impacts cause in-plane vibrations, parallel to

the surface, which couple with out-of plane motions, or perpendicular to the surface, to

produce noise.

Tests for rattle were conducted at Michigan Technological University on

3"X4"X1/8" test samples of magnesium. The samples were only constrained on the two

4" length sides opposite to each other, and thus was referred to as constrained-free-

constrained-free (C-F-C-F). In some cases, this produced different plane modes that

could change the rattle noise. Vehicular conditions were simulated using random

excitation [43].

These tests were conducted at room temperature; a Bruel & Kjaer (B&K) pre-

amplifier was positioned 30 cm away from the source, which was the impact of the rod

with the plate, and connected to a PCB Type 40AQ pre-polarized microphone. A random

excitation was used to simulate vehicle conditions for rattle testing with a material rattle

fixture. Noises were recorded using a DIGI sound card and analysed using Head

Acoustics Artemis Software. The impact was made using a rod made of polyamide or nylon 66 with a density of 1.15 grams per cubic centimetre. The mechanical properties of the nylon 66 rod, magnesium, steel, aluminum and brass were carefully characterised prior to testing. These were Young's Modulus, impact strength, yield strength, etc. It was concluded by jury testing that BSR sounds emitted from the magnesium samples were the most annoying in comparison to aluminum, steel, and brass, respectively [43].

2.3 Material Properties

Within the last decade, annual growth rates of magnesium usage for structural automotive applications have been greater than 30% on average. However, the total usage of magnesium components in automobiles is still usually less than 5 kg. Magnesium has the lowest density among any other metal that would be utilised for the dash panel firewall, which makes it favourable. Magnesium also has high specific strength, good damping characteristics, and high ductility. Specific strength is defined as the yield strength of a material divided by its density. Recent studies have shown that, based on density and specific strength, magnesium appears to be superior to both steel and aluminum. As well, magnesium alloys have good damping capacity in comparison to aluminum and steel alloys [33]. When alloyed, magnesium has the highest strength-to-weight ratio among other dash panel firewall materials [18]. Mass reduction can also be achieved by utilising magnesium. Specifically, between 35 and 50 % of the dash panel mass can be eliminated in comparison to steel [33].

Magnesium alloys are used in small amounts for automotive parts. Material, process, and design modifications of magnesium alloys are options to make the replacement of steel or aluminum economically and technically feasible. Magnesium is

the least dense engineering metal at approximately two thirds that of aluminum and one-quarter that of steel. Aluminum's density is approximately 2700 kilograms per cubic metre, and steel's density is approximately 7800 kilograms per cubic metre, for common alloys. In some dash panel firewalls, magnesium die cast alloys AM50 and AM60 have replaced the aluminum die-cast A380 alloy. The current magnesium dash panels used in industry have a thickness of 2.5 mm [30].

Over the past decade, engineers have re-assigned dash panels with magnesium alloys so that the natural frequencies are different than the structures to which the dash panel is attached. In the process of re-designing, engineers have noted that the main structural excitation sources are the engine, powertrain, and the road surface. During normal vehicle operation, it was noted that the automotive instrument support panel, made of prototype steel, aluminum or magnesium alloys, may shake due to structure-borne excitation from the powertrain. If one of the natural frequencies of the support panel is close to one of the excitation frequencies of its neighbouring components, resonance may occur. In addition, the cross-car beam connected to the panel is also connected to the steering column support brackets, making it uncomfortable for the driver during high excitation [27].

The VN127 instrument support panel, an instrument support structure designed specifically for a series of pickup trucks, was made of AM60 magnesium for these tests. The three natural frequencies of the VN127 instrument support panel alone were calculated as: 36.84 Hz, 37.45 Hz and 44.84 Hz. The purpose of testing the VN127 automotive instrument panel support structure made of magnesium alloy AM60 was to check if the NVH performance met or exceeded that of the current instrument panel made

of mild steel. If adequate, this would allow the new alloy to be used to lightweight the panel. It was found that the natural frequency of AM60 magnesium was always 1-2% lower than mild steel or AA6111-T4 aluminum when comparing different potential materials for the VN127 panel [27].

Relating to the magnesium alloy being tested, AZ31B is the code referring to the mass percent of alloying elements. In general, the first letter indicates the alloying element with the highest concentration, and the second letter indicates the alloying element in second highest concentration. The first number after the letters indicates the weight percentage of the first element, and the second number for the weight percentage of the second element. This code indicates that there is 3 percent aluminum, 1 percent zinc and balance magnesium.

2.4 Current Benefits

Automaker's studies of the relationship between vehicle mass and fuel economy over decades have concluded that for every 10% reduction in vehicle weight, there is a 6-8% reduction in the required fuel for a certain distance [24]. Automakers have also concluded in a recent study that one pound of magnesium typically replaces three pounds of steel and two pounds of aluminum, reducing the vehicle's mass without any additional safety issues. Studies of the long term effects of this mass reduction show that both the lifetime operating cost of a vehicle and its' emissions volume will be lower. More sheet magnesium is being formed for today's automotive industries due to the decreasing price per pound. Statistics in February 2007 showed that aluminum was in competition with steel at $2.20/kg. In the European Union, magnesium prices were as low as $2.20/kg,

making it most competitive with steel and aluminum for a higher volume of material for the same price [24].

Utilising magnesium in the vehicle will improve the NVH performance of the vehicle, make the vehicle more fun to drive, and improve the safety by braking and accelerating [24]. Specifically, NVH is improved by using light-weight magnesium components because they allow the various components connected to the suspension, handling and body system's natural frequencies to be changed to certain critical frequencies due to the change in Young's Modulus and density, where the NVH is reduced. Another benefit of using magnesium in automotive components is to reduce BSR, and improve psychoacoustics of the vehicle as a result of single magnesium castings being used in place of multi-component instrument panels made of steel. A single magnesium casting results in less probability of a manufacturing error in tolerances, thus reducing the BSR. An example is found in the instrument panel or dashboard, since they typically have approximately 37 elements when made of steel and only 6 elements when made of magnesium. This reduces the total tool requirements and complexity, due to the fact that a tool and gauge are required for each element of the steel dashboard fabrication [24].

2.5 Results of Modal Analysis

With regard to the physical NVH performance, Zhejiang University of China has recently conducted a test comparing the NVH performance of aluminum alloy ADC12 to magnesium alloy AZ91D. These alloys were covered with oil to simulate realistic Internal Combustion (IC) engine conditions. It was calculated that the theoretical ratio of magnesium's natural frequency to aluminum's was 0.951. The test results of modal

analysis show that for ten natural frequencies, the average ratio of the magnesium to aluminum values was 0.962 [21].

The tests were conducted using a motor, causing excitations at the side of the IC engine. These vibration tests were important relative to TL analysis, because physical resonance is what happens during coincidence. The ratio of vibration amplitudes for aluminum to magnesium was 0.63. It was assumed that the maximum speed of the motor was 6000 rpm during the test. The most destructive resonances occurred at excitations of 1400, 1500 and 1600 Hz. The damping values of both materials were assumed to be 0.06 lb-s/in. The audible response at certain excitation frequencies was calculated using Boundary Element Method (BEM) analysis. The researchers of Zhejiang University concluded that AZ91D magnesium is better for the IC engine applications because it is lighter, and has the better NVH performance [21].

2.6 Purpose of SAE J1400

The SAE J1400 Test Method was utilised rather than the ASTM E2249 Test Method because of the ease of measurement when using ten stationary microphones. Five microphones were positioned in the reverberation pit and five microphones were positioned in the semi-anechoic room in order to compare the sound intensity on each side of the sample. Also, for the SAE J1400 Test Method, the five stationary microphones were positioned 20.3 cm above the test samples and four being 12.7 cm offset diagonally from the corners of the sample. This was much easier than using a two-microphone intensity probe to scan at a steady distance from the sample face, held perpendicular to the sample face. Likewise, utilising the J1400 method with the five

fixed microphone positions above the test sample face was more accurate than using a hand-held two-microphone intensity probe.

The SAE J1400 Test Method was preferred over the ASTM E336 Test Method due to the greater resulting accuracy of STL measurements. This was due to the fact that the ASTM E336 Test Method measures what is referred to as Field Transmission Loss (FTL). This test method oversimplifies the Correlation Factor (CF) by setting it equal to 6 dB for all one-third octave bandwidth centre frequencies. This is the only difference between the ASTM E336 Test Method and the SAE J1400 Test Method, as the SAE J1400 Test Method calculates a unique CF for each one-third octave bandwidth centre frequency, using a 60cmX60cm reference sample of lead with a constant thickness. The CF is calculated utilising equation (13), which is more accurate than assuming a 6 dB CF for each one-third octave bandwidth centre frequency.

2.7 Correction of TL Errors due to Under-Sizing of Test Samples

Relating to NVH Laboratory impedance tube TL testing, it has been proven that very small differentials in diameters of test specimens in comparison with respective impedance tubes' inner diameters cause large deviations in STL. Specifically, the STL shifts upwards across the applicable frequency range as the boundary conditions are pressure loaded. This is due to the fact that the pressure-loaded boundary conditions cause the boundary pores of the automotive underlayment sample, and slightly for the metal, to close, and the barriers to stiffen. This phenomenon is much more pronounced in the small tube, since greater pressure is produced on the sample. Thus, boundary conditions pressure loading, due to diameter sizes or restraints, results in large errors in STL computations. Specifically, any test specimen under-sizing creates air between the

impedance tube wall and the specimen boundary, resulting in a pronounced localized shift in STL as compared to the large impedance tube data. Correction for the effects of test specimen under-sizing can be determined by using the following equation.

$$STL_{measured} = STL_{actual} - 10\log\left(1 + \frac{A_{gap}}{A}\left(\frac{\tau_{gap}}{\tau_{actual}} - 1\right)\right)$$ (4)

Here, A_{gap} is the surface area of the gap, A is the total surface area of the impedance tube cross section, τ_{gap} is the sound transmission coefficient of the gap fluid which is air, and τ_{actual} is the actual sound transmission coefficient of the material. Ideally, this equation is utilised when there is any difference between the diameter of the impedance tube and the active test specimen. However, results in the range of 0.0 mm to 1.5 mm will be insignificant. When utilised for small impedance tube data, the average difference between the actual STL (STL_{actual}) and the measured STL ($STL_{measured}$) is used to adjust the small tube STL upwards, in the recommended one-third octave bandwidths. Using this shift, the gap area A_{gap}, and thus the area of the material sample itself, which changes based on orientation, since A_{gap} is measured as the normal surface area, can be calculated for each one-third octave band, as recommended. The calculated surface area is compared to the actual measured surface area of small tube samples, most commonly. It is known that, if the computed test specimen diameter is within 5% of the actual measured specimen diameter, calculated from the equations

$$A_{sample} = \Pi/4*D^2$$ (5)

where $$A_{sample} = A - A_{gap}$$ (6)

then the calculated STL shift is valid. Thus, large and small impedance tube STL curves can be combined in valid frequency regions.

2.8 Summary

In summary, a review of the current knowledge of the psychoacoustics of magnesium samples in comparison to aluminum and steel in terms of BSR has been discussed. As well, the history of psychoacoustics, and the results of a recently conducted BSR test on magnesium, aluminum and steel have been presented. As well, Zwicker loudness, masking and sharpness have been thoroughly discussed. Also, the results of a modal analysis test conducted at Zhejiang University comparing a magnesium alloy to an aluminum alloy have been provided. The past and current automotive applications of magnesium have been reviewed, as well as the current benefits. The discovery of magnesium has been outlined, as well as its material properties. The methods utilised to correct errors in TL measurements involving an impedance tube due to under-sizing of the material samples has been discussed, as well as the similarities of the impedance tube four microphone method to the three STL Suite methods.

Further testing for the psychoacoustic response in terms of specific loudness, total loudness and sharpness of AZ31B magnesium dash panel samples will provide further insight to the driver and passenger subjective evaluation. As well, impedance tube and STL Suite two-room TL testing of AZ31B magnesium dash panel samples in comparison to that of 6061-T6 aluminum and 1018 cold-rolled steel dash panel samples will provide a physical NVH performance comparative evaluation. This is based on several TL values across the 100-6400 Hz frequency range, from the B&K impedance tubes - large and

small, and the 100 – 10000 Hz frequency range, from the STL Suite – reverberation pit

above or adjacent to the semi-anechoic room.

Chapter 3: THEORY

This chapter will deal with the theory or plan for impedance tube and STL Suite TL testing based on principles verifiable by experiment. The differences between the impedance tube method and the STL Suite two-room method, in general, will also be discussed. The theory behind the classical equation for TL will be discussed. Vehicular conditions in which NVH performance is most appropriately evaluated will be outlined. The details of the three STL Suite two-room methods of TL testing will be reviewed. Also, the theory behind what is physically happening in the impedance tube, including pressure waves, the derivation of the transfer matrix, and comparisons between the two-load and one-load impedance tube TL testing methods will be explained.

3.1 Differences between the Impedance Tube Method and the STL Suite Method

There are large differences between the impedance tube method and the STL Suite two-room method. Specifically, in the impedance tube method, the sound hits the specimen at a perpendicular or normal incidence angle, as opposed to the STL Suite two-room method that allows random angles of incidence for a more realistic outcome. Also, the STL Suite two-room method requires a minimum size for test specimens which may not be practical for all materials. Normal Incidence Transmission Loss (TL_n) may also be practical for certain situations in which the test specimen is placed within a small acoustical cavity close to a sound source, for example a closely fitted machine enclosure or portable electronic device such as a radio. TL is not only a property of a material test specimen, but also its boundary conditions, for example a dash panel may have flanking paths due to the cracks in the plastic surface layer. The results of the four microphone impedance tube TL test are ideal with absolutely no flanking paths, so the use of test

specimens to model systems such as a dash panel will probably not give the same performance due to different boundary conditions. For the test signal characteristics, it is recommended that it be random noise having a uniform spectral density across the frequency range of interest, for example uniform white noise [2].

It has been proven that the STL Suite two-room measurement methods of SAE J1400, ASTM E2249, and ASTM E336, and the four-microphone impedance tube method of ASTM E2611 follow the same trends. For the STL Suite two-room methods, the sound intensity method of ASTM E2249 and the FTL method of ASTM E336 yield STL curves of the same shapes, while the sound intensity method shows an increase in STL with frequency. The sound intensity method itself takes into account the sound power that is existent along a perpendicular line to the test sample in the receiver room. On the other hand, the FTL method measures SPL in the receiver semi-anechoic room, which may come from paths other than through the test specimen. The secondary sound transmission paths are known as flanking paths, and may affect results adversely.

The underlying assumptions of these two techniques are slightly different, thus the STL results are not expected to be equal. The SAE J1400 STL Suite two-room method has been proven to approximate the FTL method or ASTM E336 at low frequencies, and the sound intensity method or ASTM E2249 at higher frequencies. This is due to the difference in CFs between the ASTM E336 and the SAE J1400 methods. The frequency dependant CF formula with the SAE J1400 standard should take into account flanking transmission paths between the source and receiver rooms as well as other frequency dependant measurement errors.

It is known that the flanking transmission paths between the chambers have the greatest affect at higher frequencies, specifically greater than 3 kHz. Thus, proper sealing of all reference and test specimens along their perimeters using putty or adhesive material is essential for accuracy of TL measurements at higher frequencies. Also, it is important to note that this method is based on slightly different assumptions than the ASTM E2249 and ASTM E336 methods, so the STL results are not expected to be exactly the same. Specifically, the four-microphone impedance tube method of ASTM E2611 is most similar to the ASTM E336 FTL STL Suite two-room method, in comparison to the three, STL Suite two-room methods.

It is known that the four-microphone impedance tube method of ASTM E2611 is least suited for the two-load method for multiple-material test specimens. Symmetric materials, tested using the one-load method, are known to lack reliable results. It has been recommended that elimination of the flanking transmission paths between the reverberation pit or room and the semi-anechoic room by proper sealing of all test samples and reference samples using putty or adhesive material could produce more reliable STL results [4].

3.2 TL Equation

Relating to the air-borne NVH performance of magnesium, the TL of powertrain noise through an AZ31B magnesium alloy panel can be theoretically determined by the following equation [8].

$$TL\ (dB) = 10\log\frac{1}{\tau} \tag{7}$$

$$= 10 \log \frac{\Pi i}{\Pi r}$$

Here, the subscripts i and r refer to the incident and radiated sound power waves, respectively. The symbols Π_i and Π_r refer to the incident and reflected frequency averaged acoustic powers, respectively. The frequency averaged acoustic power is calculated by another equation, as follows [8].

$$\Pi_i = \frac{1}{N} * \sum_n^N \Pi_n \qquad (8)$$

This equation (2) is for n = 1 through N, for N number of acoustic power samples taken during a certain period of time in seconds. When a noise wave is impeded by a panel, there are two resultant moving waves incident on the panel surface, the incident power wave and the reflected power wave. Only one travelling wave passes through the panel. This is classified as the radiated power wave. Regarding sound pressure wave behaviour, coincidence is a condition in which resonance of a material specimen occurs due to the frequency of vibration being equal to that of noise or sound transmitted through it [8].

3.3 Details of STL Suite Two-Room Methods

3.3.1 Sound Intensity Method of ASTM E2249

A standard two-room STL Suite test method for TL testing, described by ASTM E2249 uses uniform white noise generated in the reverberation room and measurements are conducted in the receiver or semi-anechoic room to characterise the material's STL performance. For this method, the SPL is measured at five different locations by five microphones on stands in the reverberation room. Then, the sound intensity is calculated using the following equation.

$$I_i = \frac{P^2}{4\rho c} \tag{9}$$

Here, P is referred to as the space-averaged sound pressure in the reverberation room, ρ is the density of the ambient air, and c is the speed of sound inside the reverberation room. The sound intensity transmitted through the material, I_t, is measured on the face of the dash panel layer specimen visible in the semi-anechoic room using a standard two-microphone intensity probe. Specifically, the intensity probe is to be held perpendicular to the test sample and can be moved from point to point or scanned over the material surface to internally calculate the average transmitted sound intensity in units of watts per square metre. Then, the transmission coefficient is calculated utilising the following equation.

$$\tau = \frac{I_t}{I_i} \tag{10}$$

Also, the STL can be computed using another equation, as follows [4].

$$TL = 10 \log(\frac{1}{\tau}) \tag{11}$$

3.3.2 Unique CF Method of SAE J1400

For another standard, a second two-room STL Suite test method exists which is described by the SAE Standard J1400. This method also uses a reverberation room and an adjacent semi-anechoic room with a transmission hole between them. However, SPLs are utilised to calculate the Measured Noise Reduction (MNR) rather than the sound intensity. The MNR is defined as the difference between the volume-averaged SPL in the source room, which is the reverberation pit below, or the reverberation room beside the main semi-anechoic chamber, and the dash panel material surface transmitted SPL in

the semi-anechoic receiver room. MNR is obtained using free-field microphones. A frequency-dependant CF is subtracted from the MNR to directly yield the STL. This CF is calculated using the mass law for a homogeneous limp mass material, given by the following equation.

$$STL_{Theory} = 20\log_{10} m + 20\log_{10} f - 47.2 \ dB \qquad (12)$$

Here, m is the mass density of the entire reference specimen, and f is the frequency in units of Hz. The CF is computed utilising another equation, as follows.

$$CF = MNR - STL_{theory} \qquad (13)$$

In equation (13), the theoretical TL is subtracted from the MNR. Finally, the actual TL is calculated by the following equation.

$$STL_{actual} = MNR - CF \qquad (14)$$

It is important to note that the CF is computed with only the reference specimen in place, while the MNR is computed with the entire 60cmX60cm dash panel sample in place after the reference specimen has been taken out. Also, a CF is needed to relate the testing material to the reference material, which is lead for the J1400 test [4].

3.3.3 FTL Method of ASTM E336

A third standard for TL testing utilising a two-room STL Suite is defined by ASTM E336. This method measures what is defined as the FTL. It is proposed to measure FTL of partitions that are installed in a working environment, such as the vehicle dash panel. This method also involves either a reverberation room below or adjacent to the main receiver room, or semi-anechoic room. As well, the space-averaged SPL in the

source room and the dash panel surface averaged SPL in the semi-anechoic receiver room
are utilised to find the MNR. The FTL is then calculated using the following equation.

$$FTL = MNR - 6\,dB \tag{15}$$

It is observed that this is the same equation utilised in the J1400 test standard, except that
the CF has been set to 6 dB for all one-third octave measurement bandwidth centre
frequencies. The lower frequency limit for the two-room methods of measuring STL or
FTL is usually 100 Hz. So, measurements are usually made in one-third octave bands
from 100 Hz to 10000 Hz [4].

3.4 Theory behind Physical Phenomena in Impedance Tube

3.4.1 Pressure Waves

The scenario for the incident and reflected complex sound pressures in the
impedance tube with an anechoic termination is shown in the following figure [2].

Figure 3: Schematic Drawing of the Measurement Setup (ASTM E2611 Technical Committee, 2009)

The following equations show the incident and reflected pressure waves expressed in terms of the pressures at the microphone locations [28].

$$A = \frac{J\left(P_1 e^{Jkx_2} - P_2 e^{Jkx_1}\right)}{2\sin\left(k(x_1 - x_2)\right)} \tag{16}$$

$$B = \frac{J\left(P_2 e^{-Jkx_1} - P_1 e^{-Jkx_2}\right)}{2\sin\left(k(x_1 - x_2)\right)} \tag{17}$$

$$C = \frac{J\left(P_3 e^{Jkx_4} - P_4 e^{Jkx_3}\right)}{2\sin\left(k(x_3 - x_4)\right)} \tag{18}$$

$$D = \frac{J\left(P_4 e^{-Jkx_3} - P_3 e^{-Jkx_4}\right)}{2\sin\left(k(x_3 - x_4)\right)} \tag{19}$$

3.4.2 Derivation of the Transfer Matrix

Assuming that the cylindrical plug of the dash panel material specimen under investigation can be described as a four-pole, two-port, or outer surfaces not in contact with one another, non-absorbent, linear acoustic sub-system, a transfer matrix can be utilised. This will be to relate the exterior complex sound pressures P_1 and acoustic particle velocities V_1 on the two exterior faces of the test specimen, as follows [34].

$$\begin{bmatrix} P \\ V \end{bmatrix}_{x=0} = \begin{bmatrix} T_{11} & T_{12} \\ T_{21} & T_{22} \end{bmatrix} \begin{bmatrix} P \\ V \end{bmatrix}_{x=d} \tag{20}$$

This is the one-load transfer matrix equation as well. The transfer matrix entries of the general form T_{ij} are frequency-dependant quantities directly related to the acoustical properties of the dash panel test specimen. The previous matrix equation for the acoustic particle velocities and complex sound pressures represents two equations in four unknowns. Thus, in order to be solvable, the transfer matrix elements must be spread over four equations by introducing two independent equations by introducing a second

termination condition. This can be blocked by the plunger at the end of the impedance tube opposite the sound source, or open ended by removal of the plunger and tube top at the end opposite the sound source. This will allow for reverberation with the NVH laboratory room walls, instead of the inner tube walls of the impedance tube. This second termination condition is represented by the superscript notations 'b' or 'o', respectively, assuming the one-load termination condition was anechoic. Thus, the matrix equation is modified for the blocked case, most commonly utilised, as the following [34].

$$\begin{bmatrix} P^{(a)} & P^{(b)} \\ V^{(a)} & V^{(b)} \end{bmatrix}_{x=0} = \begin{bmatrix} T_{11} & T_{12} \\ T_{21} & T_{22} \end{bmatrix} \begin{bmatrix} P^{(a)} & P^{(b)} \\ V^{(a)} & V^{(b)} \end{bmatrix}_{x=d} \tag{21}$$

This is the two-load transfer matrix. The superscript 'a' refers to the first anechoic termination using open-cell foam. For the open-ended second termination condition option, replace the superscript 'b' with 'o'. The transfer matrix elements are determined by multiplying the above equation from the right-side to the left with the inverse matrix of the $P^{(a)}$ and $V^{(a)}$ matrix when x = d, to get the solution for the two-load method of the following [34].

$$\begin{bmatrix} T_{11} & T_{12} \\ T_{21} & T_{22} \end{bmatrix} = \frac{1}{P_{x=d}^{(a)}V_{x=d}^{(b)} - P_{x=d}^{(b)}V_{x=d}^{(a)}} * \begin{bmatrix} P_{x=0}^{(a)}V_{x=d}^{(b)} - P_{x=0}^{(b)}V_{x=d}^{(a)} & -P_{x=0}^{(a)}P_{x=d}^{(b)} + P_{x=0}^{(b)}P_{x=d}^{(a)} \\ V_{x=0}^{(a)}V_{x=d}^{(b)} - V_{x=0}^{(b)}V_{x=d}^{(a)} & -P_{x=d}^{(b)}V_{x=0}^{(a)} + P_{x=d}^{(a)}V_{x=0}^{(b)} \end{bmatrix} \tag{22}$$

The resulting solutions for the complex sound pressures and complex particle velocities for the incident and transmitted sides of the material sample for any arbitrary termination condition 's' are given by the following [34].

$$P_{x=0}^{(s)} = A^{(s)} + B^{(s)} \tag{23}$$

$$V^{(s)}_{x=0} = \frac{A^{(s)} - B^{(s)}}{\rho_0 c} \tag{24}$$

$$P^{(s)}_{x=d} = C^{(s)} e^{-jkd} + D^{(s)} e^{+jkd} \tag{25}$$

$$V^{(s)}_{x=d} = \frac{C^{(s)} e^{-jkd} - D^{(s)} e^{+jkd}}{\rho_0 C} \tag{26}$$

The coefficients $A^{(s)}$ to $D^{(s)}$ are dependent on the termination condition 's', and the transfer matrix entries T_{ij} are independent of the termination conditions [34].

3.4.3 Comparisons between the Two-Load and One-Load Methods

Comparisons between the two-load, or two different termination conditions STL technique and the one-load, preferably anechoic STL technique using a four-microphone impedance tube, in which two pairs are on opposite sides of the test specimen, have been conducted. Scientists performing these comparisons, B. Yousefzadeh, M. Mahjoub, N. Mohammadi, and A. Shahsavari, designed and built a modified version of the common B&K Type 4206-T impedance tube. They utilised the one-load method for three homogeneous and isotropic materials with disk-type test specimens of equal diameters and different thicknesses. The results of the four-microphone impedance tube techniques were also compared to those of the classical, and thought to be reliable methods of reverberation pit or room source rooms and semi-anechoic receiver rooms. For both methods, the effects of downstream boundary conditions, anechoic or reverberant-blocked tube terminations, and two-room terminations have been studied [46].

One trial for the two-room method consisted of two reverberation rooms being utilised, one with the loudspeaker source and one with the receiving microphones and data acquisition system. Also, the two-load four-microphone impedance tube method for

these symmetric materials yielded results which matched the two-room method measurements. The one-load method, most appropriate for symmetric materials along their thickness, results were significantly dependant on the boundary conditions of the anechoic wedges. Impedance tubes were noted to be originally used by the scientist Kundt to prove the wave properties of sound, but are today considered as economical alternatives for the classical two-room methods of J1400, ASTM E336 and ASTM E2249. An added advantage to cost reduction is that the entire testing apparatus can be set up on a laboratory desk [46].

The one-load method halves the number of measurements in comparison with the two-load method. However, it is not reliable for accurate STL results of test specimens due to the difficulty in implementing a perfectly anechoic termination condition. The reflection coefficient of the downstream section of an impedance tube has a significant effect on the STL measurements and is the reason why there are fluctuations in STL curves. Scientist Pispola et Al [46] has studied this effect and improved the accuracy of the anechoic termination method [46].

Specifically, the impedance tube setup construction for STL measurements at the Noise, Vibrations and Acoustics (NVA) Research Centre at the University of Tehran for these measurements consisted of the identical 1100 mm long stainless steel tubes of wall thickness 5 mm. The internal diameter of each tube was 35 mm, while the internal diameter of the sample holder and all of the samples was approximately 40 mm, which was equal to the external diameters of the main tubes with wall thicknesses included. The microphone spacing for each pair was set to 25 mm; the distance between microphones 2 and 3 to the tube ends facing the sample inside the middle piece and not

the sample face itself was 125 mm. A 7 W Samsung loudspeaker within a wooden speaker cabinet lined with absorptive material was used as the sound source. A removable cap was made part of the impedance tube to apply the open and closed termination conditions, excluding the anechoic condition. A B&K Type 2719 power amplifier, a four-channel B&K Type 3560-C signal analyzer platform, and a personal computer with PULSE 8.0 software were utilised [46].

The lower and upper applicable frequency limits were determined as 650 Hz and 5600 Hz, based on microphone spacing and tube diameters, respectively. It is noted that any microphone phase calibration was neglected since the microphones were 0.5" diameter B&K free-field, and manufacturer phase-calibrated. Specifically, STL tests were performed for three disk-type samples of plywood, lead, and steel with equal diameters and thicknesses of 18, 3 and 6 mm, respectively. To analyse the effect of the tube termination conditions, two rolled 10 cm long pieces of glass wool were utilised as absorbents for three conditions: 20 cm, 10 cm and no absorptive treatment. These three conditions contributed to three different test configurations for the one-load or anechoic method. For the one-load anechoic termination method, all samples provided the best results in the case utilising 10 cm of glass wool at the impedance tube's end [46].

The best results were obtained using the two-load method for plywood with a maximum deviation of 6 dB using the two-room method data. The one and two-load methods utilising the four-microphone impedance tube are best correlated in the case of plywood, with a maximum difference of 5 dB. The results of the test provide justification that the two-load method is a reliable alternative to the anechoic termination

one-load method using the four-microphone impedance tube, since it is more accurate and stable over a broad frequency range, and has better repeatability [46].

3.5 Summary

In summary, the differences between the STL Suite method and the impedance tube method, in general, have been discussed. Also, the TL equation, and the vehicular condition most appropriate for NVH testing have been outlined briefly. The standard test methods available to guide scientists in testing magnesium alloy along with underpad dash panel samples for TL in an STL Suite have been presented. These standards also provide a guide for TL testing of currently utilised aluminum and steel alloys, along with an underpad, dash panel samples in comparison to those of the same thickness, or within 1 mm, proposed magnesium alloy dash panel samples. In addition, theoretical issues pertinent to what physically occurs within an impedance tube during TL testing of circular dash panel samples of magnesium, aluminum, and steel alloys, along with an underpad, were reviewed. Also, variations between the one-load and two-load transfer matrix methods of TL testing with an impedance tube were compared.

Chapter 4: EXPERIMENTAL DETAILS

This chapter will present the experimental setup involved with B&K impedance tube testing in the NVH Laboratory at the University of Windsor for TL_n measurements of circular dash panel samples of AZ31B magnesium, 6061-T6 aluminum, and 1018 cold-rolled steel for comparison purposes. As well, the experimental setup for absorption coefficient testing of the 15 mm and 19 mm thick circular samples of RUL will be briefly reviewed. In addition, the experimental setup for the J1400 test in the STL Suite at the B&K ARC Centre in Canton, Michigan for the 60cmX60cm dash panel samples will be discussed. With regard to the vehicle's state of motion during the active powertrain NVH performance, it is believed that the most important conditions in which powertrain NVH can be evaluated are those at idle. Idle conditions do not involve any road or wind noises, so powertrain noise is the primary concern. It can be transferred as vibrations or structure-borne noise through the steering wheel, seat, firewall and floor pan. For all impedance tube TL measurements, a B&K Type 4206-T TL impedance tube is recommended, or a similar NVH laboratory impedance tube set with modified frequency ranges. The inner diameters of the 50-1600 Hz and 500-6400 Hz frequency range B&K Type 4206-T impedance tubes are 100 mm and 29 mm, respectively. The microphone spacings of the large and small tubes are 50 mm and 20 mm, respectively. For the greatest accuracy and ease of machining, water-jet cutting of the dash panel cylindrical sample plugs is recommended. It is recommended that the diameters of the test specimens be within 0.5 mm to 1.5 mm less than the inner diameters of the respective impedance tubes, and be sealed with acoustic rings and petroleum jelly [4].

4.1 B&K Impedance Tubes Setup

The impedance tube test setup in general consists of two tubes that cover the entire frequency range desired, as shown in the following figures.
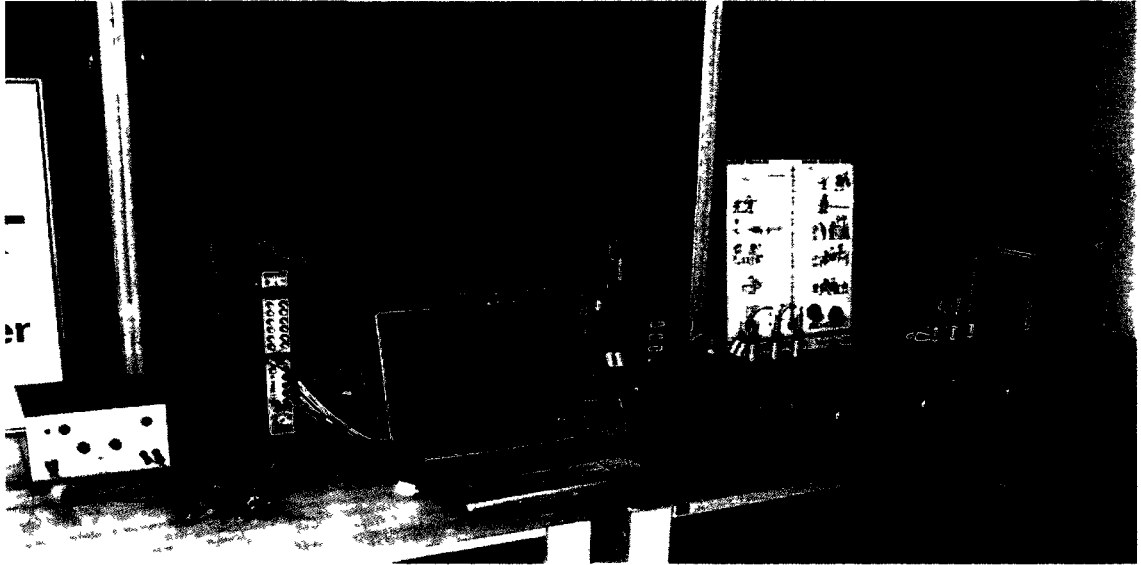
Figure 4: Picture of Full Measurement Setup using the Low Frequency Type 4206-T B&K Impedance Tube with Amplifier, Front-End and Laptop for Data Acquisition

Figure 5: Picture of the High Frequency Type 4206-T B&K Impedance Tube with Extension

The four-microphone Type 4206-T B&K impedance tube set is used to measure the TL_n of small test samples, which are 100 mm in diameter for the low frequency tube, and 29 mm in diameter for the high frequency tube. This is conducted by the use of the transfer

matrix two-load method, for multiple-layered samples. For single-layered samples, the one-load method can be utilised [7].

The one-load method is a four-microphone method of TL testing of symmetric or single-layered material samples utilising a single tube termination, preferably anechoic. The two-load method is also a four-microphone method of TL testing, but for multi-layered samples, for example metal with underpad, utilising two different tube terminations, preferably anechoic and then blocked, or open. The frequency ranges for the low frequency and high frequency tubes of the Type 4206-T impedance tube set are 50 Hz – 1.6 kHz and 1.6 kHz – 6.4 kHz, respectively [7].

The transfer matrix for the one or two-load methods is obtained by measuring the incident and reflected components of random or pseudo-random noise on the incident and transmitted sides of the material sample tested, inside the impedance tube. These components are generated inside the impedance tube by the sound source. The reflected components on the incident and transmitted sides of the material specimen, and the transmitted incident component are affected by the acoustic properties of the material sample under test [7].

The low frequency 100 mm inner diameter Type 4206-T B&K impedance tube has a frequency weighting unit or band-pass filter, defined as a dial that controls the range of frequencies emitted from the source, and a sound source mounted at one end. It also has six couplers for mounting microphones flush with the inside of the tube, since there are three maximum possible microphones on opposite sides of the test specimen. This tube has an intermediate specimen holder, with a foam layer insulating the outside

coupling edges of the connecting ends and the inner walls of the two connecting tubes to eliminate flanking paths [7].

The high frequency impedance tube has four microphone couplers, and an intermediate sample holder. Note that the high frequency tube end needs to be separated from the low frequency tube to take individual, high-frequency measurements. So, two tests are required for the entire frequency range of 100 – 6400 Hz. The high frequency 29 mm inner diameter impedance tube also has foam sealing between the outer edges of the connecting sections and the inner walls of the connecting tubes with microphone couplers. The test specimen holder is attached to the connected tubes also by longitudinal clamps, securing it in place as shown in the following figure. Note that the sample holders are disconnected [7].
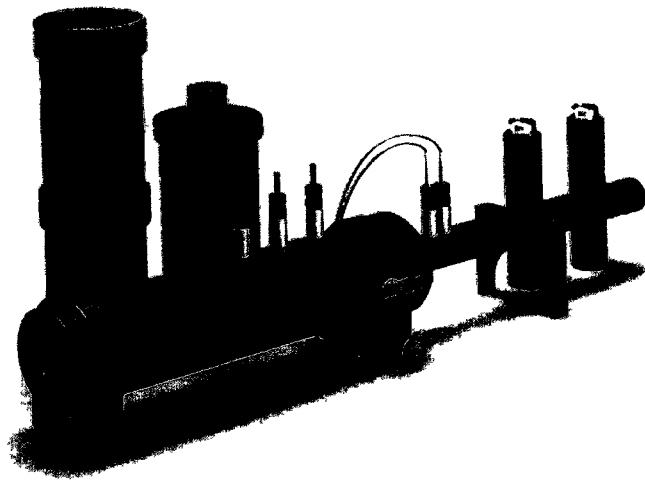
Figure 6: Two-microphone Impedance Measurement Tube Type 4206 (Bruel & Kjaer Impedance/Transmission Loss Measurement Tubes Type 4206 Technical Committee, 2007)

Specifically, the TL sample holders are tubes that are open-ended at both ends. They are mounted after the measurement tubes and before the TL measurement tubes, or extensions. Though the TL sample holders have fixed lengths, samples of variable length can be measured. For TL calculations only, the thickness of the sample is not needed, but

if other, more complex parameters are to be calculated, the thickness and positions of the sample are important [7].

For the low frequency and high frequency TL measurement tubes, there are two extension tubes for each setup. These tubes are threaded at each end, so they can be coupled directly with the sample holders. Specifically, this applies between the two halves of the small sample holder for the high frequency tube setup, and between the threaded plastic plug and the threaded end of the large sample holder in the low frequency tube setup. Either one or both extension tubes can be added to each tube setup. Each pair of extension tubes can be screwed together using Type DB-2359 Couplers for the tubes as required, and added to the setup. Each extension tube essentially increases the length of the measurement tube by 200 mm. This gives the user the option of establishing larger air gaps behind the test sample, and, especially for the high frequency tube setup due to the narrow diameter, allows better access to the rear of the sample [7].

4.2 Setup for Absorption Coefficient Measurement

The previous figure showed the simple setup for two-microphone measurement of sound absorption coefficients using the high frequency B&K Type 4206 impedance tube. The setup for measurement of absorption coefficients using the low frequency B&K Type 4206 impedance tube is similar, only with two active microphones being in the low frequency impedance tube, and the low frequency tube extension with the appropriate sized plunger being attached. For both setups, instead of the material sample being placed in a sample holder, it is placed directly in front of the plunger, with sufficient space between the face of the sample and the second microphone, to ensure accurate measurements. The impedance tube should be straight and it's inner surface smooth,

nonporous, and free of dust in order to ensure low sound attenuation. The tube's wall thickness is sufficiently thick so that sound transmission through it is negligible compared to transmission through the test specimen sample, depending on the SPL of the loudspeaker [7].

4.3 Frequency Weighting Types

In general, three types of weighting are selectable with the B&K Type 4206-T impedance tube set's frequency weighting unit. The first is high-pass for high frequency measurements in the high frequency tube. The second is linear pass for measurements in the low frequency tube. The third type is low-pass, for extra-measurement accuracy below 100 Hz. Measurements are recommended to be made with 0.25" diameter Type 4187 Condenser Microphones that are supplied. These are specially designed to reduce errors due to pressure leaks at high frequencies. Regarding the software, the Type 4206-T impedance tube setup is suitable for use with the PULSE Material Testing System [7].

4.4 Microphones

The B&K Type 4206-T impedance tube set has four microphones, which are each Type 4187 Condenser of 0.25" diameter, and four preamplifiers, which are each Type 2670. There is more than four microphone position holders located on the low frequency impedance tube so that the user can select which positions are appropriate for the microphone spacing desired, depending on the frequency range chosen. The high frequency impedance tube only has four microphone position holders, since the frequency range is fixed at 1600-6400 Hz. The microphones have a specially designed diaphragm that reduces air-leakage, and thus sound pressure absorption, from the inside of the impedance tubes. This gives a coupling between the impedance tube and the

microphones that is well-defined with respect to phase. For measurements, the microphones are positioned in special holders that ensure that they are mounted flush with the inside of the measurement tube. A silicon O-ring, inside the holder, seals the microphone holder itself against air leakage from inside the impedance tube, as shown in the following figure [7].

Condenser Microphone 4187

Microphone Holder
DP-0809

Microphone Position
DB-3213

Mounting Screw
DB-3266

"O"-ring
YJ-0071

Mounting Cup
YJ-0832

913477/1
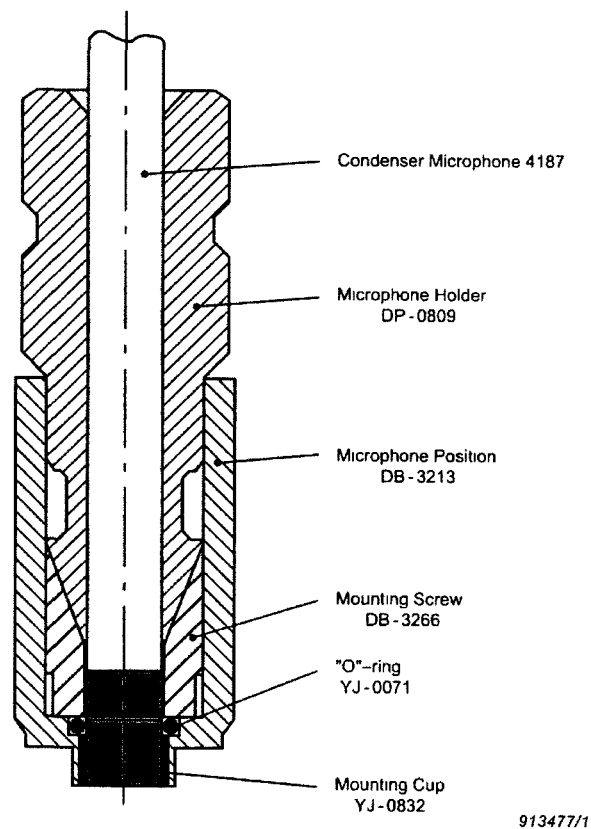
Figure 7:   The Internal Structure of a Microphone's Position and Holder (Bruel & Kjaer Impedance/Transmission Loss Measurement Tubes Type 4206 Technical Committee, 2007)

Dummy microphones are also supplied with the impedance tubes, for microphone mounting in holders that are not used in the active measurement setup. For example, one microphone position when using the low frequency tube setup is blocked, and all three low frequency tube positions when using the high frequency tube setup are blocked [7].

4.5 High Frequency Impedance Tube Setup

The high frequency TL tube setup consists of the low frequency measurement impedance tube, the high frequency measurement impedance tube, the small TL sample holder, and the high frequency impedance tube sample holder, which is an extension. The high frequency measurement tube has two microphone positions and holders that are identical to those on the low frequency tube. These positions are 20 mm apart. The free end of the tube is threaded so that the small sample holder can be screwed directly onto it [7].

In more detail, each measurement tube has its own sample holder. The sample holders consist of an aluminum tube, open at one end, through which a piston or plunger can be moved back and forth. The open ends of the tubes attach directly onto their respective measurement tubes [7].

For the high frequency impedance tube, the small sample holder is divided into two halves that can be unscrewed, so that extension tubes can be attached. This also gives access to the back of the test sample. The piston head or top of plunger is made of a flat circular brass disk. A rubber O-ring is positioned behind the disk to ensure that the piston or plunger slides smoothly inside the tube. The disk and O-ring are mounted onto a base of variable diameter that is screwed onto the plunger push-rod. When the user turns the handle clockwise, viewed from the end of the impedance tube, the diameter of the piston base increases, locking the piston or plunger into place in the impedance tube. When the user turns the handle counter-clockwise, the base loosens again, freeing the plunger to move along the tube's axis [7].

The high frequency TL measurement tube is mounted after the small TL sample holder. The small TL sample holder is 65 mm long. The distance from the sample holder to the microphone positions is 100 mm. A 29 mm length section of this must be air, leaving the other 71 mm available to be occupied by sample material. This gives a maximum possible sample length of 136 mm which is not recommended, since the thickness should be less than the diameter of the test samples. The measurement tube has two-microphone positions with holders that are identical to those on the low frequency tube. The positions are 20 mm apart and numbered 12 and 13. The free end of the tube is threaded so that the small sample holder can be screwed directly onto it. This is illustrated in the following figure [7].
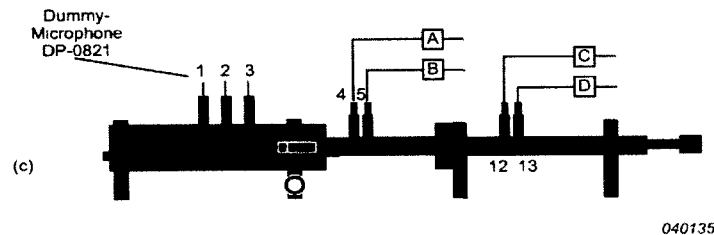
Figure 8: **Standard High Frequency Transmission Loss Tube (Bruel & Kjaer Impedance/Transmission Loss Measurement Tubes Type 4206 Technical Committee, 2007)**

The labels indicate the microphone numbers, recommended dummy microphones for unused microphone holders, and alphabetical position indicators of active microphones.

4.6 Low Frequency Impedance Tube Setup

The major component of the Type 4206-T B&K impedance tube set is the low frequency impedance tube. An 80 mm diameter sound source and frequency weighting unit are mounted at one end of the tube. The frequency weighting unit is controlled by a switch on the back side of the tube. This switch enables the user to select low-pass,

linear, or high-pass weighting of the input signal. The back plate of the low frequency impedance tube also has two input ports for standard B&K test connectors of the AQ-0100 Banana Plug type. These generally connect to a power amplifier, for signal conditioning. Three microphone holders are at a fixed 50 mm spacing between each consecutive microphone along the top of the tube, and are numbered 1 to 3. These holders specifically fit the 0.25" diameter Type 4187 Microphones, with Type 2670 Preamplifiers, and the Type DP-0821 Dummy Microphones that come supplied [7].

An adjustable support is positioned at the open end of the low frequency measurement tube. The support has a screw that can be loosened to allow it to slide freely along the length of the tube. A securing clamp is positioned on each side of the collar of the adjustable support. These clamps are used when mounting the large sample holder or the high frequency measurement tube onto the low frequency measurement tube. This ensures that half of the high frequency measurement tube is secured to the low frequency tube. For the inter-tube size arrangement, a tubular block of foam is supplied and fits snugly between the outside edge of the high frequency tube and the inside edge of the low frequency tube [7].

The low frequency TL measurement tube is mounted after the large TL sample holder. The large TL sample holder is 150 mm long. The TL measurement tube is a symmetrical unit with adjustable supports at both ends of the tube. Accordingly, the way it is mounted is not particularly important, but the user must be aware of the microphone position indicators. The numbers of the microphone positions increase with sound propagation, that is, the lowest numbers are closest to the loudspeaker. The low frequency impedance tube has a gap into which the securing clamps of the adjustable

support are clamped onto. Three microphone holders are spaced at 50 mm along the top

of the tube and are numbered 9 to 11. These holders fit the 0.25" diameter Type 4187

Microphones with Type 2670 Preamplifiers, and the Type DP-0821 Dummy

Microphones that come supplied with the Type 4206-T impedance tube set [7].

4.7 Alternative Impedance Tube Setups

For measurement preparations, two complete measurement setups are needed for

the Type 4206-T impedance tube set to operate over the complete frequency range from

50 Hz to 6.4 kHz. These are the Standard High Frequency Tube Setup, covering 1.6 kHz

– 6.4 kHz, and the Standard Low Frequency Tube Setup, covering 100 Hz – 1.6 kHz. In

addition to the standard tube setups, a wide spacing or alternative Low Frequency Tube

Setup can be assembled. These three setups are shown in the following figure, with the

positions of the two active microphones on one side of the material specimen indicated.

Note that an extension tube with two additional microphone holders is required for TL

measurements, since these setups are only for absorption coefficient measurements [7].
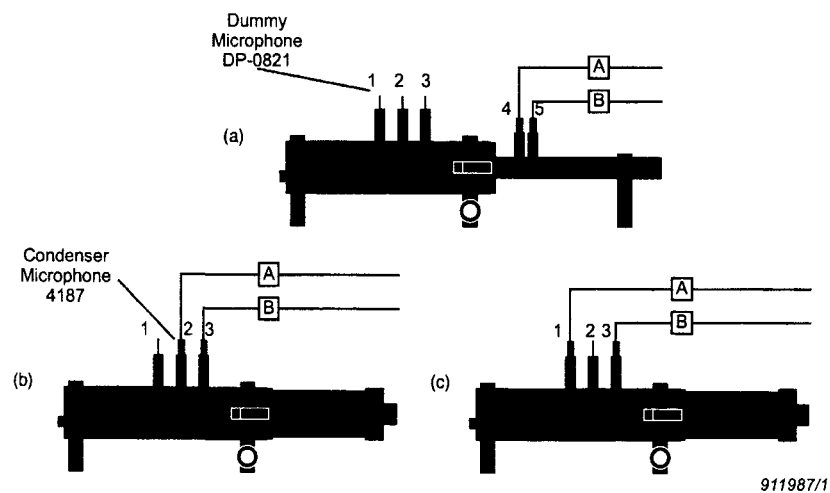
Figure 9: The Tube Setups for Type 4206: a) Standard High Frequency Tube; b) Standard Low Frequency Tube; c) Wide Spacing Low Frequency Tube (Bruel & Kjaer Impedance/Transmission Loss Measurement Tubes Type 4206 Technical Committee, 2007)

The labels indicate the microphone numbers, recommended dummy microphones for unused microphone holders, recommended Type 4187 Condenser microphones for active use, and alphabetical position indicators of active microphones. Both the high frequency and low frequency tube setups can be extended using one, or both, of the corresponding extension tubes. An extended tube setup can be used to create air gaps of measurable length behind the test specimen. This type of setup can be utilised, for example, to simulate measurements of high-volume vehicle cabin automotive applied dash panel underpads, for absorption coefficient measurements only. An extended tube setup also allows the user to have better access to the rear of the mounted test sample, especially when using the high frequency tube setup [7].

The simplest of the low frequency tube setups are the Standard Low Frequency Tube setup and the Wide Spacing Low Frequency Tube setup. These setups are identical except for the positioning of the microphones, as was shown in the previous figure. These setups consist of the low frequency measurement tube and the sample holder. The following figure depicts examples of correctly mounted test samples, for absorption coefficient measurements only [7].
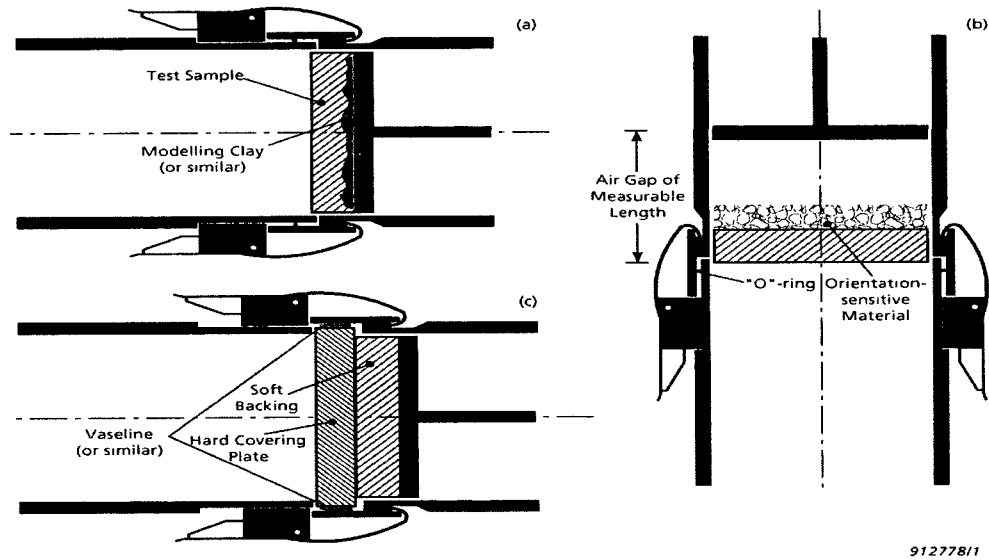
Figure 10: Three Examples of Correctly Mounted Test Samples: a) Uneven with Modelling Clay, b) Sample Mounted Horizontally with Vertical Tube with Air Gap in front of Plunger, c) Sample with Hard Surface and Soft Backing (Bruel & Kjaer Impedance/Transmission Loss Measurement Tubes Type 4206 Technical Committee, 2007)

4.8 Preparation and Mounting of Test Samples

The shape and size of the test specimens is essential to ensure the accuracy of the measurements. So, the user must take great care when preparing and mounting the test samples [7]. Each test specimen must have the same shape and area as the impedance tube's cross section. The mounting conditions, for example acoustic rings, will strongly affect the measured TL. The test specimen may be rigidly mounted or clamped to the wall of the impedance tube, being freely suspended with a dense flexible seal, for example acoustic rings. Any flexible mounting material, for example plastic for acoustic rings, must be proven to have a TL greater than the test specimen. Any exposed gaps in acoustic plastic rings will have a tremendous impact on the TL results. Any visible cracks should be well-sealed with petroleum jelly [2].

The B&K impedance tube setup is critical for accurate TL_n measurements of circular dash panel samples of AZ31B magnesium, 6061-T6 aluminum, and 1018 cold-

rolled steel for comparison. Each of these dash panel samples is with either a 15 mm or 19 mm thick, circular sample of RUL automotive underpad. The alternative two-microphone setup depicted in Figure 6 is also critical for accurate two-microphone absorption coefficient measurements of circular samples of 15 mm or 19 mm thick RUL automotive underpad. When TL measurements on larger, square 60cmX60cm samples of the same materials with a 15 mm or 19 mm thick, square 60cmX60cm sample of RUL automotive underpad are required, the experimental setup for TL_r measurements according to the test standard of SAE J1400 is essential.

4.9 Sample Setup for SAE J1400 Testing

The SAE J1400 Test was conducted in the B&K ARC Centre for Research in Canton, Michigan utilising an STL Suite. The STL Suite consisted of a very large semi-anechoic room above a reverberation pit in which the speaker source, and five microphones, positioned at least 1 m above the floor, 1 m away from the wall, the ground and each other on tripods, were placed. This is shown in the following figure, with two microphones being out of view.

Figure 11: A Speaker Source and Five Type 4189 B&K Free-Field Microphones Placed on Tripods in a Reverberation Pit below the Semi-Anechoic Room, with Two Microphones being Out of View

The reverberation pit was sealed from the semi-anechoic room by a 2.1 m long, 1.2 m wide, 11.4 cm thick acoustic buck made out of Medium Density Fibreboard (MDF). This acoustic buck was sealed around its edges, which could have exposed flanking paths, by putty sealant. The acoustic buck consisted of an adaptor plate placed in the 1mX1m hole in the centre, which consisted of a 60cmX60cm hole in its centre. This is shown in the following figure, with five microphones on tripods positioned above the sample.

Figure 12: The Acoustic Buck with Adaptor Plate in the 1mX1m Hole in the Centre, Consisting of an MDF Sample Frame Holding a 60cmX60cm Steel Sample in Place

All holes had lips that protruded in at certain heights to support the weight of the object placed on top of it. This was the MDF adaptor plate, and an MDF sample holder with a metal sample sealed with putty along the bottom perimeter. The 60cmX60cm hole in the adaptor plate was filled during each four, 10 second signal tests with an MDF sample holder, with a 60cmX60cm sample of either 1018 cold-rolled steel, 6061-T6 aluminum, or AZ31B magnesium within it. Each metal was tested by itself, and also with a 15 mm or 19 mm thick, 60cmX60cm sample of RUL automotive under-padding, which were tested separately, to simulate realistic dash panel arrangements. There were eight different metal samples and two different RUL underpads, which were tested alone as well, total, for a total of 26 different sample arrangements.

Each dash panel sample was tested using four signals of 10-second durations from the speaker source. These were tested in this order: random or uniform white noise, periodic random or scattered white or pseudorandom noise, diesel generator noise, and electric motor noise. These signals were utilised since random noise and periodic random noise are standard for uniform pressure response across the frequency range. Also, diesel generator noise and electric motor noise are more subjective, for a more 'real world' TL and psychoacoustic evaluation. Random noise was required for the J1400 TL calculations, for a uniform sound pressure response across the frequency range.

The tests were conducted utilising a laptop computer with a B&K front end, which was connected to the ten Type 4189 Free-Field B&K microphones via BNC to BNC cables. The five microphones in the semi-anechoic room were also on tripods, positioned 20.3 cm above the test sample front face, with four microphones being 12.7 cm diagonally offset from the corners of the test sample. The laptop was equipped with PULSE Labshop Version 15.1 software, utilised to acquire the SPL data of the ten microphones over the four, 10-second signals. The latter two test signals, diesel generator noise and electric motor noise, were utilised in addition to the more common first two to also analyse the psychoacoustic response of the dash panel test samples. This was done for microphones 6 and 10, which were randomly chosen to best represent the specific loudness, total loudness and sharpness above the test sample.

Referring to Figure 11 and viewing from above the test sample, microphone 6 is at the upper right-hand corner of the sample, microphone 7 is at the upper-left, microphone 8 is at the bottom left, microphone 9 is at the bottom right, and microphone 10 is in the centre. So, it is clear how the microphone 6 and 10 averaged specific

loudness, total loudness and sharpness is a good psychoacoustic response over the surface of the sample.

As mentioned, the psychoacoustic parameters were chosen to be specific loudness, total loudness and sharpness in the time domain, since sharpness has not been standardised yet. TL_r, and the two-microphone averaged values of specific loudness, total loudness and sharpness were calculated for all four signals. The psychoacoustic evaluations were only needed once in the reverberation pit for characterisation of the source signal, but once for every material arrangement in the semi-anechoic room, for the microphones 6 and 10 average.

Chapter 5: RESULTS AND DISCUSSION

As discussed previously, the metals aluminum, magnesium, and steel were tested, each utilising 15 mm and 19 mm thick RUL under-padding. TL results obtained using B&K impedance tubes at the University of Windsor were compared to the B&K results obtained utilising the buck within the semi-anechoic room with the reverberation pit underneath in Canton, Michigan, both utilising random or uniform white noise. Also, sharpness in the time domain, specific loudness, and total loudness results were presented for all three metals, both by themselves, and also involving the usage of stated under-padding. In addition, absorption coefficients for circular samples only of the RUL automotive underpads were presented. As well, TL for the large 60cmX60cm dash panel samples, and metals and underpads alone for three additional signals for the purpose of a more 'real world' response outside of the J1400 test method were reviewed. These signals were periodic random or scattered white or pseudorandom noise, diesel generator noise, and electric motor noise. The actual test results from experimentation utilising the B&K impedance tubes, and the STL Suite at the ARC Centre in Canton, Michigan will be discussed in this chapter.

5.1 Experimental TL_n Results

The 4.7 mm, 2 mm, and 1.27 mm thicknesses of 6061-T6 aluminum, the 4 mm, and 2 mm thicknesses of AZ31B magnesium, and the 4.9 mm, 2 mm and 1 mm thicknesses of 1018 cold-rolled steel dash panel materials were machined as disks of 99.5 mm diameter and 28.5 mm diameter. Each of these disks was tested for TL_n in combination with either a 15 mm or 19 mm thick circular sample of RUL automotive under-padding. All material disks were machined from sheet material. As well, the 15

mm and 19 mm thick, 99.5 mm diameter and 28.5 mm diameter samples of RUL automotive under-padding were tested for normal incidence absorption. Also, for the TL_r and psychoacoustic measurements in the STL Suite, 60cmX60cm samples of these material thicknesses were machined, and the RUL underpad samples were cut to specification. The TL_n results of the eight different metal disks, with either a 15 mm or 19 mm thick circular sample of RUL automotive underpad dash panel samples, are shown in the following figures.

5.2 Discussion of Experimental TL_n Results

Referring to Figure 13, it is clear that 2 mm Mg 15 mm RUL is higher than 4 mm Mg 15 mm RUL, due to problems with the measurement setup within the impedance tube, for example acoustic rings, sealing with petroleum jelly, etc. As well, 2 mm Mg 15 mm RUL is clearly a better dash panel arrangement than 2 mm Steel 15 mm RUL at some frequencies, 2 mm Al 15 mm RUL for almost all frequencies, and 1.27 mm Al 15 mm RUL for all frequencies. Figure 13 also depicts that the only good competitor with 1.27 mm Al 15 mm RUL is 4 mm Mg 15 mm RUL for some frequencies.

Referring to Figure 14, it is clear that the TL_n performance of 2 mm Mg 19 mm RUL and 4 mm Mg 19 mm RUL is almost identical. However, 2 mm Mg 19 mm RUL is shown to be the better dash panel sample based on slightly higher TL_n values. This may be due to the measurement setup issues noted previously. A good competitor with 2 mm Al 19 mm RUL is 4 mm Mg 19 mm RUL, while 2 mm Mg 19 mm RUL is shown to be a good competitor with 1.27 mm Al 19 mm RUL at most frequencies, and 2 mm Al 19 mm RUL at all frequencies.

Referring to Figure 15, it is clear that 2 mm Mg 15 mm RUL is a better dash panel arrangement than the 4 mm Mg 15 mm RUL, since its TL_n values are higher in most cases. This is due to measurement setup issues. The 2 mm Mg 15 mm RUL is a good competitor with 4.7 mm Al 15 mm RUL at almost all frequencies, 1 mm Steel 15 mm RUL at some frequencies, 2 mm Steel 15 mm RUL at some frequencies, and 4.9 mm Steel 15 mm RUL at some frequencies. The 4 mm Mg 15 mm RUL is a good competitor with 4.7 mm Al 15 mm RUL at most frequencies.

Referring to Figure 16, it is clear that the TL_n performance of 2 mm Mg 19 mm RUL is superior to that of 4 mm Mg 19 mm RUL, since its TL_n values are higher in most cases. Again, this is only due to problems with the measurement setup already noted. A good competitor with 1.27 mm Al 19 mm RUL is 2 mm Mg 19 mm RUL at some frequencies, while the 4 mm Mg 19 mm RUL is a good competitor with 2 mm Steel 19 mm RUL at some frequencies, 2 mm Al 19 mm RUL at some frequencies, and 1.27 mm Al 19 mm RUL at some frequencies.

Figure 13: TLₙ Results of Three Consecutive Trials Averaged Arithmetically for each Material Thickness with a 15 mm Thick RUL Underpad in the Low Frequency B&K Impedance Tube

Figure 14: TLₙ Results of Three Consecutive Trials Averaged Arithmetically for each Material Thickness with a 19 mm Thick RUL Underpad in the Low Frequency B&K Impedance Tube

Figure 15: TL_n Results of Three Consecutive Trials Averaged Arithmetically for Each Material Thickness with a 15 mm Thick RUL Underpad in the High Frequency B&K Impedance Tube
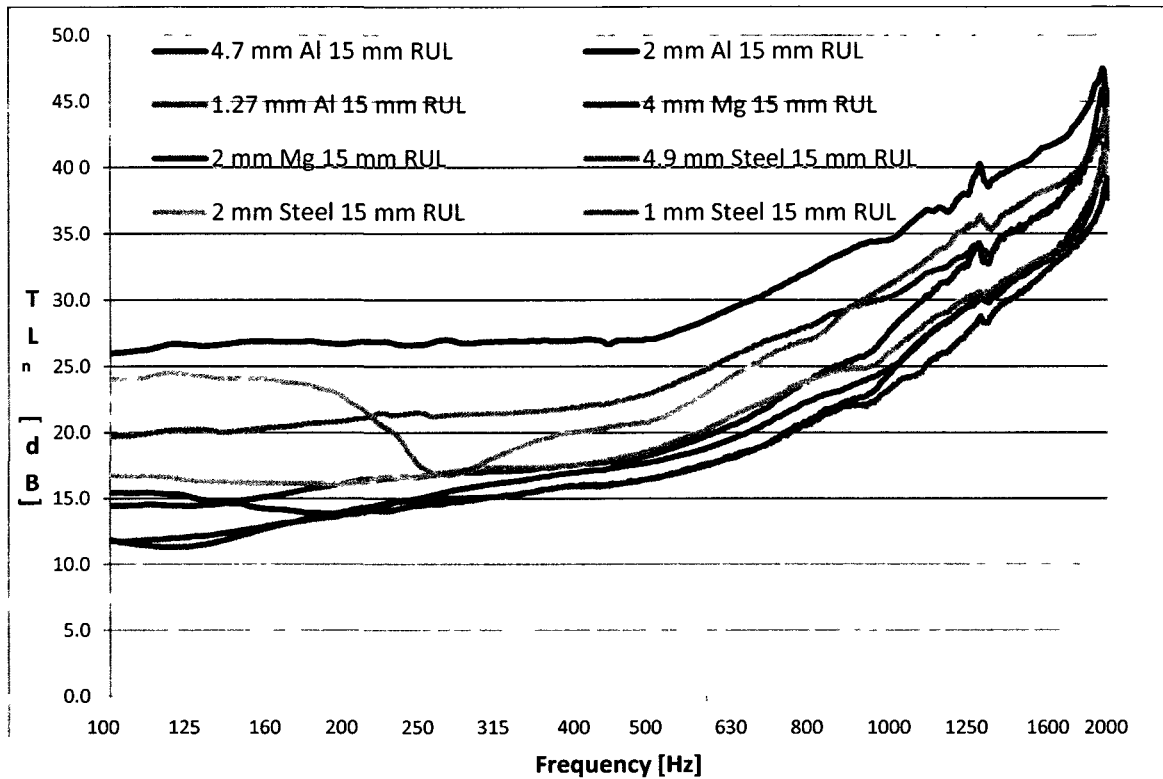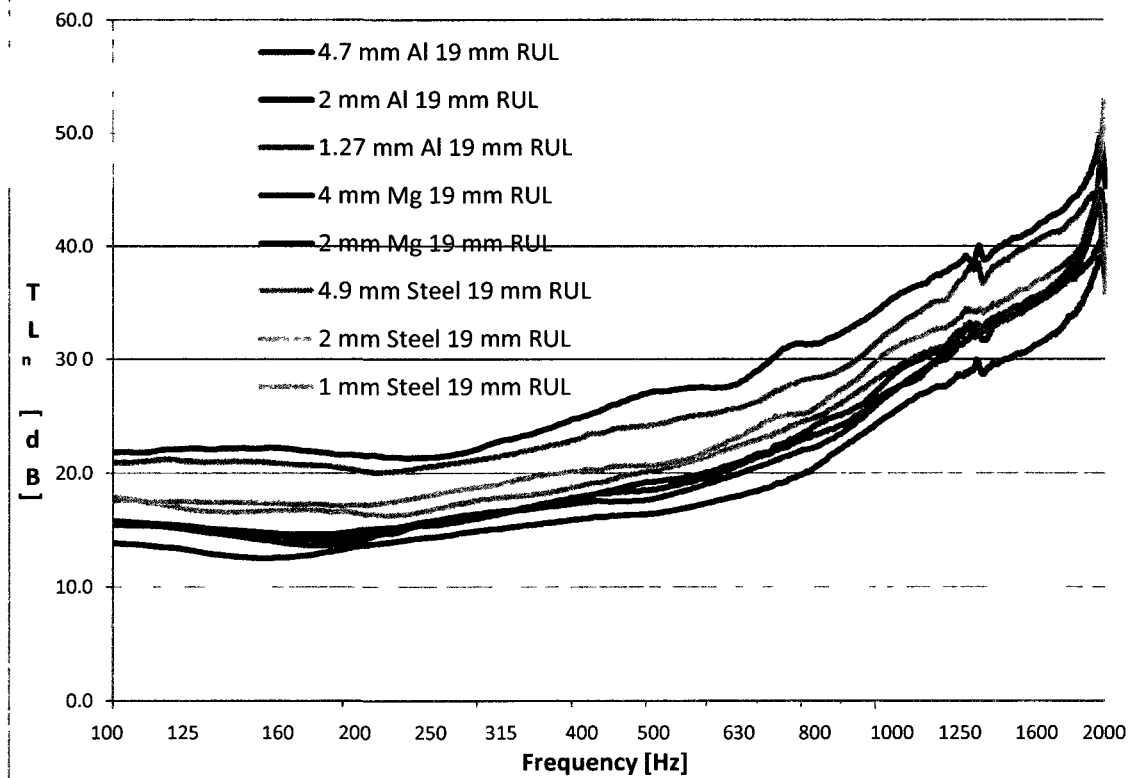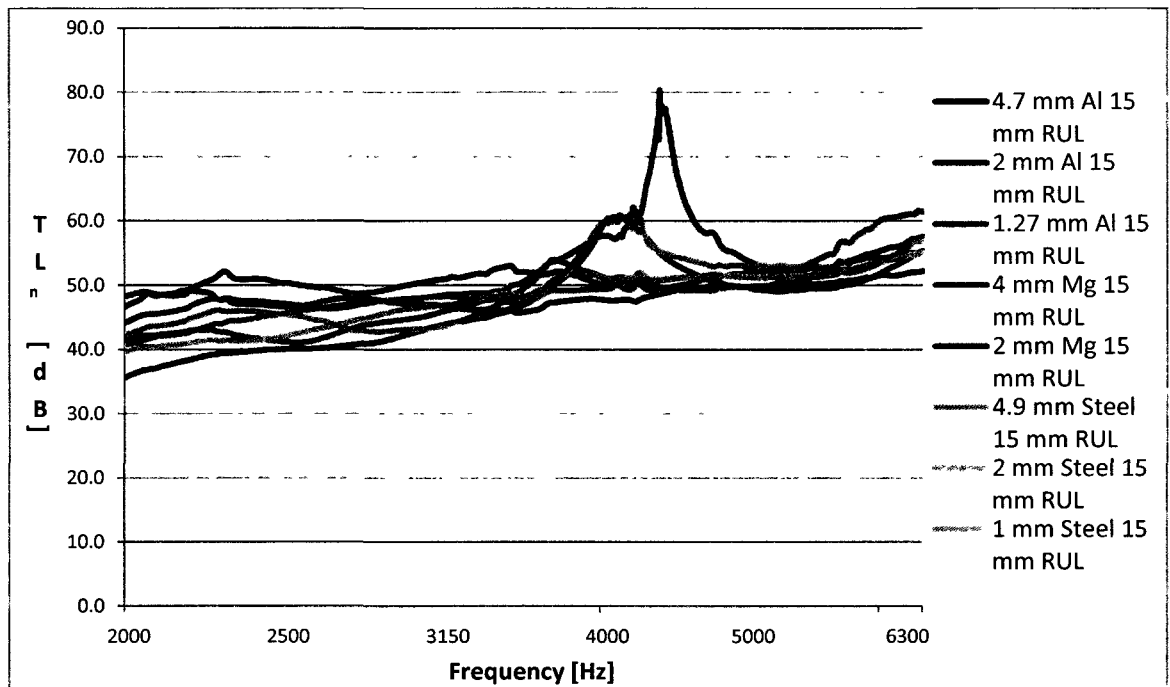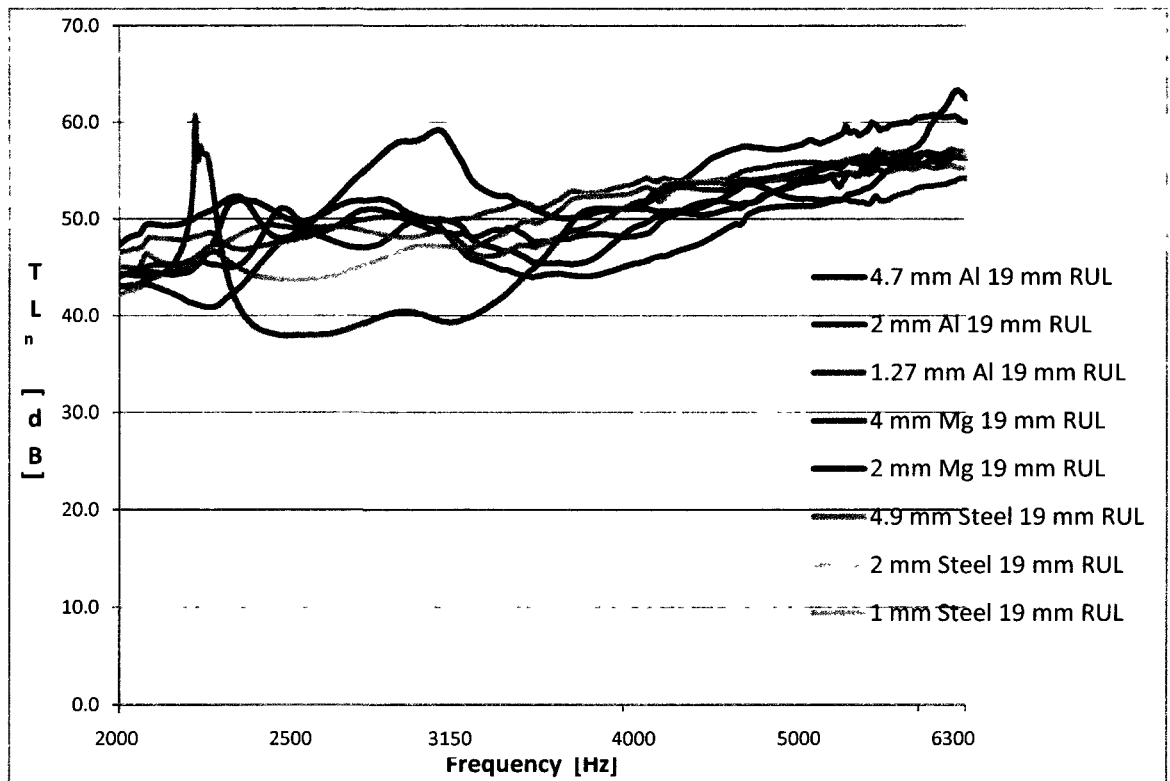

Figure 16: TL_n Results of Three Consecutive Trials Averaged Arithmetically for Each Material Thickness with a 19 mm Thick RUL Underpad in the High Frequency B&K Impedance Tube

5.3 Experimental Absorption Coefficient Results

The following figures show the normal incidence absorption coefficient results for one-third octave bandwidth centre frequencies starting from 50 Hz up to 6300 Hz, for the 15 mm and 19 mm thick, 99.5 mm diameter and 28.5 mm diameter circular samples of RUL.

Referring to Figure 17, the normal incidence absorption coefficients tend to increase with frequency from 0.01 at 50 Hz to 0.45 at 800 Hz. The absorption then decreases to a local minimum of 0.37 at 1600 Hz, due to a small resonance. The absorption then increases to a final maximum of 0.54 at 2000 Hz.

Referring to Figure 18, the normal incidence absorption coefficients tend to increase from 0.02 at 50 Hz up to 0.49 at 630 Hz. The absorption then decreases to a minimum of 0.35 at 1250 Hz, due to a small resonance. The absorption then increases to 0.40 at 1600 Hz, followed by a decrease to a final minimum of 0.38 at 2000 Hz.

Referring to Figure 19, the normal incidence absorption coefficients tend to decrease from 0.55 at 2000 Hz to a minimum of 0.49 at 2500 Hz, due to a small resonance. The absorption then rises to a maximum of 0.80 at 6300 Hz.

Referring to Figure 20, the normal incidence absorption coefficients tend to increase from 0.38 at 2000 Hz to a maximum of 0.42 at 2500 Hz. The absorption then decreases to a minimum of 0.41 at 3150 Hz, due to a small resonance. The absorption then increases to a maximum of 0.56 at 6300 Hz.

Figure 17: Normal Incidence Absorption Coefficients of the 99.5 mm Diameter, 15 mm Thick Circular Sample of RUL Automotive Underpad

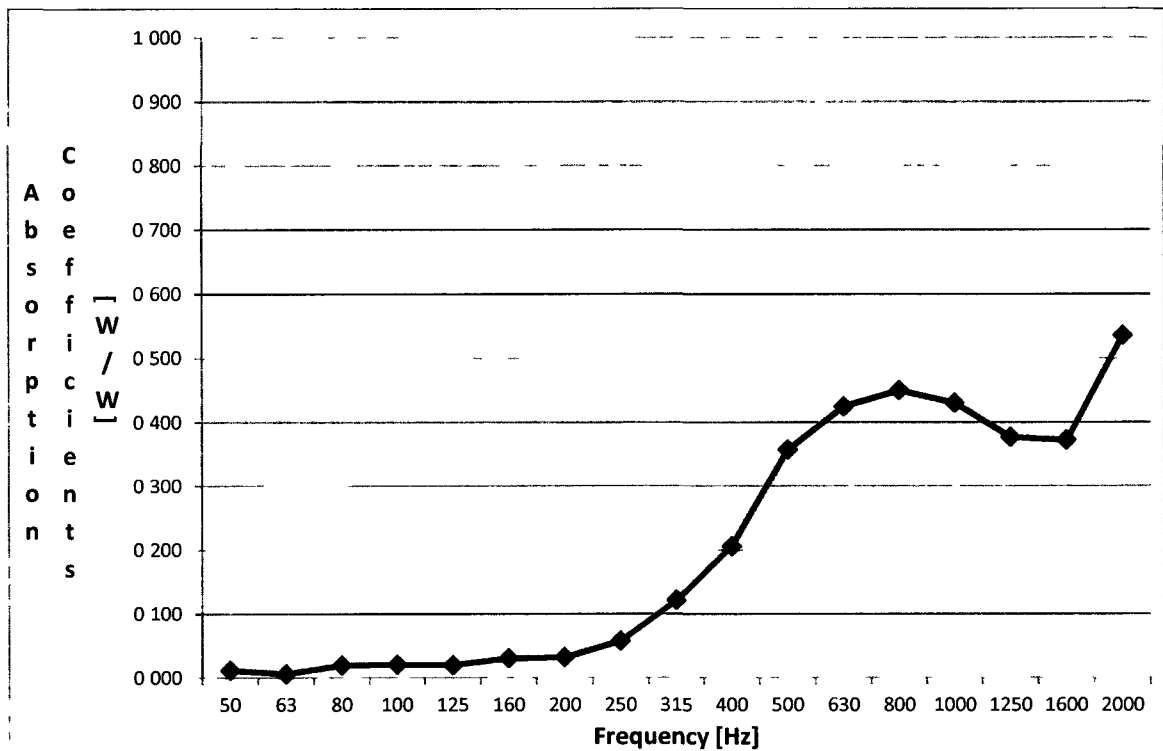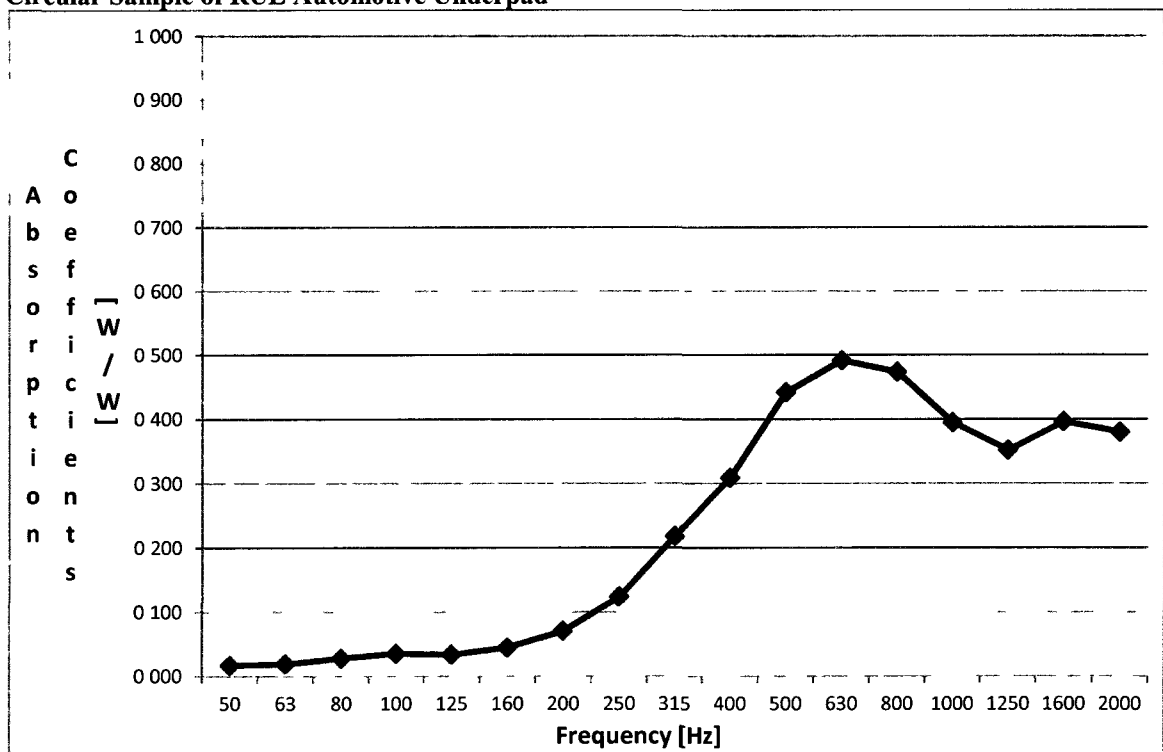**Figure 18:** Normal Incidence Absorption Coefficients of the 99.5 mm Diameter, 19 mm Thick Circular Sample of RUL Automotive Underpad
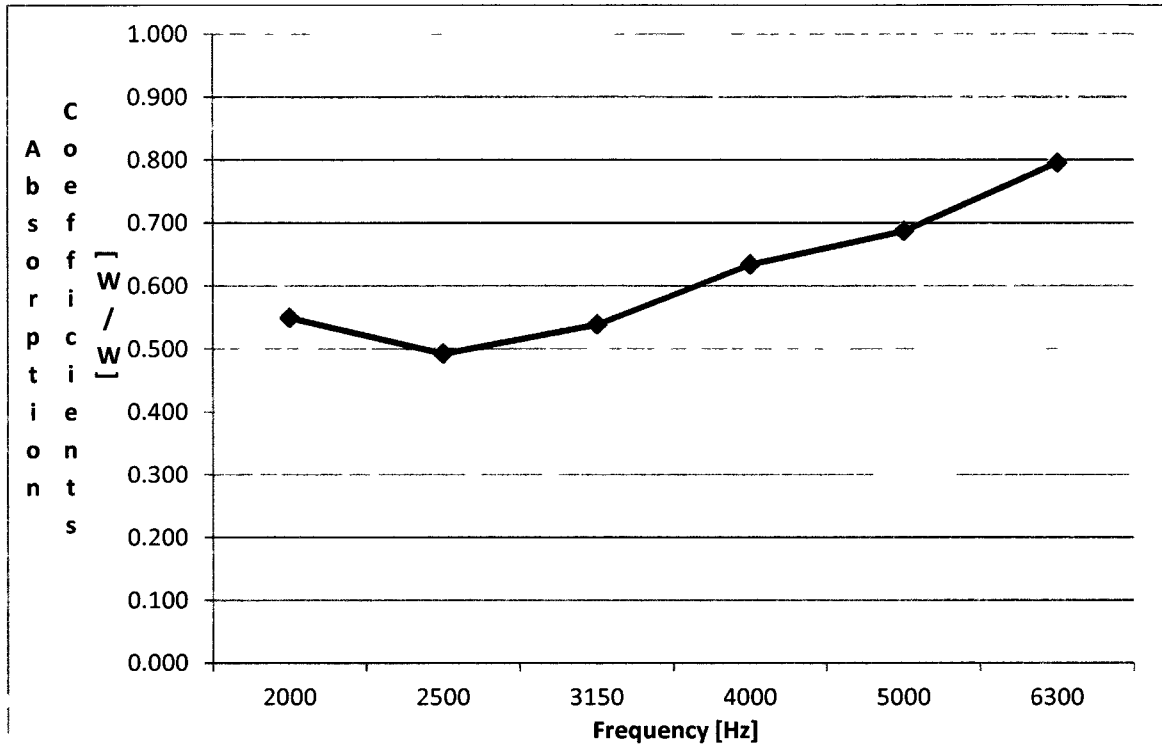
Figure 19: Normal Incidence Absorption Coefficients of the 28.5 mm Diameter, 15 mm Thick Circular Sample of RUL Automotive Underpad
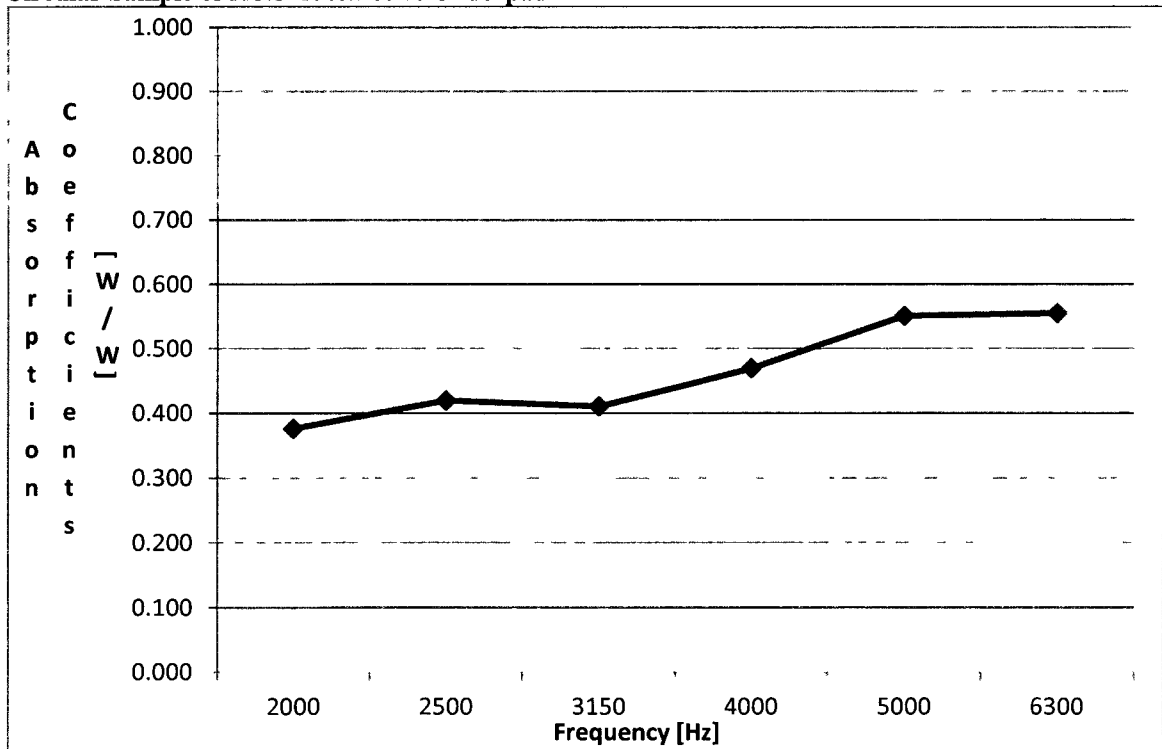

Figure 20: Normal Incidence Absorption Coefficients of the 28.5 mm Diameter, 19 mm Thick Circular Sample of RUL Automotive Underpad

5.4 Uniform White Noise Experimental TL_r Results

The following figures are graphs showing the random or uniform white noise TL_r results from the 24, 60cmX60cm dash panel samples, and two RUL underpads tested using the acoustic buck in the STL Suite at the B&K ARC Centre in Canton, Michigan, in July 2010. The separate J1400 test results are shown in the Appendix, for ease of comparison of the TL_n data in the B&K impedance tubes to the TL_r data of the J1400 test, which is a new comparison that has not been researched by many, other than those of reference [34].

Referring to Figure 21, both the 4 mm Mg 15 mm RUL and 2 mm Mg 15 mm RUL prove to be acceptable dash panel arrangements, since their TL_r performance is in the same region as the 1018 cold-rolled steel and 6061-T6 aluminum dash panel samples, for respective thickness comparisons. Specifically, their TL_r performance is never more than 11.4 dB less than those of competing dash panel samples for respective firewall thicknesses, and even exceeds them at times. This was determined by the difference in TL_r values at 500 Hz for 4 mm Mg 15 mm RUL in comparison to 4.9 mm Steel 15 mm RUL.

Referring to Figure 22, both the 4 mm Mg 19 mm RUL and 2 mm Mg 19 mm RUL prove to be worthy competitors, since their TL_r performance is in the same region as the 1018 cold-rolled steel and 6061-T6 aluminum dash panel samples, for respective thickness comparisons. For statistical purposes, the greatest difference in TL_r values occurs at 250 Hz, where the TL_r for 4.9 mm Steel 19 mm RUL is 40.3 dB, while the TL_r for 4 mm Mg 19 mm RUL is 25.9 dB. This results in an inferior difference of 14.4 dB. Otherwise, the 4 mm Mg 19 mm RUL and 2 mm Mg 19 mm RUL dash panel samples

were proven to perform in the same range as the other dash panel samples, and even exceeding in some cases.

Referring to Figure 23, a similar outcome was reached, with different statistical values. The RUL underpads were also shown to have significant contributions to the TL_r performance of the two-layered dash panel samples.

Figure 21: Random or Uniform White Noise TL_r Results of All Material 60cmX60cm Samples with the 15 mm Thick, 60cmX60cm Sample of RUL Automotive Underpad from the J1400 Test in Canton, Michigan

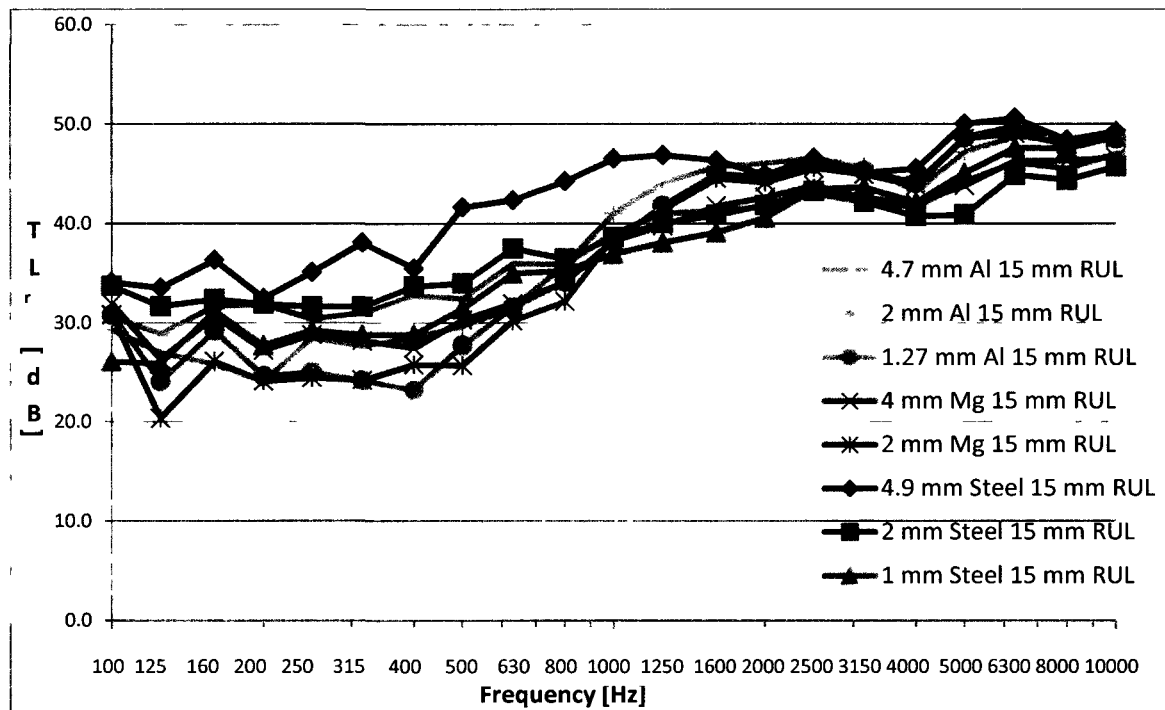**Figure 22: Random or Uniform White Noise TL_r Results of All Material 60cmX60cm Samples with the 19 mm Thick, 60cmX60cm Sample of RUL Automotive Underpad from the J1400 Test in Canton, Michigan**
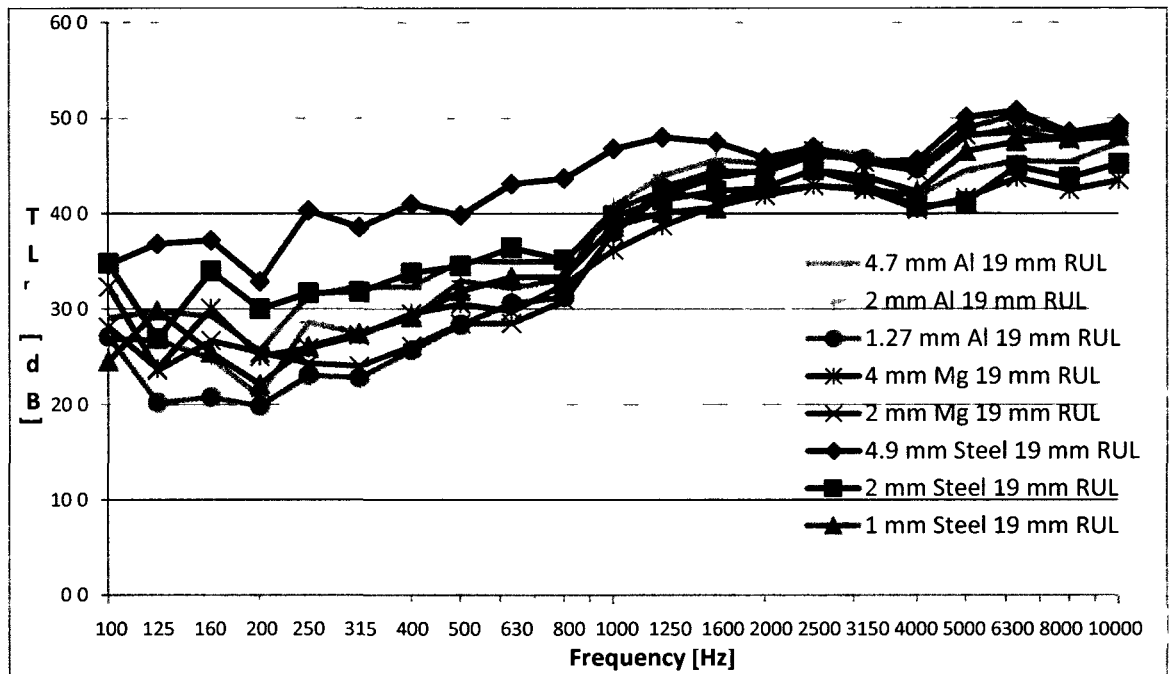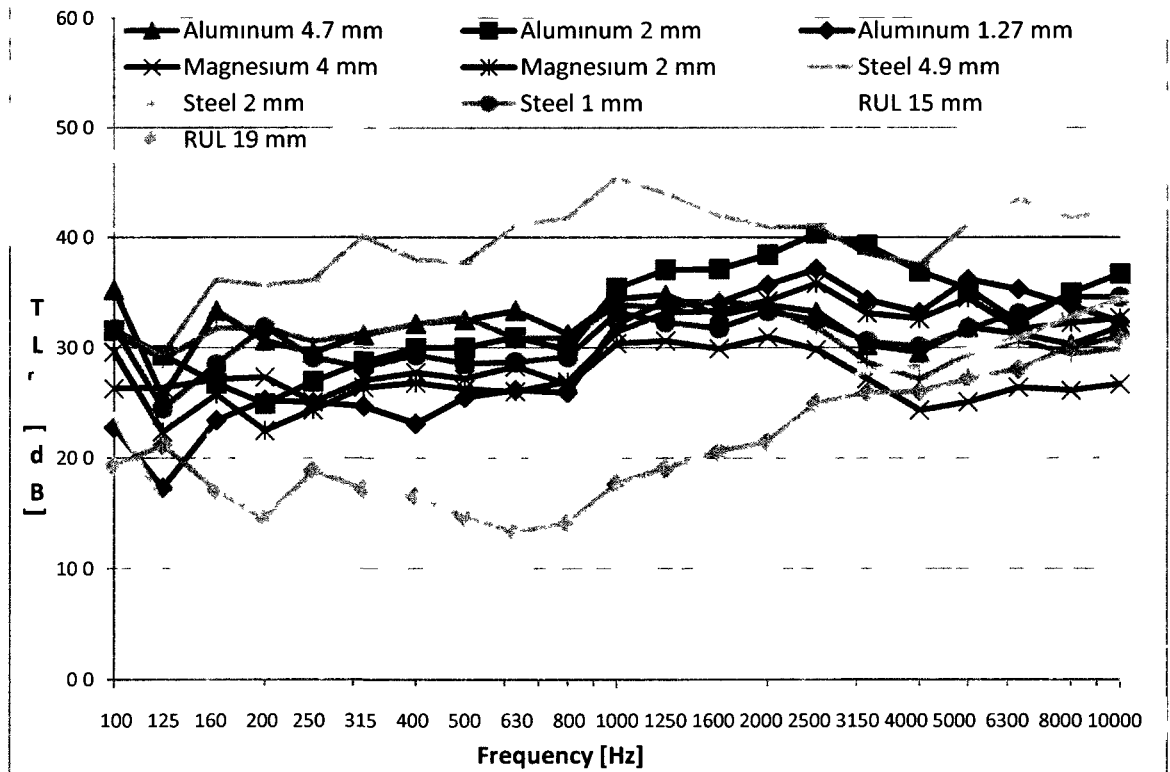

Figure 23: Random or Uniform White Noise TL_r Results of All Material 60cmX60cm Samples Alone, and the 15 mm and 19 mm Thick, 60cmX60cm Samples of RUL Automotive Underpad Alone from the J1400 Test in Canton, Michigan

5.5 Discussion of J1400 Results Comparison to Impedance Tube TL_n Results

Comparing Figures 13, 14, 15 and 16 from the B&K impedance tubes to Figures 21 and 22 from the STL Suite at the ARC Centre in Canton, Michigan, it is clear that the TL_r results are generally much higher than the TL_n results. This is due to many reasons. One reason is that the impedance tube method utilised many theoretical equations. From the Theory section of this thesis, equations (16), (17), (18), (19), (21), (22), (23), (24), (25), and (26) were used for the two-load method only, since only two-layered dash panel samples were tested.

The theoretical equation approach utilised was found to be very different than the SAE J1400 method, where SPL data from the five microphones in each room was logarithmically averaged for respective one-third octave bandwidth centre frequencies. The averages in the semi-anechoic room were then subtracted from the averages in the reverberation room for each one-third octave bandwidth centre frequency. This gave the MNR. This approach was found to be very different than that used in the impedance tube.

The impedance tube approach utilised the preliminary ratios of complex sound pressure at microphones 3 and 4, positioned after the test samples in the sample holder in the middle of the tube, to microphone 1, in the incident wall of the tube. Furthermore, the impedance tube method used the complex sound pressure ratios from microphone 1 to microphones 2, 3, and 4, or transfer functions, to calculate the incident and reflected complex sound pressures on opposite sides of the two-layered test sample. These complex sound pressures were then used to calculate the complex sound pressures and complex particle velocities on each face of the two-layered test sample. Then, the

calculated complex sound pressures and complex particle velocities were used to calculate the four entries of the 2X2, two-load transfer matrix. The transfer matrix entries were then used to calculate the Transmission Coefficient t, which was then used to calculate TL_n. So, the impedance tube method in itself is very theoretical.

The impedance tube method attempts to approximate the SPL data from the reverberation pit for the incident side of the test samples with only two microphones. It also attempts to approximate the SPL data from the semi-anechoic room on the transmitted side of the material samples, with an anechoic termination with only two microphones. If the termination is blocked, the impedance tube method tries to approximate SPL data from a second reverberation room above the test samples, in addition to the first. If the termination is open, the impedance tube method attempts to approximate the SPL data from a much larger, second reverberation room. Thus, it is not realistic to approximate the SPL data from a large reverberation pit and semi-anechoic room in a relatively tiny tube, on incident and transmitted sides of the test samples, respectively. Otherwise, the J1400 results should be the same as the impedance tube results, but they are found to be much higher.

The reflection off the tube walls is also very different, since they are circular, while the walls of the reverberation pit are flat. The floor of the semi-anechoic room is flat, while the four side walls and ceiling are padded with large anechoic wedges. This is similar to the transmitted side of the test samples in the impedance tubes. However, the walls of the tubes are circular, and the anechoic condition is much less effective than that in the semi-anechoic room.

The impedance tube method also has many sources of error. These include not having a test sample mounted correctly, or normal to the tube's longitudinal axis, with acoustic rings that are required to possess a higher TL than the two-layered test sample. Also, the gap in the acoustic rings may not be sealed properly with vibro-acoustic sealing material. In addition, the test samples may not be sealed between the two acoustic rings in the sample holder with sufficient petroleum jelly to seal the clearance between the test samples diameter and the impedance tube's inner diameter.

The SAE J1400 method, on the other hand, gives a more realistic outcome of TL, since it uses the physical SPL data from each separate microphone located in two high-volume rooms, separated by much larger, square two-layered test samples, with any flanking paths sealed off with putty. The five microphones in the reverberation room are spread out over a large volume to capture the physical changes in the air from sound reflected off the six walls. These are the floor, the four side walls, and the ceiling. During testing, the five microphones in the semi-anechoic room were positioned 20.3 cm above the test sample, with four being 12.7 cm diagonally offset from the sample corners, and one being in the geometric centre. These provided a realistic SPL average across the surface of the test samples, after sound was transmitted through from the reverberation pit.

5.6 Real World Experimental TL_r Results from Three Additional Signals

The following figures show the TL_r values from all the metals with a 15 mm or 19 mm thick RUL underpad, which were tested separately, and the metals alone along with the RUL underpads alone. These were all 60cmX60cm samples, and were tested with three additional signals to the standard J1400 random or uniform white noise signal, in

order to present a more 'real world' TL response of the metals and underpads alone, and the two different dash panel sample types. These signals were periodic random or scattered white or pseudorandom noise, diesel generator noise, and electric motor noise.

Figures 24, 25 and 26 are proof that AZ31B magnesium dash panels are acceptable when subjected to periodic or scattered white or pseudorandom noise. This is because the TL_r values are within reasonable dB intervals from those of competing dash panel materials of respective thicknesses for comparison. For statistical purposes, the largest difference occurs at 6300 Hz for 4 mm Magnesium in comparison to the 4.9 mm Steel. Here, the 4 mm Magnesium is at 39.9 dB, while the 4.9 mm Steel is at 56.4 dB, for a difference of 16.5 dB in favour of 4.9 mm Steel. Otherwise, the AZ31B magnesium dash panel samples perform in the same TL_r region, match, and even exceed the TL_r performance of competing dash panel samples, for respective thickness comparisons. These are 4 mm Magnesium to 4.9 mm Steel and 4.7 mm Aluminum; 2 mm Magnesium to 2 mm Steel, 1 mm Steel, 2 mm Aluminum, and 1.27 mm Aluminum.
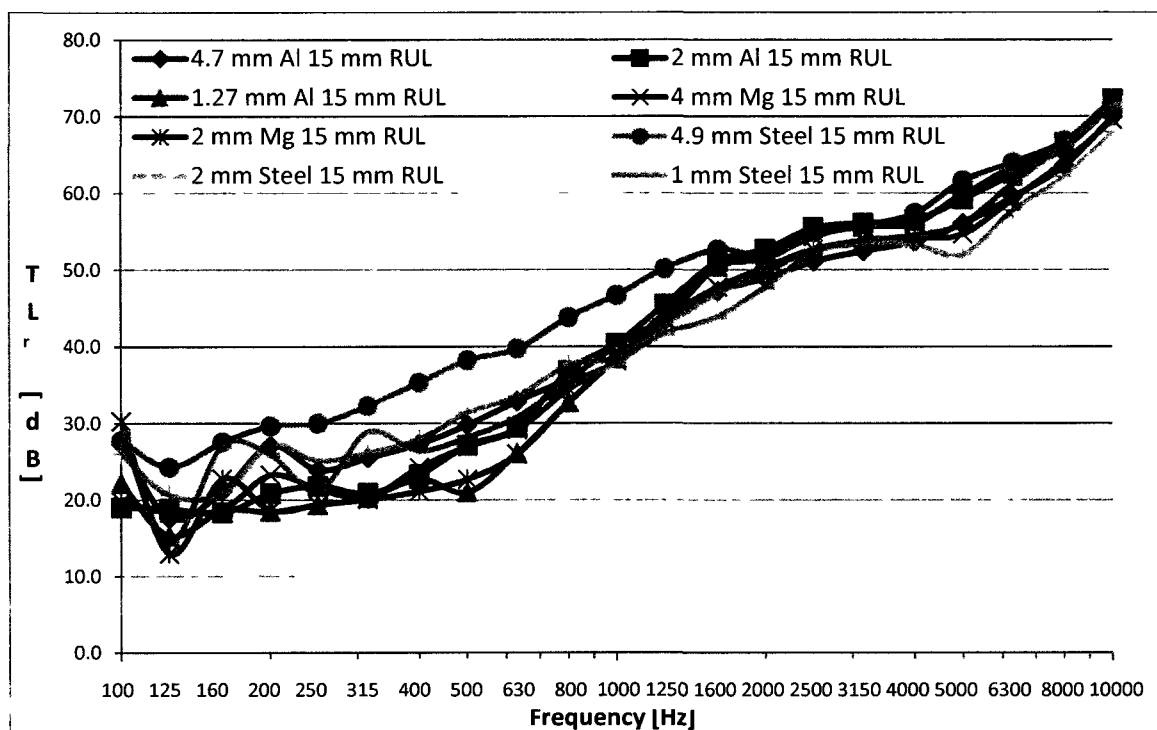
Figure 24: Periodic Random or Scattered White or Pseudorandom Noise TL$_r$ Results of All Material 60cmX60cm Samples with the **15 mm** Thick, **60cmX60cm** Sample of RUL Automotive Underpad from the Tests in Canton, Michigan
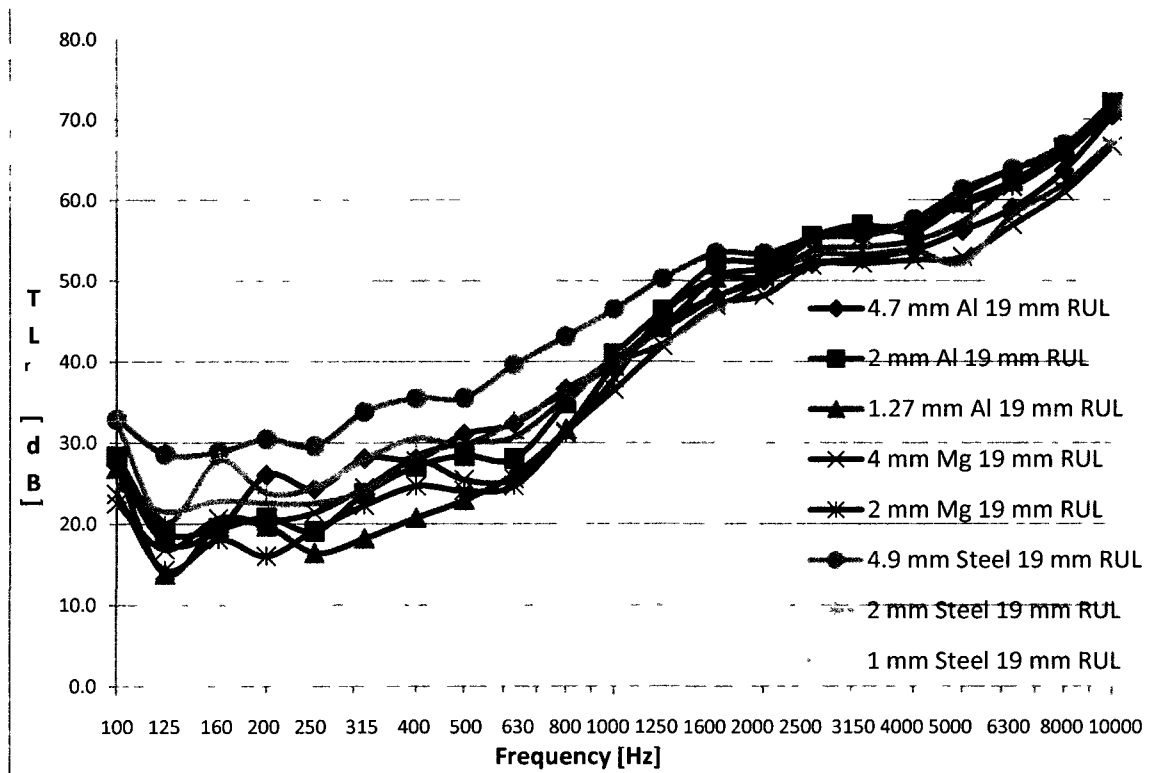

Figure 25: Periodic Random or Scattered White or Pseudorandom Noise TL$_r$ Results of All Material 60cmX60cm Samples with the **19 mm** Thick, **60cmX60cm** Sample of RUL Automotive Underpad from the Tests in Canton, Michigan
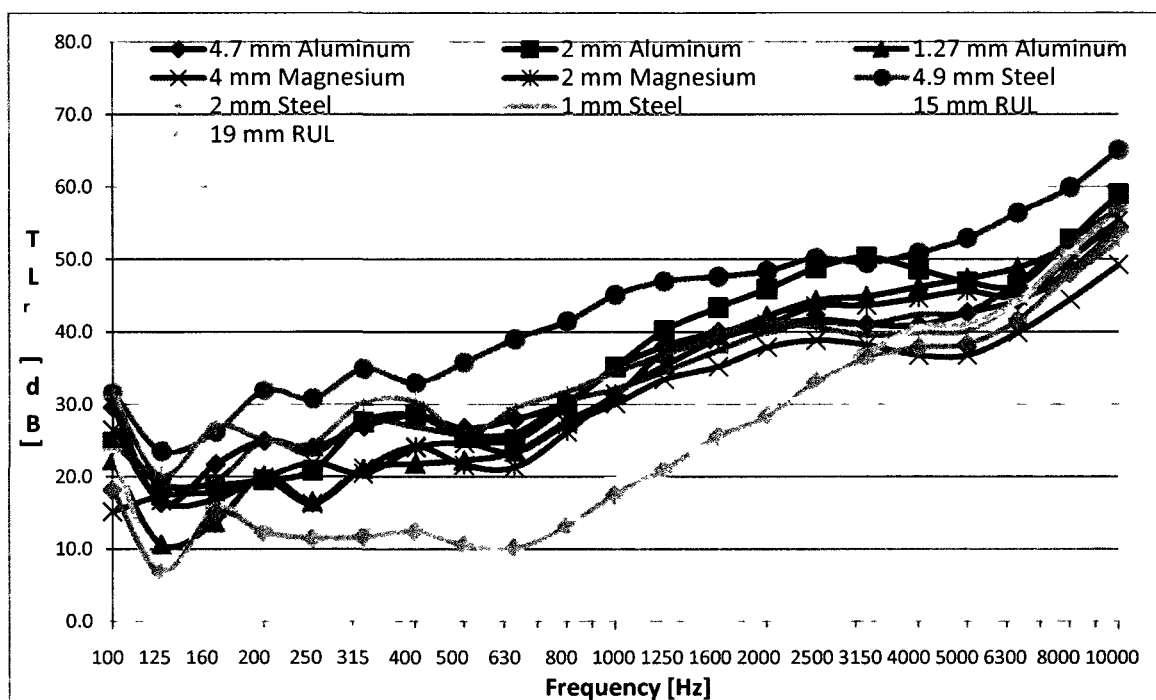
Figure 26: Periodic Random or Scattered White or Pseudorandom Noise TL_r Results of All Material 60cmX60cm Samples Alone, and the 15 mm and 19 mm Thick, 60cmX60cm Samples of RUL Automotive Underpad Alone from the Tests in Canton, Michigan

Figures 27, 28 and 29 provide evidence of AZ31B magnesium dash panel acceptance when subjected to a more subjective noise, specifically diesel generator noise. This results in a more 'real world' TL response of AZ31B magnesium dash panel samples in comparison to those of competing materials, for respective thickness comparisons. The worst case for magnesium occurs at 630 Hz for the 4 mm Magnesium firewall alone in comparison to the 4.9 mm Steel firewall. Specifically, the 4.9 mm Steel firewall has a TL_r of 42.0 dB, while the 4 mm Magnesium firewall has a TL_r of 25.5 dB. This gives a negative difference of 16.5 dB, in favour of the 4.9 mm Steel firewall. Otherwise, for all three types of dash panel samples tested, AZ31B magnesium performs in the same TL_r region, matches, and even exceeds the competing dash panel materials, for respective thickness comparisons.

Figure 27: Diesel Generator Noise TL$_r$ Results of All Material 60cmX60cm Samples with the 15 mm Thick, 60cmX60cm Sample of RUL Automotive Underpad from the Tests in Canton, Michigan

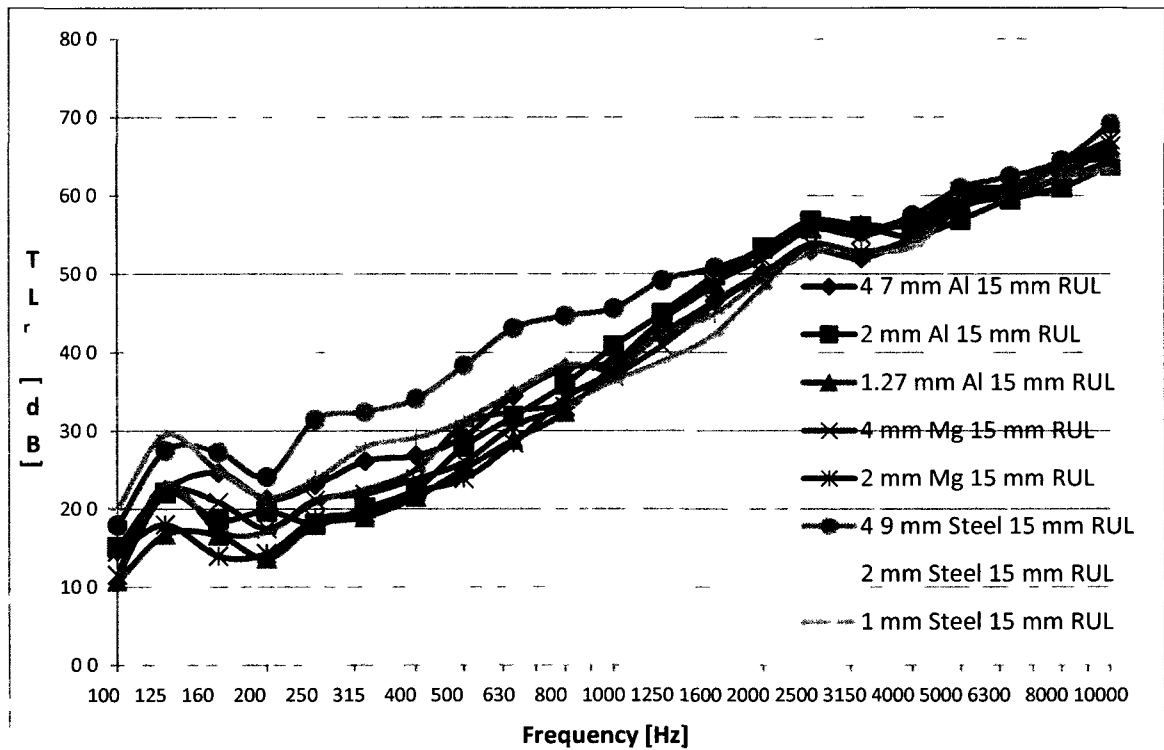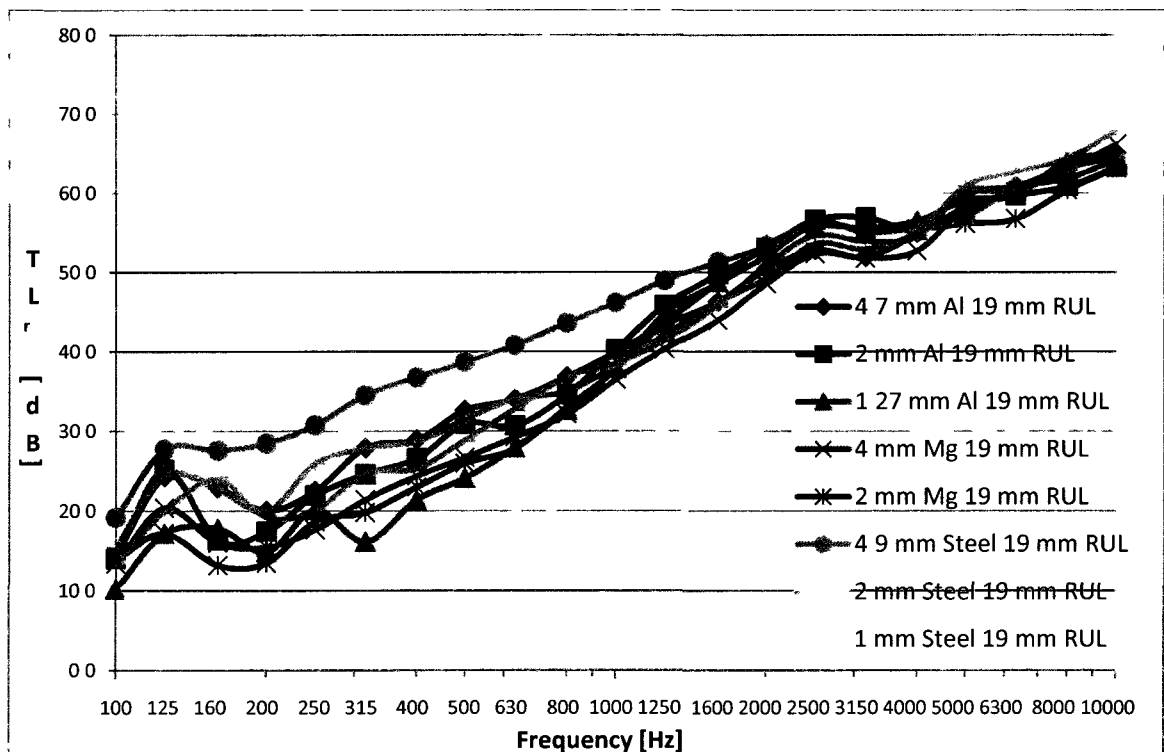**Figure 28: Diesel Generator Noise TL$_r$ Results of All Material 60cmX60cm Samples with the 19 mm Thick, 60cmX60cm Sample of RUL Automotive Underpad from the Tests in Canton, Michigan**

Figure 29: Diesel Generator Noise TL$_r$ Results of All Material 60cmX60cm Samples Alone, and the 15 mm and 19 mm Thick, 60cmX60cm Samples of RUL Automotive Underpad Alone from the Tests in Canton, Michigan

The Figures 30, 31 and 32 are proof that dash panels consisting of an AZ31B magnesium firewall are acceptable when subjected to electric motor noise. This is also a more subjective signal type, for a more 'real world' TL response of magnesium, aluminum and steel dash panel samples that exceeds the SAE J1400 Standard. For a good performance comparison, the worst TL$_r$ result for AZ31B magnesium occurs at 315 Hz. At this one-third octave bandwidth centre frequency, the 4 mm Magnesium dash panel firewall has a TL$_r$ of 17.8 dB, while the 4.9 mm Steel firewall material has a TL$_r$ of 35.7 dB. This gives a negative difference for AZ31B magnesium of 17.9 dB. Otherwise, for all three dash panel types, AZ31B magnesium performs in the same TL$_r$ region, matches, and even exceeds the TL$_r$ performance of competing dash panel materials, for respective thickness comparisons.

Figure 30: Electric Motor Noise TL_r Results of All Material 60cmX60cm Samples with the 15 mm Thick, 60cmX60cm Sample of RUL Automotive Underpad from the Tests in Canton, Michigan

Figure 31: Electric Motor Noise TL_r Results of All Material 60cmX60cm Samples with the 19 mm Thick, 60cmX60cm Sample of RUL Automotive Underpad from the Tests in Canton, Michigan
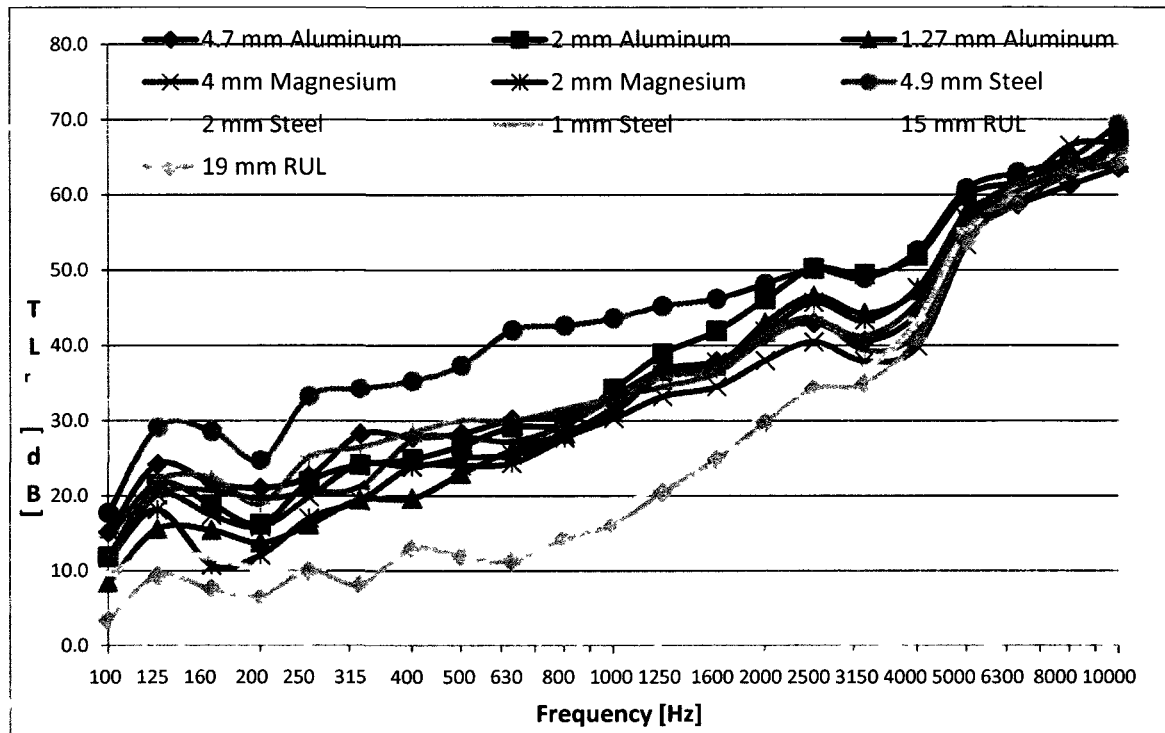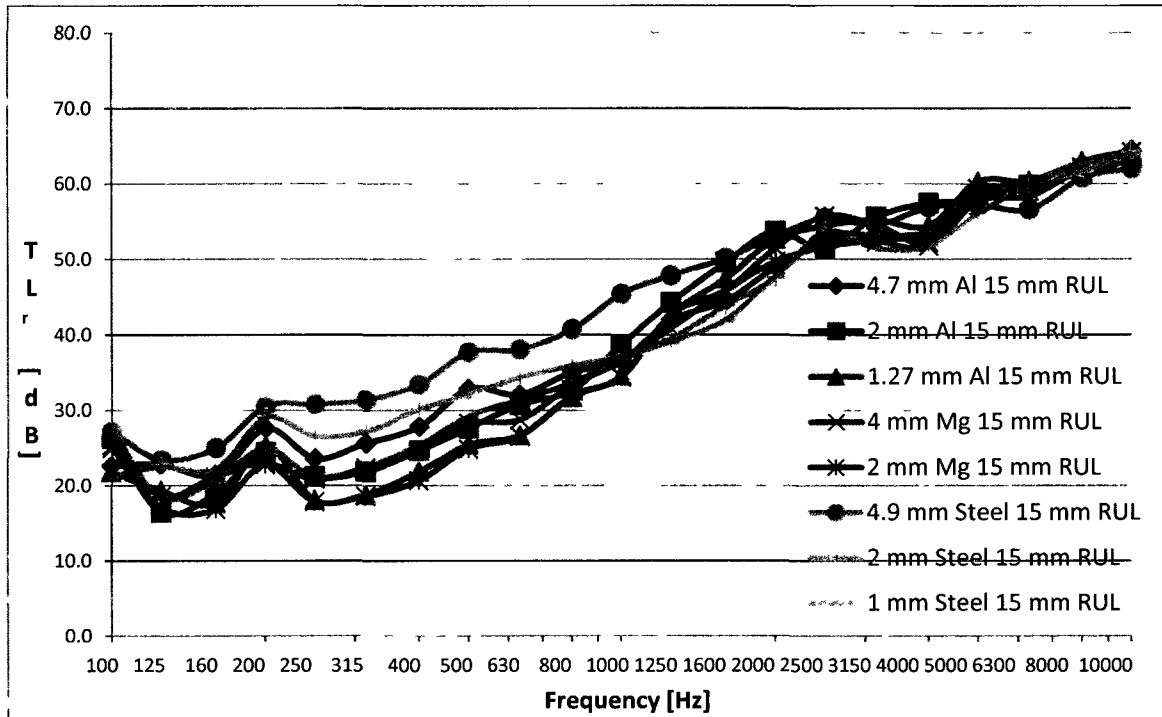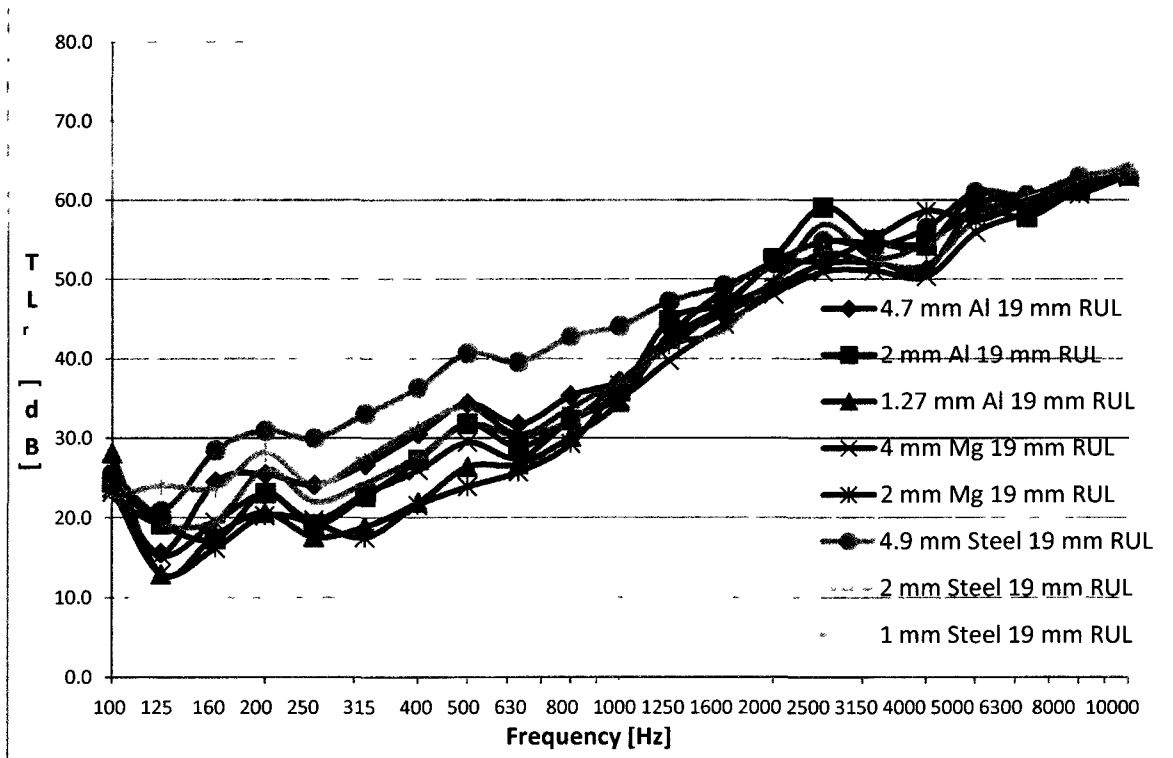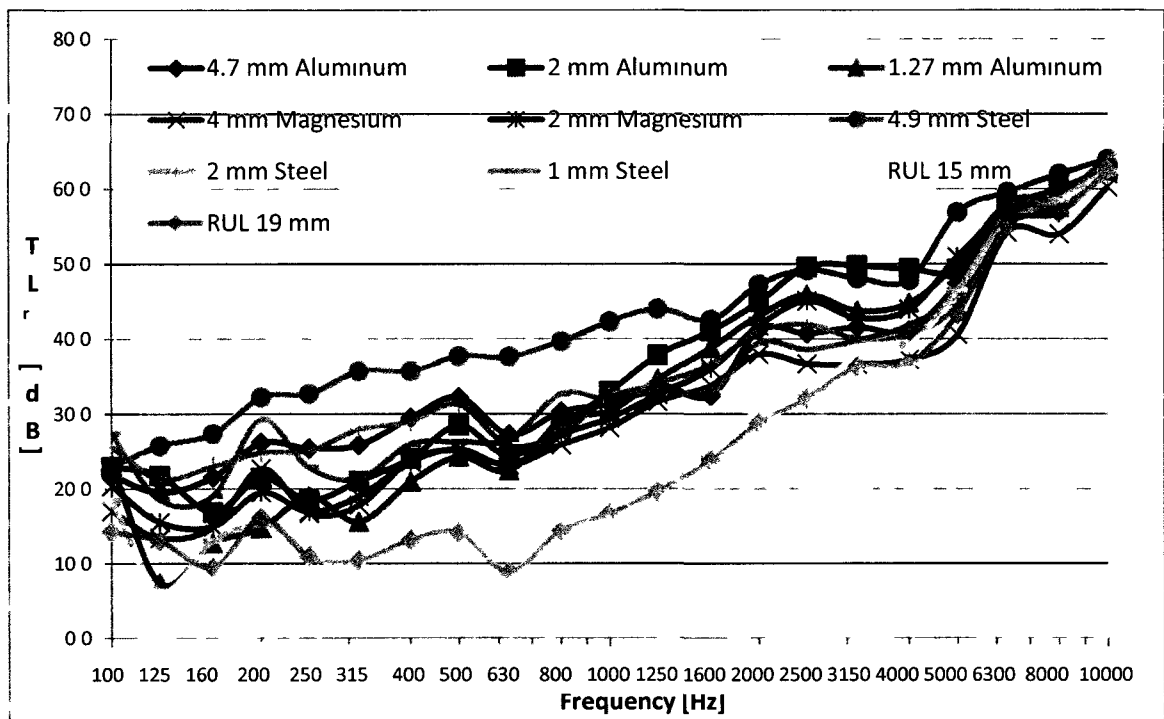
Figure 32: Electric Motor Noise TL$_r$ Results of All Material 60cmX60cm Samples Alone, and the 15 mm and 19 mm Thick, 60cmX60cm Samples of RUL Automotive Underpad Alone from the Tests in Canton, Michigan

5.7 Experimental Specific Loudness Results

The following figures show the averaged specific loudness from microphones 6 and 10, which were randomly chosen for the best results over the surface area, and positioned 20.3 cm above the samples in the semi-anechoic room. For evaluation purposes, these are compared to each other for each Bark band frequency closest to the one-third octave band centre frequencies of J1400 for TL$_r$ in Barks, and the lower values are superior. The graphs for the underpads alone are shown in the Appendix.

The specific loudness results are for four different signals: random or uniform white noise, periodic random or scattered white or pseudorandom noise, diesel generator noise, and electric motor noise, each with 10 seconds signal duration. Also, for referral to the source only, four figures in the Appendix show the averaged specific loudness for microphones 1 and 5, chosen for a more accurate response in the reverberation pit, as

compared to one microphone, for each signal. Note that the averaged specific loudness results for microphones 6 and 10 were for a free field sound field condition, while those for microphones 1 and 5 in the reverberation pit were for a diffuse field sound field condition. For these figures, Table 1 provides equivalent Bark band frequency values closest to the one-third octave bandwidth centre frequencies of J1400, converted to Barks for specific loudness evaluation.

Frequency [Hz]	Frequency [Barks]	Frequency [Hz]	Frequency [Barks]	Frequency [Hz]	Frequency [Barks]
99.7		632.6	6	4017	17.44
124.3	1.23	801.6	7.23	4989	18.69
161.8	1.63	996.8	8.5	6269	19.94
		1249	9.89	8079	21.23
					22.11
		2503			

Table 1: Equivalent Frequencies in Barks Closest to the One-third Octave Bandwidth Centre Frequencies of J1400 for Specific Loudness Evaluation

Unfortunately, for random or uniform white noise, Figures 33, 34, and 35, show that AZ31B magnesium performs poorly in comparison to competing dash panel materials, for respective thickness comparisons. The best case for AZ31B magnesium dash panel samples in this situation occurs at a Bark band frequency of 17.44 barks. Here, the 2 mm Magnesium automotive dash panel firewall material has an averaged specific loudness of 0.80 sones/bark, while the 2 mm Steel firewall has an averaged specific loudness of 1.14 sones/bark. This gives a difference in averaged specific loudness of 0.34 sones/bark, in favour of the 2 mm Magnesium. Otherwise, the AZ31B

magnesium dash panel samples perform poorly in comparison, since they have higher
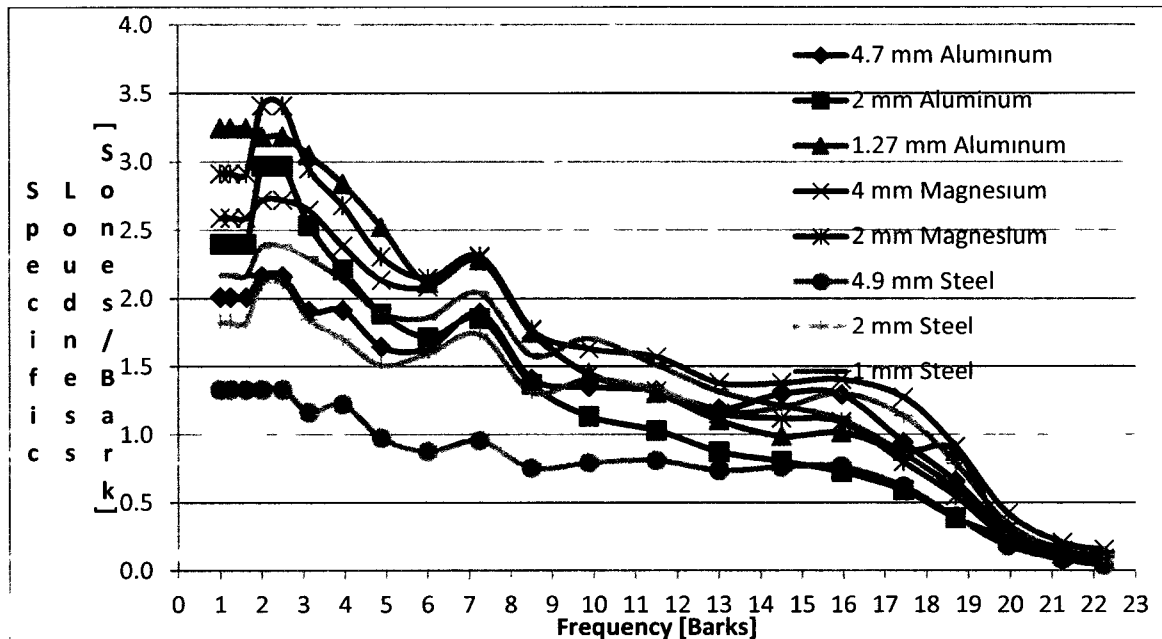
averaged specific loudness values.

Figure 33: Averaged Specific Loudness for a Free Field Sound Field Condition from Microphones 6 and 10 for the Eight Different Metal Thicknesses of AZ31B Magnesium, 6061-T6 Aluminum and 1018 Cold-Rolled Steel of 60cmX60cm Surface Area with Random or Uniform White Noise 10 Seconds Signal Duration

Figure 34: Averaged Specific Loudness for a Free Field Sound Field Condition from Microphones 6 and 10 for the Eight Different Metal Thicknesses of AZ31B Magnesium, 6061-T6 Aluminum and 1018 Cold-Rolled Steel with the 15 mm Thick, 60cmX60cm Sample of RUL Automotive Underpad with Random or Uniform White Noise 10 Seconds Signal Duration
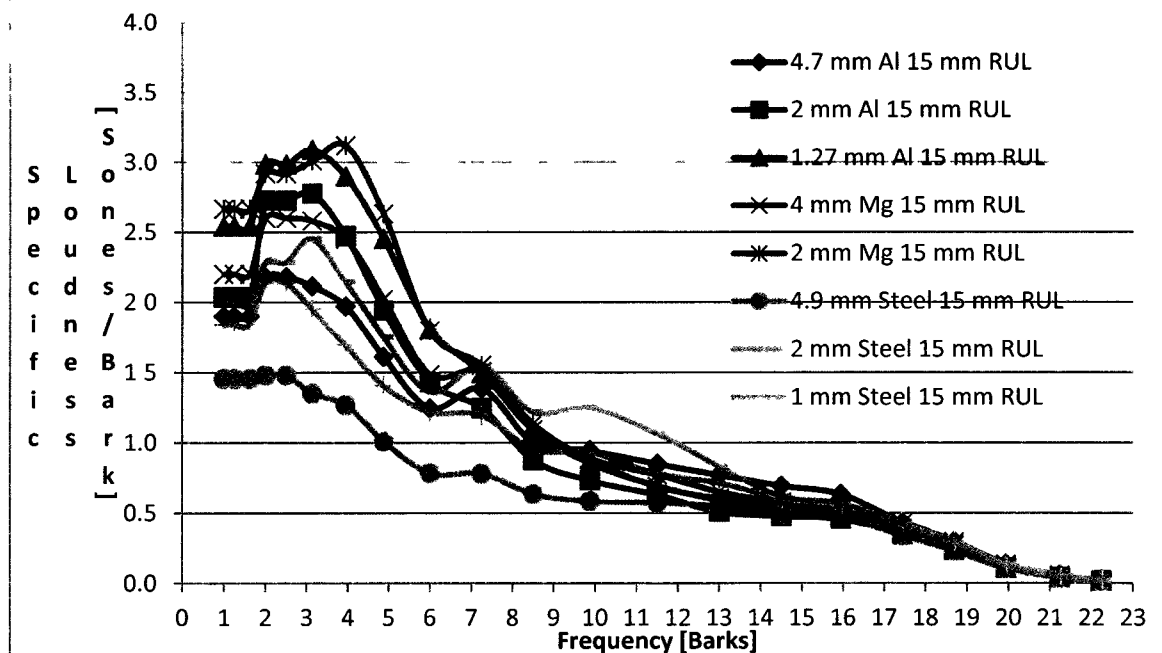
Figure 35: Averaged Specific Loudness for a Free Field Sound Field Condition from Microphones 6 and 10 for the Eight Different Metal Thicknesses of AZ31B Magnesium, 6061-T6 Aluminum and 1018 Cold-Rolled Steel with the 19 mm Thick, 60cmX60cm Sample of RUL Automotive Underpad with Random or Uniform White Noise 10 Seconds Signal Duration

In regards to Figures 36, 37, and 38, AZ31B magnesium performs poorly in comparison to competing dash panel firewall materials for periodic or scattered white or pseudorandom noise. The best case for AZ31B magnesium occurs at a Bark band frequency of 9.88 barks. At this frequency, the 2 mm Mg 15 mm RUL dash panel sample has an averaged specific loudness of 0.88 sones/bark, while the 1 mm Steel 15 mm RUL dash panel sample has an averaged specific loudness of 1.25 sones/bark. This gives a difference of 0.37 sones/bark in favour of the 2 mm Mg 15 mm RUL. Otherwise, the three types of AZ31B magnesium dash panel samples perform relatively poorly.
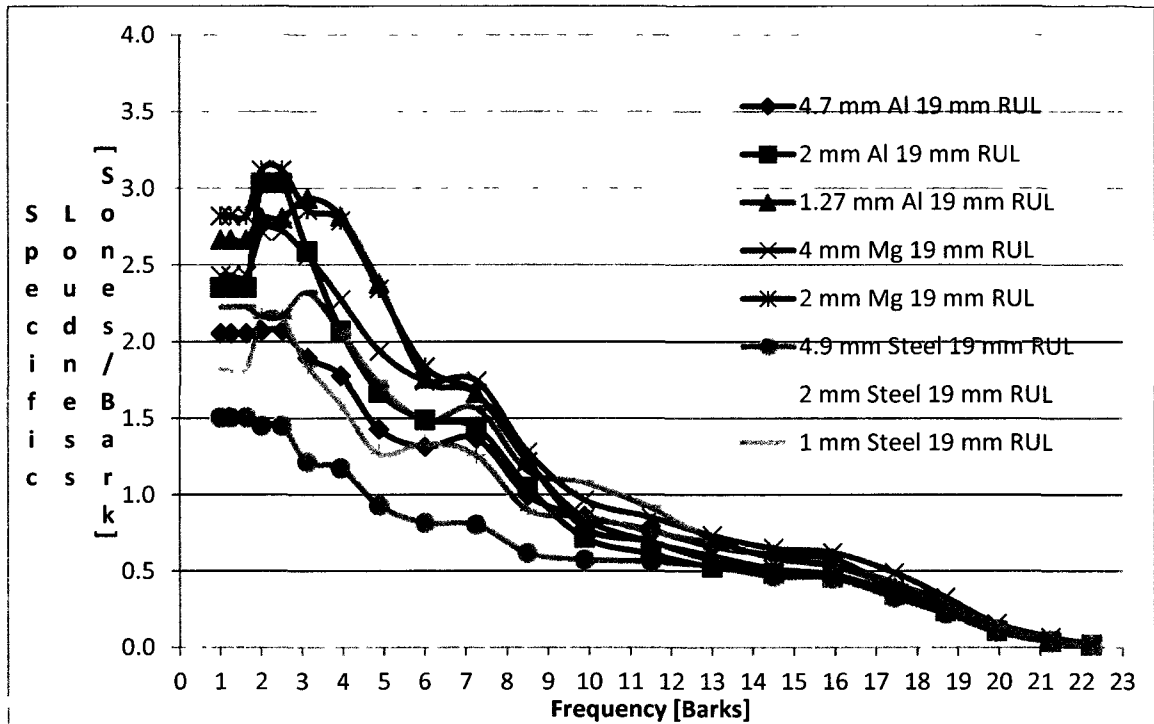

Figure 36: Averaged Specific Loudness for a Free Field Sound Field Condition from Microphones 6 and 10 for the Eight Different Metal Thicknesses of AZ31B Magnesium, 6061-T6 Aluminum and 1018 Cold-Rolled Steel of 60cmX60cm Surface Area with Periodic Random or Scattered White or Pseudorandom Noise 10 Seconds Signal Duration

Figure 37: Averaged Specific Loudness for a Free Field Sound Field Condition from Microphones 6 and 10 for the Eight Different Metal Thicknesses of AZ31B Magnesium, 6061-T6 Aluminum and 1018 Cold-Rolled Steel with the 15 mm Thick, 60cmX60cm Sample of RUL Automotive Underpad with Periodic Random or Scattered White or Pseudorandom Noise 10 Seconds Signal Duration
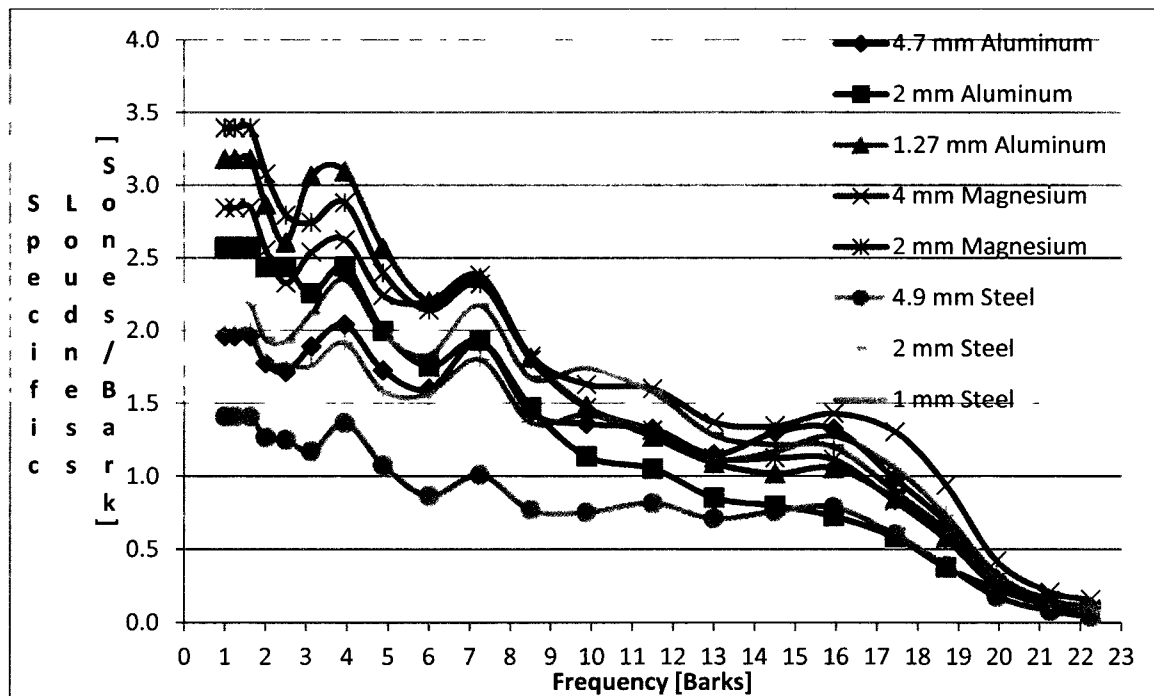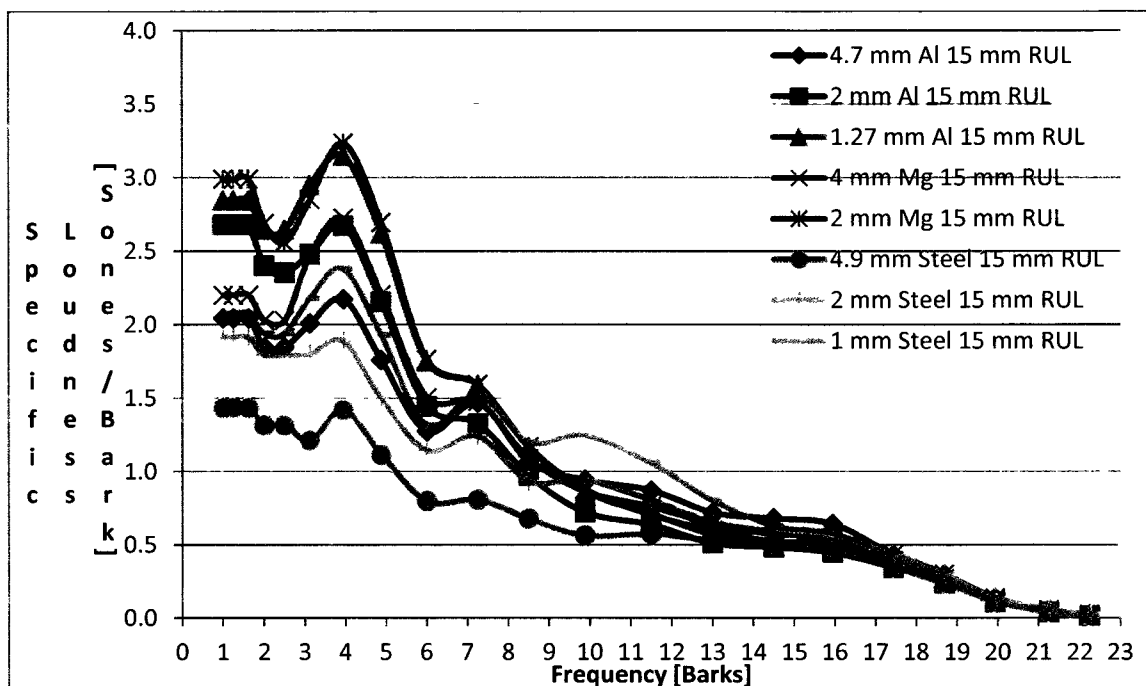

Figure 38: Averaged Specific Loudness for a Free Field Sound Field Condition from Microphones 6 and 10 for the Eight Different Metal Thicknesses of AZ31B Magnesium, 6061-T6 Aluminum and 1018 Cold-Rolled Steel with the 19 mm Thick, 60cmX60cm Sample of RUL Automotive Underpad with Periodic Random or Scattered White or Pseudorandom Noise 10 Seconds Signal Duration

Figures 39, 40, and 41, show that AZ31B magnesium performs poorly in comparison to 6061-T6 aluminum, and 1018 cold-rolled steel dash panel samples. This is for a more subjective signal of diesel generator noise, for the specific loudness evaluation of a more 'real world' signal. The most favourable comparison for AZ31B magnesium occurs at a Bark band frequency of 11.5 barks. At this frequency, the averaged specific loudness for 2 mm Mg 15 mm RUL is 0.31 sones/bark, while the averaged specific loudness for 1 mm Steel 15 mm RUL is 0.49 sones/bark. This gives a difference of 0.18 sones/bark in favour of the 2 mm Mg 15 mm RUL. Otherwise, the AZ31B magnesium dash panel samples perform relatively poorly, for respective thickness comparisons.
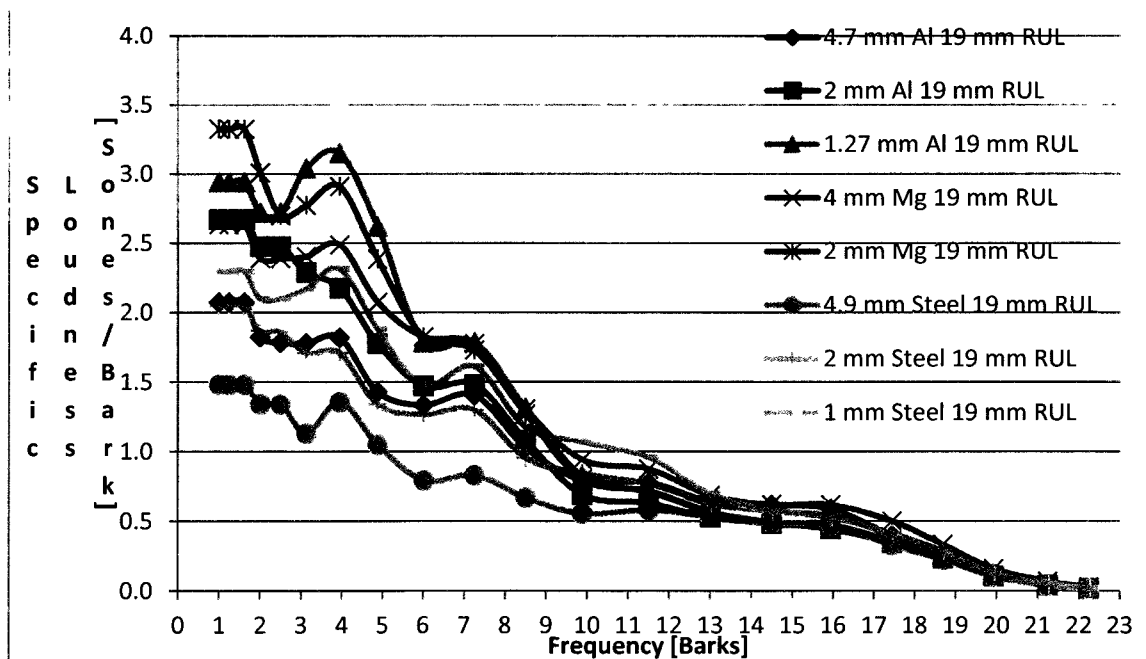

Figure 39: Averaged Specific Loudness for a Free Field Sound Field Condition from Microphones 6 and 10 for the Eight Different Metal Thicknesses of AZ31B Magnesium, 6061-T6 Aluminum and 1018 Cold-Rolled Steel of 60cmX60cm Surface Area with Diesel Generator Noise 10 Seconds Signal Duration

Figure 40: Averaged Specific Loudness for a Free Field Sound Field Condition from Microphones 6 and 10 for the Eight Different Metal Thicknesses of AZ31B Magnesium, 6061-T6 Aluminum and 1018 Cold-Rolled Steel with the 15 mm Thick, 60cmX60cm Sample of RUL Automotive Underpad with Diesel Generator Noise 10 Seconds Signal Duration
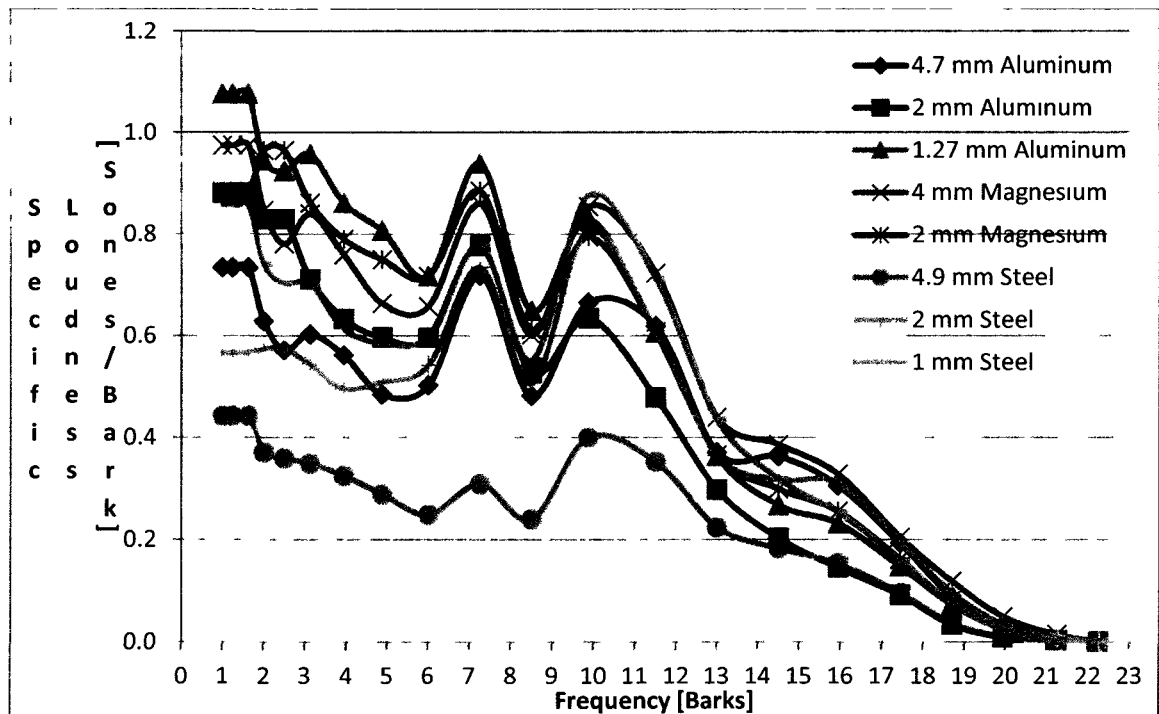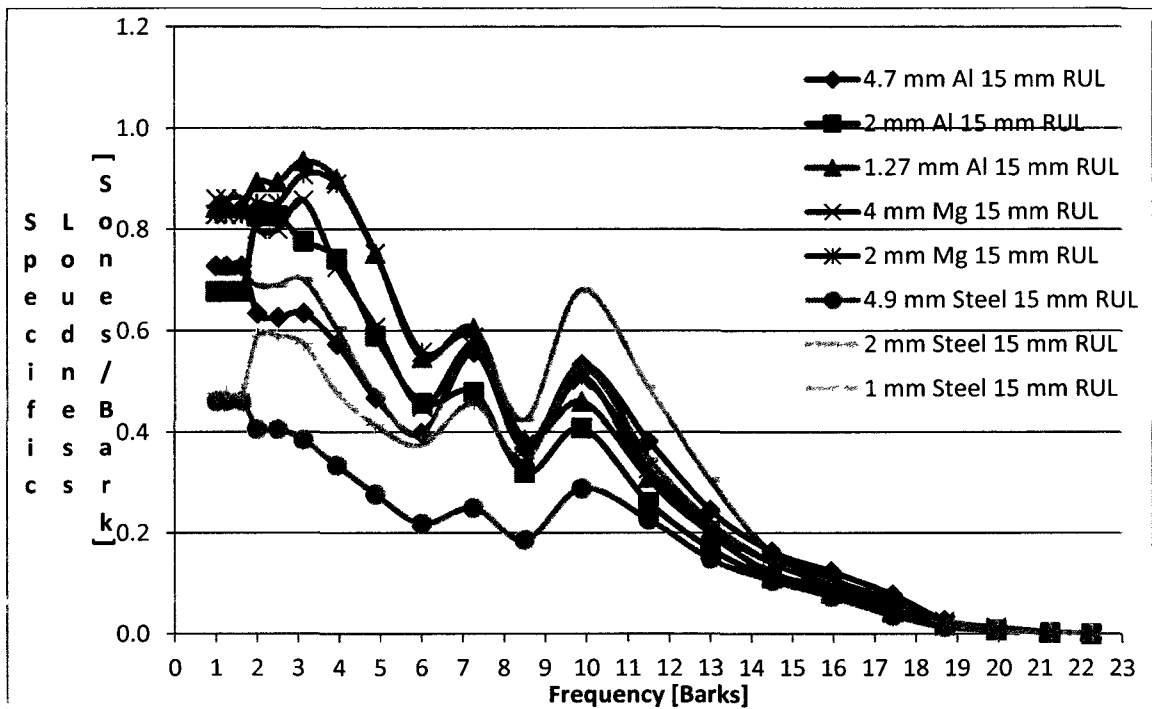

Figure 41: Averaged Specific Loudness for a Free Field Sound Field Condition from Microphones 6 and 10 for the Eight Different Metal Thicknesses of AZ31B Magnesium, 6061-T6 Aluminum and 1018 Cold-Rolled Steel with the 19 mm Thick, 60cmX60cm Sample of RUL Automotive Underpad with Diesel Generator Noise 10 Seconds Signal Duration

For averaged specific loudness with another subjective signal of electric motor

noise, Figures 42, 43, and 44, show that the AZ31B magnesium dash panel firewall

performs poorly in comparison. The best supportive argument for AZ31B magnesium

occurs at a Bark band frequency of 3.13 barks. Here, the averaged specific loudness for

the 2 mm Magnesium dash panel firewall material is 2.06 sones/bark, while that for the

1.27 mm Aluminum is 2.73 sones/bark. This gives a difference of 0.67 sones/bark in

favour of the 2 mm Magnesium dash panel firewall material. Also, the 2 mm Magnesium

performs well in comparison to the 1.27 mm Aluminum. Otherwise, the AZ31B

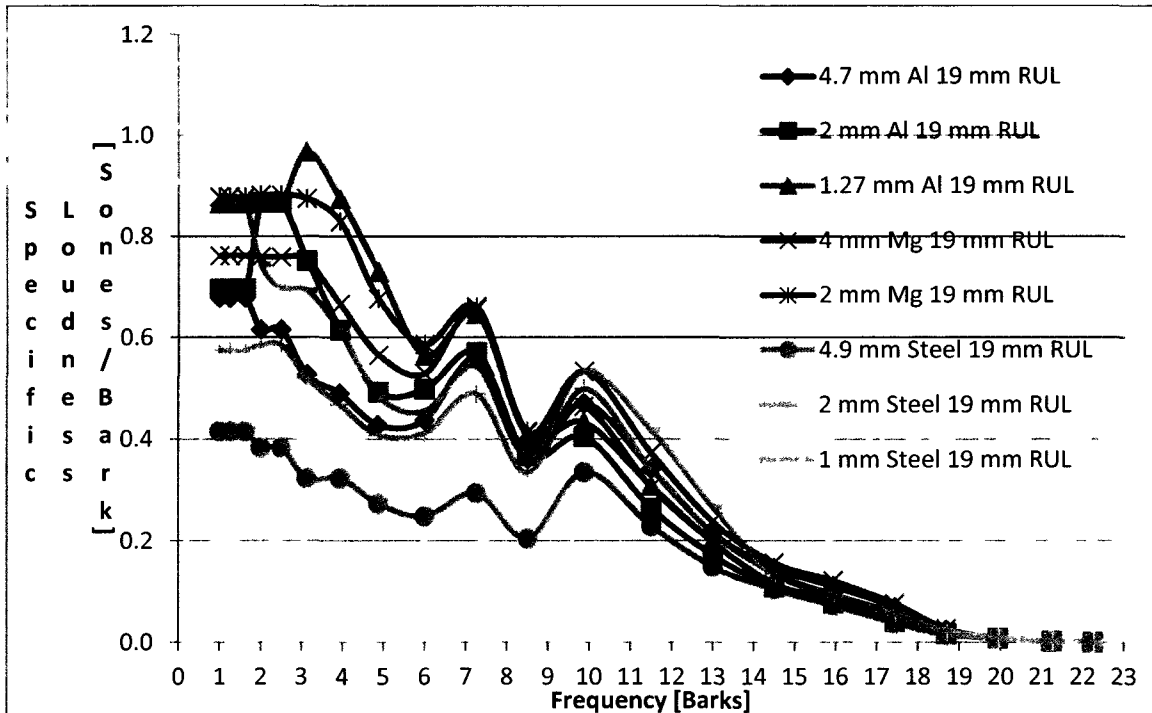magnesium dash panel samples perform relatively poorly.

Figure 42: Averaged Specific Loudness for a Free Field Sound Field Condition from Microphones 6 and 10 for the Eight Different Metal Thicknesses of AZ31B Magnesium, 6061-T6 Aluminum and 1018 Cold-Rolled Steel of 60cmX60cm Surface Area with Electric Motor Noise 10 Seconds Signal Duration

Figure 43: Averaged Specific Loudness for a Free Field Sound Field Condition from Microphones 6 and 10 for the Eight Different Metal Thicknesses of AZ31B Magnesium, 6061-T6 Aluminum and 1018 Cold-Rolled Steel with the 15 mm Thick, 60cmX60cm Sample of RUL Automotive Underpad with Electric Motor Noise 10 Seconds Signal Duration
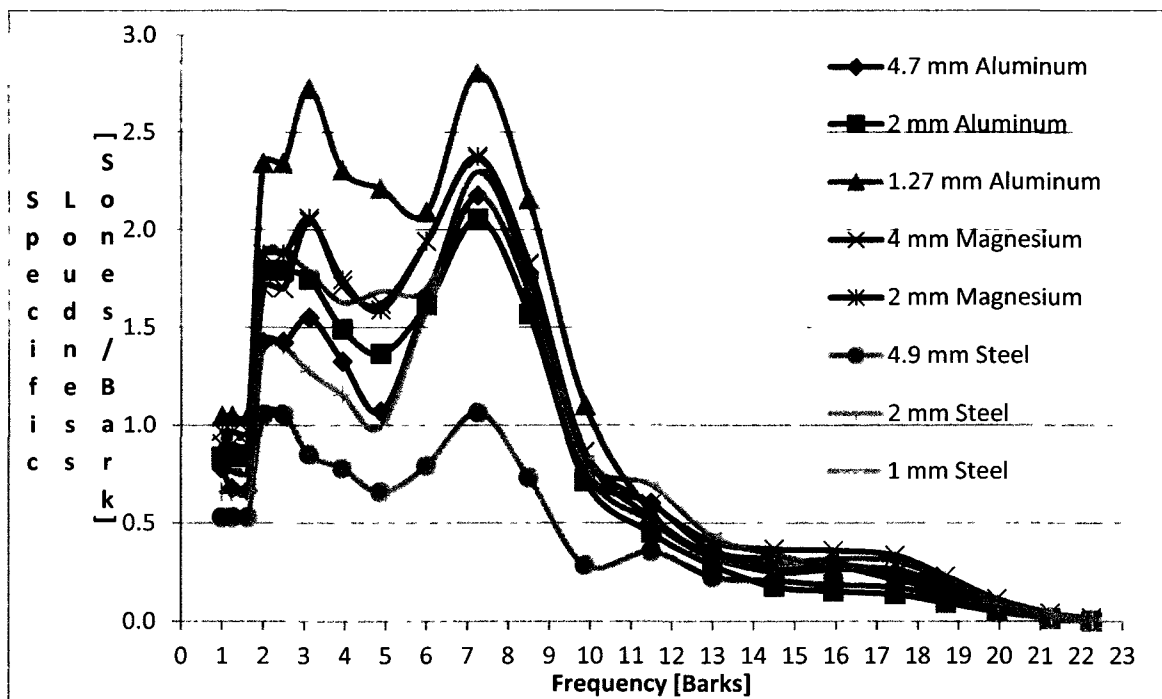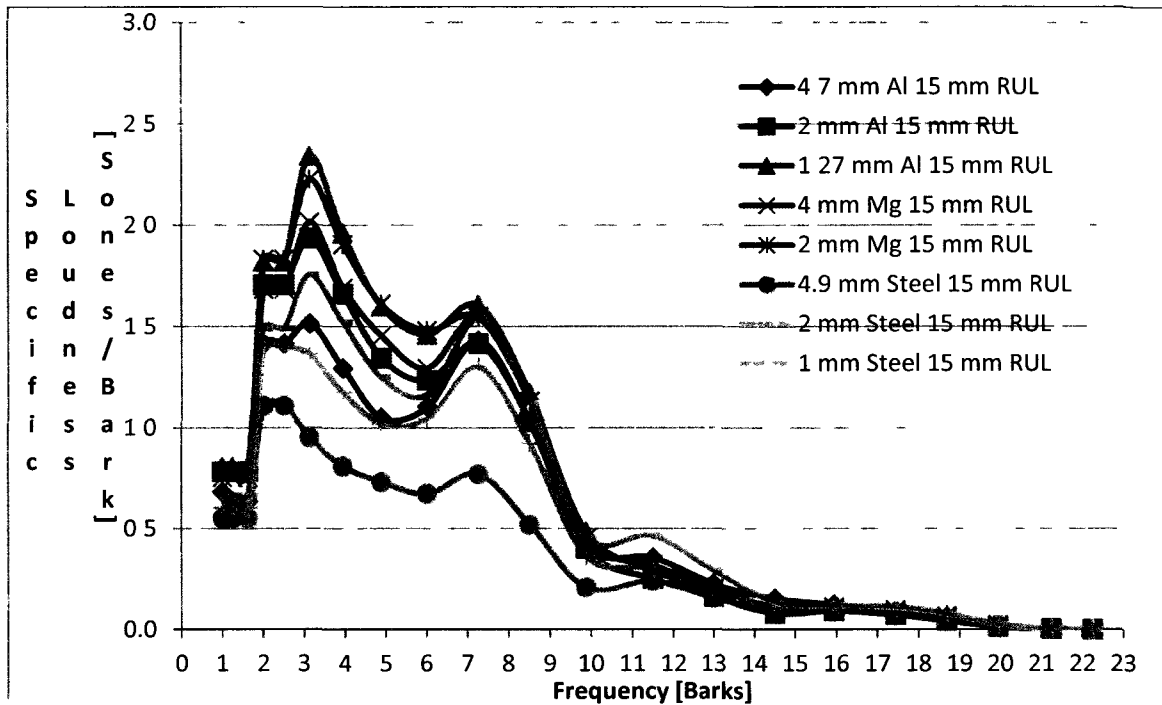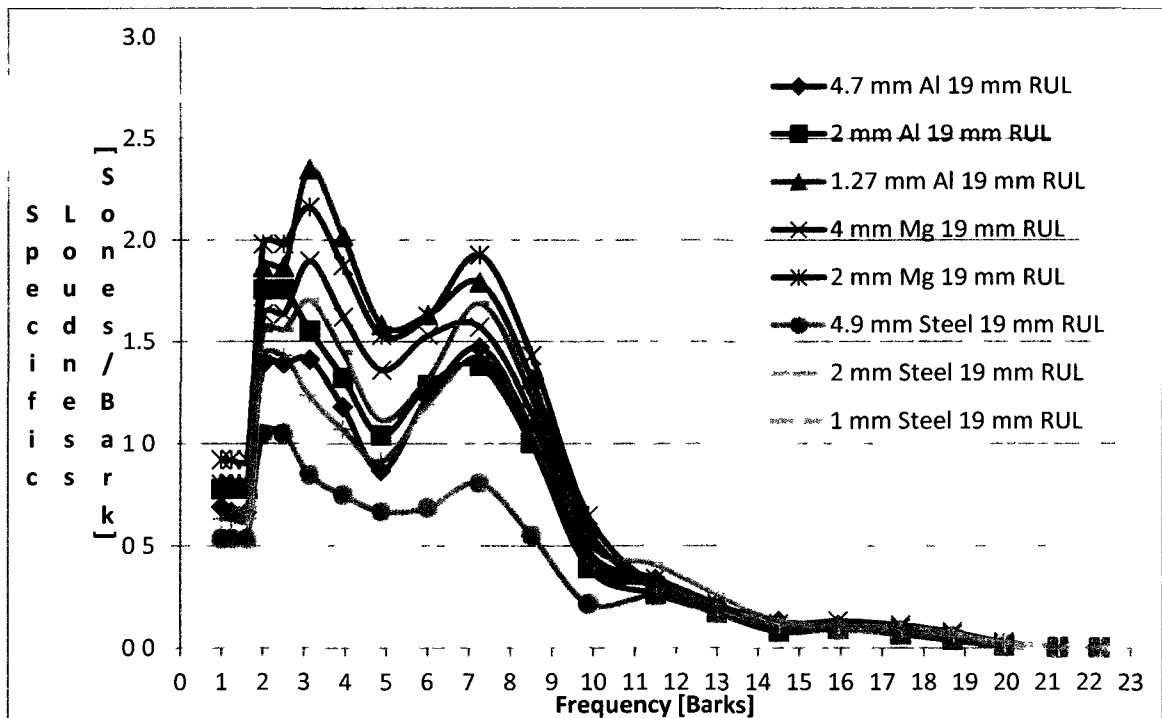

Figure 44: Averaged Specific Loudness for a Free Field Sound Field Condition from Microphones 6 and 10 for the Eight Different Metal Thicknesses of AZ31B Magnesium, 6061-T6 Aluminum and 1018 Cold-Rolled Steel with the 19 mm Thick, 60cmX60cm Sample of RUL Automotive Underpad with Electric Motor Noise 10 Seconds Signal Duration

5.8 Experimental Total Loudness Results

The following tables show the time-averaged total loudnesses from microphones 6 and 10, from 0.2 s to 1.18 s, originally with a 20 ms resolution with very small deviations from value to value. The tables for the underpads are shown in the Appendix. As well, the time-averaged total loudness values from microphones 1 and 5 are shown in the Appendix for references to the source. Note, there is one table and that the results for the total loudness from microphones 6 and 10 were for a free field sound field condition, while those for microphones 1 and 5 were for a diffuse field sound field condition in the reverberation pit for all further related discussion.

Unfortunately, for random or uniform white noise, Tables 2, 3 and 4 show that AZ31B magnesium performs poorly in comparison to competing dash panel materials, for respective thickness comparisons. The best case for AZ31B magnesium dash panel samples in this situation occurs for the 2 mm Magnesium automotive dash panel firewall. This sample has an averaged total loudness of 32.95 sones, while the 1.27 mm Aluminum firewall has an averaged total loudness of 33.6 sones. This gives a difference in averaged total loudness of 0.65 sones, in favour of the 2 mm Magnesium. Otherwise, the AZ31B magnesium dash panel samples perform poorly in comparison, since they have higher averaged total loudness values.

In regards to Tables 2, 3 and 4, AZ31B magnesium performs poorly in comparison to competing dash panel firewall materials for periodic or scattered white or pseudorandom noise. The best case for AZ31B magnesium occurs for the 2 mm Mg 19 mm RUL dash panel sample. The 2 mm Mg 19 mm RUL dash panel sample has an averaged total loudness of 25.25 sones, while the 1.27 mm Al 19 mm RUL dash panel

sample has an averaged total loudness of 25.45 sones. This gives a difference of 0.2 sones in favour of the 2 mm Mg 19 mm RUL. Otherwise, the three types of AZ31B magnesium dash panel samples perform relatively poorly.

Tables 2, 3 and 4, show that AZ31B magnesium performs poorly in comparison to 6061-T6 aluminum, and 1018 cold-rolled steel dash panel samples. This is for a more subjective signal of diesel generator noise, for the averaged total loudness evaluation of a more 'real world' signal. The best case for AZ31B magnesium occurs for the 2 mm Magnesium firewall sample. This has an averaged total loudness value of 10.75 sones, while the 1.27 mm Aluminum firewall sample has an averaged total loudness value of 11.35 sones. This gives a difference of 0.6 sones in favour of the 2 mm Magnesium. Otherwise, the three types of AZ31B magnesium dash panel samples perform relatively poorly.

For averaged total loudness with another subjective signal of electric motor noise, Tables 2, 3, and 4, show that the AZ31B magnesium dash panel samples perform poorly in comparison. The best supportive argument for AZ31B magnesium occurs for the 2 mm Magnesium dash panel firewall sample. This has an averaged total loudness of 19.2 sones, while that for the 1.27 mm Aluminum is 22.6 sones. This gives a difference of 3.4 sones in favour of the 2 mm Magnesium dash panel firewall material. Another supportive argument is for the 2 mm Mg 19 mm RUL dash panel sample. This has an averaged total loudness of 16.0 sones, while that for the 1.27 mm Al 19 mm RUL dash panel sample is 16.3 sones. This gives a difference of 0.3 sones in favour of the 2 mm Mg 19 mm RUL dash panel sample. Otherwise, the AZ31B magnesium dash panel samples perform relatively poorly.

SIGNAL TYPE	METAL & THICKNESS							
	4 mm Mg	2 mm Mg	4.7 mm Al	2 mm Al	1.27 mm Al	4.9 mm Steel	2 mm Steel	1 mm Steel
Random	34.9	32.95	27.75	26.8	33.6	16.6	27.4	30.1
Periodic Random	35.0	33.3	27.9	26.65	32.9	16.6	27.25	29.85
Diesel Generator	11.35	10.75	9.01	8.96	11.35	4.99	8.82	10.25
Electric Motor	19.4	19.2	16.75	16.25	22.6	9.16	15.85	19.05

Table 2: Averaged Total Loudness in Sones for a Free Field Sound Field Condition from Microphones 6 and 10 in the Time Domain from 0.2 s to 1.18 s, representing each Second in the 10-Second Long Signals of Random or Uniform White Noise, Periodic Random or Scattered White or Pseudorandom Noise, Diesel Generator Noise, and Electric Motor Noise for the Eight Metal Thicknesses of AZ31B Magnesium, 6061-T6 Aluminum and 1018 Cold-Rolled Steel of 60cmX60cm Surface Area

SIGNAL TYPE	LAYERS & THICKNESSES							
	4 mm Mg	2 mm Mg	4.7 mm Al	2 mm Al 15 mm RUL	1.27 mm Al 15 mm RUL	4.9 mm Steel 15 mm RUL	2 mm Steel 15 mm RUL	1 mm Steel 15 mm RUL
Random	52.0	28.45	21.3	24.08	24.65	14.0	13.6	23.??
Periodic Random	?7.?	28.?	21.0	?1.?	?4.0	1?.?	1?.25	22.8
Diesel Generator	?.0?	8.05	?.0?	?.??	?.??	?.?	?.0?	?.??
Electric Motor	13.75	15.0	12.35	13.4	15.25	7.84	11.0	13.4

Table 3: Averaged Total Loudness in Sones for a Free Field Sound Field Condition from Microphones 6 and 10 in the Time Domain from 0.2 s to 1.18 s, representing each Second in the 10-Second Long Signals of Random or Uniform White Noise, Periodic Random or Scattered White or Pseudorandom Noise, Diesel Generator Noise, and Electric Motor Noise for the Eight Metal Thicknesses of AZ31B Magnesium, 6061-T6 Aluminum and 1018 Cold-Rolled Steel with the 15 mm Thick, 60cmX60cm Sample of RUL Automotive Underpad Dash Panel Samples

SIGNAL TYPE	LAYERS & THICKNESSES							
	4 mm Mg 19 mm RUL	2 mm Mg 19 mm RUL	4.7 mm Al 19 mm RUL	2 mm Al 19 mm RUL	1.27 mm Al 19 mm RUL	4.9 mm Steel 19 mm RUL	2 mm Steel 19 mm RUL	1 mm Steel 19 mm RUL
Random	24.75	25.1	20.05	21.35	24.7	13.85	19.2	22.3
Periodic Random	24.55	25.25	19.35	21.1	25.45	13.75	18.75	22.2
Diesel Generator	7.8	8.13	6.57	6.88	7.99	4.12	6.14	7.32
Electric Motor	14.45	16.0	11.9	12.45	16.3	7.57	11.5	13.7

Table 4: Averaged Total Loudness in Sones for a Free Field Sound Field Condition from Microphones 6 and 10 in the Time Domain from 0.2 s to 1.18 s, representing each Second in the 10-Second Long Signals of Random or Uniform White Noise, Periodic Random or Scattered White or Pseudorandom Noise, Diesel Generator Noise, and Electric Motor Noise for the Eight Metal Thicknesses of AZ31B Magnesium, 6061-T6 Aluminum and 1018 Cold-Rolled Steel with the 19 mm Thick, 60cmX60cm Sample of RUL Automotive Underpad Dash Panel Samples

5.9 Experimental Sharpness Results

The following tables show the time-averaged sharpness from microphones 6 and 10, from 0.2 s to 1.18 s, originally with a 20 ms resolution with very small deviations from value to value. The tables for the underpads alone are shown in the Appendix. As well, the time-averaged sharpness from microphones 1 and 5 are shown in the Appendix for references to the source.

Tables 5, 6, and 7, show that AZ31B magnesium dash panel samples perform relatively well for random or uniform white noise. The worst case occurs with 2 mm Mg in comparison to 2 mm Al. For this case, the 2 mm Mg has an averaged sharpness value of 1.04 acum, while the 2 mm Al has an averaged sharpness value of 1.00 acum. This gives a difference of 0.04 acum against the 2 mm Mg. Otherwise, the AZ31B magnesium dash panel samples perform well in comparison.

For the case of periodic random or scattered white or pseudorandom noise, Tables 5, 6, and 7, give evidence that AZ31B magnesium dash panel samples perform well in

comparison, for respective thicknesses. The worst case for AZ31B magnesium occurs with 4.9 mm Steel, for the 4 mm Mg dash panel firewall sample. Here, the 4 mm Mg has an averaged sharpness value of 1.23 acum, while the 4.9 mm Steel has an averaged sharpness value of 1.18 acum. This gives a difference of 0.05 acum against the 4 mm Mg. Otherwise, AZ31B magnesium dash panel samples perform well in comparison, for respective thicknesses.

When averaged sharpness is evaluated for diesel generator noise, Tables 5, 6, and 7, show that AZ31B magnesium dash panel samples perform relatively well, for respective thickness comparisons. The worst case for AZ31B magnesium occurs for 2 mm Mg in comparison to 2 mm Al. For this case, the 2 mm Mg has an averaged sharpness value of 0.90 acum, while the 2 mm Al has an averaged sharpness value of 0.81 acum. This gives a difference of 0.09 acum against the 2 mm Mg. Otherwise, the AZ31B magnesium dash panel samples perform well in comparison, for respective thicknesses.

In regards to electric motor noise for averaged sharpness evaluation, Tables 5, 6, and 7, show that AZ31B magnesium dash panels perform well in comparison to the competitors, for respective thicknesses. The worst case for AZ31B magnesium occurs with 2 mm Mg in comparison to 2 mm Al. For this case, the 2 mm Mg has an averaged sharpness value of 0.82 acum, while the 2 mm Al has an averaged sharpness value of 0.78 acum. This gives a difference of 0.04 acum against the 2 mm Mg. Otherwise, the AZ31B magnesium dash panel samples perform relatively well, for respective thickness comparisons.

SIGNAL TYPE	METAL & THICKNESS							
	4 mm Mg	2 mm Mg	4.7 mm Al	2 mm Al	1.27 mm Al	4.9 mm Steel	2 mm Steel	1 mm Steel
Random	1.22	1.04	1.21	1.00	1.03	1.19	1.27	1.14
Periodic Random	1.23	1.05	1.23	1.01	1.05	1.18	1.27	1.16
Diesel Generator	0.96	0.90	1.00	0.81	0.86	0.96	1.05	0.94
Electric Motor	0.92	0.82	0.90	0.78	0.81	0.89	0.96	0.88

Table 5: Averaged Sharpness in Acum from Microphones 6 and 10 in the Time Domain from 0.2 s to 1.18 s, representing each Second in the 10-Second Long Signals of Random or Uniform White Noise, Periodic Random or Scattered White or Pseudorandom Noise, Diesel Generator Noise, and Electric Motor Noise for the Eight Metal Thicknesses of AZ31B Magnesium, 6061-T6 Aluminum and 1018 Cold-Rolled Steel of 60cmX60cm Surface Area

SIGNAL TYPE	LAYERS & THICKNESSES							
	4 mm Mg 15 mm RUL	2 mm Mg 15 mm RUL	4.7 mm Al 15 mm RUL	2 mm Al 15 mm RUL	1.27 mm Al 15 mm RUL	4.9 mm Steel 15 mm RUL	2 mm Steel 15 mm RUL	1 mm Steel 15 mm RUL
Random	0.88	0.82	0.91	0.88	0.81	1.04	0.90	0.91
Periodic Random	0.90	0.83	0.92	0.89	0.87	1.00	0.93	0.94
Diesel Generator	0.78	0.74	0.80	0.72	0.76	0.87	0.84	0.82
Electric Motor								

Table 6: Averaged Sharpness in Acum from Microphones 6 and 10 in the Time Domain from 0.2 s to 1.18 s, representing each Second in the 10-Second Long Signals of Random or Uniform White Noise, Periodic Random or Scattered White or Pseudorandom Noise, Diesel Generator Noise, and Electric Motor Noise for the Eight Metal Thicknesses of AZ31B Magnesium, 6061-T6 Aluminum and 1018 Cold-Rolled Steel with the 15 mm Thick, 60cmX60cm Sample of RUL Automotive Underpad Dash Panel Samples

SIGNAL TYPE	LAYERS & THICKNESSES							
	4 mm Mg 19 mm RUL	2 mm Mg 19 mm RUL	4.7 mm Al 19 mm RUL	2 mm Al 19 mm RUL	1.27 mm Al 19 mm RUL	4.9 mm Steel 19 mm RUL	2 mm Steel 19 mm RUL	1 mm Steel 19 mm RUL
Random	0.90	0.81	0.93	0.82	0.81	0.97	0.96	0.91
Periodic Random	0.92	0.80	0.94	0.83	0.80	0.99	0.97	0.92
Diesel Generator	0.80	0.73	0.81	0.73	0.72	0.84	0.84	0.79
Electric Motor	0.73	0.70	0.74	0.69	0.70	0.76	0.77	0.75

Table 7: Averaged Sharpness in Acum from Microphones 6 and 10 in the Time Domain from 0.2 s to 1.18 s, representing each Second in the 10-Second Long Signals of Random or Uniform White Noise, Periodic Random or Scattered White or Pseudorandom Noise, Diesel Generator Noise, and Electric Motor Noise for the Eight Metal Thicknesses of AZ31B Magnesium, 6061-T6 Aluminum and 1018 Cold-Rolled Steel with the 19 mm Thick, 60cmX60cm Sample of RUL Automotive Underpad Dash Panel Samples

In summary, a thorough analysis of the absorption coefficients of the RUL automotive underpad, and the TL_n, TL_r, specific loudness, total loudness, and sharpness results for AZ31B magnesium dash panel samples in comparison to those of the 1018 cold-rolled steel and 6061-T6 aluminum dash panel samples has been undertaken. The results for the J1400 TL_r test were presented with uniform white or random noise. They were also presented for periodic random or scattered white or pseudorandom noise, diesel generator noise, and electric motor noise, for a more 'real world' TL_r response that goes beyond the J1400 standard. The results for specific loudness, total loudness and sharpness were also presented for all four signals.

Chapter 6: CONCLUSIONS AND RECOMMENDATIONS

6.1 Conclusions

Upon reviewing the results of this study, the following are conclusions that have been reached.

1. AZ31B magnesium, based on its density, has the highest strength-to-weight ratio when compared to 6061-T6 aluminum and 1018 cold-rolled steel. It also has the best manufacturability, since it has superior specific strength, as noted in the literature survey. Knowing these important general properties, the NVH performance of AZ31B magnesium dash panels can be evaluated.

2. Comparing the TL_n results to the TL_r results for respective circular and square dash panel samples, it is evident that the TL_r results are much higher than the impedance tube TL_n results. This is due to many reasons as discussed in Chapter 5, including the impedance tube method utilising many theoretical transfer function equations for ratios of complex sound pressures found at microphones 2, 3, and 4 to the complex sound pressure detected at microphone 1, instead of evaluating the SPL for each separate microphone. The conclusion reached is that the impedance tube method is an unrealistic TL measurement approach. This is because it attempts to approximate the SPL data from the reverberation pit in the incident side of the two-layered test samples, and the SPL data from the semi-anechoic room on the transmitted side of the test samples, in the impedance tube.

3. In terms of specific and total loudness, the results proved that, in general, AZ31B magnesium performed poorly in comparison to 1018 cold-rolled steel and 6061-T6 aluminum, with or without the two different thicknesses of RUL underpad stated,

respectively. This is because magnesium dash panel and firewall samples almost always had higher specific loudness and total loudness values than the competing material dash panel samples, for respective thickness comparisons. There are few cases for specific and total loudness where AZ31B magnesium is favoured over 1018 cold-rolled steel and/or 6061-T6 aluminum. Also, AZ31B magnesium dash panel samples sharpness values were usually lower for respective thickness comparisons, indicating that AZ31B magnesium performs well. So, in terms of specific and total loudness, it is safe to say that AZ31B magnesium proves to be the most annoying of the three dash panel firewall metals or the least supportive for irritating powertrain, wind or tire road noise. In terms of sharpness, AZ31B magnesium is the least annoying firewall material, for high-frequency content of powertrain noise.

4. Separately comparing the TL_n and TL_r values for AZ31B magnesium to 1018 cold-rolled steel and 6061-T6 aluminum samples of respective areas and thicknesses, AZ31B magnesium proves to be a worthy competitor. This is because its TL_n values and TL_r values were relatively close to the other metals, even exceeding some, as discussed in Chapter 5. For the TL_r values, these included the signal types of periodic random or scattered white or pseudorandom noise, diesel generator noise, and electric motor noise, for a more 'real world' TL_r response of the metals and dash panel samples that goes beyond the J1400 standard. The TL_r and TL_n results were within reasonable dB intervals if inferior, and were sometimes higher or superior to other dash panel samples, for respective thickness comparisons.

6.2 Recommendations

The following is a recommendation for further NVH performance research of AZ31B magnesium dash panels. Obtain panels of AZ31B magnesium of 1 mm and 1.27 mm thickness to perform TL_n, TL_r, specific loudness, total loudness, and sharpness measurements for comparison to the exact same thicknesses of the most commonly utilised 1018 cold-rolled steel and 6061-T6 aluminum dash panel arrangements, respectively. This will provide further insight into the relative performance of AZ31B magnesium when compared to 1018 cold-rolled steel and 6061-T6 aluminum. This could be accomplished by consultation with the donors from the United States.

REFERENCES

1. Aleksander, S. & Moore, B. C. J. (1994). The critical modulation frequency and its relationship to auditory filtering at low frequency. *J. Acoust. Soc. Am.*, 95(5), 2606-2615.

2. ASTM E 2611-09 Technical Committee. (2009). *Standard test method for measurement of normal incidence sound transmission of acoustical materials based on the transfer matrix method.* West Conshohocken (PA): ASTM E2611-09 Technical Committee.

3. Beals, R. S. (2007). *Magnesium global development: outcomes from the TMS 2007 annual meeting.* Retrieved July 28th, 2008, from a JOM Web site: http://findarticles.com/p/articles/mi_qa5348/is_200708/ai_n21295

4. Bernard, A. R., & Rao, M.D. (2004). *Measurement of sound transmission loss using a modified four microphone impedance tube.* Retrieved October 3rd, 2009, from an MTU Web site: http://www.me.mtu.edu/courses/meem4704/project/papers/nc04_transmission_loss.pdf

5. Brown, B. (n.d.). *Magnesium applications in the short term.* Retrieved August 18th, 2008, from a Magnesium.Com Web site: http://www.magnesium.com/w3/data-bank/article.php?mgw=199&magnesium=286

6. Brown, B. (2003). *The men who made it happen.* Retrieved February 1st, 2009, from a Magnesium.Com Web site: http://www.magnesium.com/w3/data-bank/print.php?mgw=196&magnesium=270

7. Bruel & Kjaer Impedance/Transmission Loss Measurement Tubes Type 4206 Technical Committee. (2007). *Technical documentation-impedance/transmission loss measurement tubes type 4206-user manual.* Denmark: Bruel & Kjaer Impedance/Transmission Loss Measurement Tubes Type 4206 Technical Committee.

8. Carneal, J. P., & Fuller, C. R. (2003). An analytical and experimental investigation of active structural acoustic control of noise transmission through double panel systems. *Journal of Sound and Vibration,* 272, 749-771.

9. Charbonneau, J. (2010). *Comparison of Loudness Calculation Procedure Results to Equal Loudness Contours.* University of Windsor Faculty of Graduate Studies Theses, 6-35.

10. Cortex Instruments. (n.d.). *Psychoacoustics: A Tool for Industrial Sound Design.* Cortex Instruments. Cortex Instruments.

11. Dafoe, J. (2007). *Evaluation of Loudness Calculation Techniques with Applications for Product Evaluation.* University of Windsor, Faculty of Graduate Studies Theses, page 5.

12. Das, S. (2003). *JOM.* Retrieved July 28th, 2008, from a Find Articles Web site: http://findarticles.com/p/articles/mi_qa5348/is_200311/ai_n21339344

13. DeJong, C. A. (2007). *Magnesium: the other light metal.* Retrieved August 17th, 2008, from an Autofield Guide Web site: http://www.autofieldguide.com/articles/article_print.cfm

14. Edgar, J. (2001). *Magnesium: coming soon to a car near you.* Retrieved July 28th, 2008, from an AutoSpeed Web site: http://autospeed.com/cms/A_1103/printArticle.html

15. Fletcher, H.C, & Munson, W.A. (n.d.). *Equal loudness curves.* Retrieved February 25th, 2011 from a Webervst Web site: http://www.webervst.com/fm.htm

16. Fletcher, H. & Munson, W.A. (1933). Loudness, its definition, measurement and calculation. *Bell System Technical Journal,* 12(4), 377-430.

17. Fletcher, H. & Munson, W.A. (1933). Loudness, Its Definition, Measurement and Calculation. *The Journal of the Acoustical Society of America,* 5(2), 82-108.

18. Gaines, L., Cuenca, R., Stodolsky, F., & Wu, S. (1996). *Potential automotive uses of wrought magnesium alloys.* Argonne (IL).

19. Glasberg, B. R., & Moore, B. C. J. (1990). *Derivation of auditory filter shapes from notched-noise.* Hearing Research, 47(1-2), 103-138.

20. Glasberg, B. R., & Moore, B. C. J. (2006). Prediction of absolute thresholds and equal loudness contours using a modified loudness model (L). *Journal of the Acoustical Society of America,* 120(2), 585-588.

21. Guang-tai, Z., Zhi-yong, H., Jun, C., & Rong-jie, M. (2008). *Comparison of NVH performance of magnesium alloy casting and aluminium alloy casting.* Retrieved February 6th, 2009, from a Chinese Internal Combustion Engine Engineering Web site: http://en.cnki.com.cn/Article_en/CJFDTOTAL-NRJG200802019.htm

22. Human Factors Course. (n.d.). *Measuring Loudness.* Retrieved June 6th, 2011, from a Perception Enhancement Web site: http://www.perceptionenhancement.com/docs/human_factors_course/human_factors_course_lec14_sound_exposure.pdf

23. International Organization for Standardization. (2003). *Acoustics – Normal Equal Loudness Contours.* Standard, Geneva International Organization for Standardization.

24. Karabin, L., & Hunt Jr., H. (2007). *Die cast magnesium in automotive applications.* Retrieved June 10th, 2008, from a Materials Technology Web site: http://www.materialstechnology.org

25. Kingsbury, B. A. (1927). *A Direct Comparison of the Loudness of Pure Tones.* Phys. Rev. Vers. 29, 588.

26. Kramer, D. A. (2003). *Magnesium metal.* United States.

27. Lam, K. P., Behdinan, K., & Cleghorn, W.L. (2003). *A material and gauge thickness sensitivity analysis on the NVH and crashworthiness of automotive instrument panel support.* Retrieved January 25th, 2009 from a Science Direct Web site:
http://www.sciencedirect.com/science?_ob=ArticleURL&_udi=B6V59-48R1WTV-2&_user=1010624&_coverDate=11%2F30%2F2003&_rdoc=1&_fmt=high&_orig=gateway&_origin=gateway&_sort=d&_docanchor=&view=c&_searchStrId=167962
2661&_rerunOrigin=google&_acct=C000050266&_version=1&_urlVersion=0&_us
erid=1010624&md5=f4c04477f6d4d4b009bde72d534b57eb&searchtype=a

28. Levitt, H. (1970). Transformed up-down methods in psychoacoustics. *The Journal of the Acoustical Society of America,* 4.1, 4.5, 467-77.

29. Lin, J. Z., Lanka, S., & Ruden, T. (2005). *Physical and virtual prototyping of magnesium instrument panel structures.* Detroit (MI).

30. Luo, A. A. (2002). *Magnesium: current and potential automotive applications.* Retrieved July 28th, 2008, from a JOM Web site: http://findarticles.com/p/articles/mi_qa5348/is_200202/ai_n21308970/

31. Metal Bulletin Monthly. (2006). *Magnesium.* Retrieved January 8th, 2008, from a Metal Bulletin Monthly Web site: http://www.mmta.co.uk/uploaded_files/MagnesiumMBM.pdf

32. Moore, B. C. J., & Glasberg, B. R. (1996). *A revision of Zwicker's loudness model.* Acustica – Acta Acustica, 82(2), 335-345.

33. NVH-SQ Research Group. (2007). *Magnesium alloys in structural automotive applications: a review.* Windsor (ON).

34. Olivieri, O., Bolton, J. S., & Yoo, T. (2006). *Measurement of transmission loss of materials using a standing wave tube.* Retrieved October 6th, 2009, from a Bruel & Kjaer Web site:

http://www.bksv.com/doc/bn0216.pdf

35. Paulus, E., & Zwicker, E. (1972). *Programme Zur Automatischen Bestimmura Der Lautheit Aus Terzpegeln Oder Frequenzgur-pisenpegelen (Computer Program for Calculating Loudness from Third-Octave Band Levels or from Critical Band Levels).* Acustica, 27(5), 253-266.

36. Robinson, D. W., & Dadson, R. S. (1956). A re-determination of the equal loudness relations for pure tones. *Br. J. Appl. Phys.* V7, 166-181.

37. SAE Sound & Heat Insulation Materials Committee. (1990). *Surface vehicle recommended practice.* Warrendale (PA). SAE Sound & Heat Insulation Materials Committee.

38. SAE Sound Presentation. (n.d.). *Soundc.* Retrieved June 6th, 2011, from an SAE Web site:
http://www.sae.org/events/nvc/ws-wed-soundc.pdf

39. Schumann, S. (2005). *The paths and strategies for increased magnesium applications in vehicles.* Wolfsburg (Germany).

40. Stevens, S. S. (1936). *A scale for the measurement of psychological magnitude: loudness.* Psychological Review, V43, 405-416.

41. Stevens, S. S. (1961). Procedure for Calculating Loudness: Mark VI. *J. Acoust. Soc. Am.*, 33(11), 1577-1585.

42. Suzuki, Y., & Takeshima, H. (2004). Equal-loudness-level contours for pure tones. *J. Acoust. Soc. Am.* 116(2), 918-933.

43. Trapp, M.A., & Hodgdon, K.K. (2008). An evaluation of friction and impact induced acoustic behaviour of selected automotive materials, part II: impact induced acoustics. *International Journal of Vehicle Noise and Vibration,* 4(1), 17-31.

44. United States Automotive Materials Partnership Committee. (2006). *Magnesium vision 2020: a north american automotive strategic vision for magnesium.* United States: United States Automotive Materials Partnership Committee.

45. Vasilash, G. S. (2003). *Almost famous: magnesium.* Retrieved August 17th, 2008, from an Autofield Guide Web site:
http://www.autofieldguide.com/articles/article_print1.cfm

46. Yousefzadeh, B., Mahjoob, M., Mohammadi, N., & Shahsavari, A. (2008). *An experimental study of sound transmission loss (STL) measurement techniques using an impedance tube.* Retrieved September 30th, 2009, from an Acoustics'08 Paris Web site:

http://intelligence.eu.com/acoustics2008/acoustics2008/cd1/data/articles/002077.pdf

47. Zwicker, E., & Fastl, H. (1990). *Psychoacoustics: Facts and Models.* Springer.

48. Zwicker, E., & Fastl, H. (1999). *Psychoacoustics: Facts and Models.* Heidelberg, Germany. Springer-Verlag.

49. Zwicker, E., & Feldtkeller, R. (1955). *Uber die Lautstarke von Gleichformiger Gerauschen (On the loudness of stationary noises).* Acustica, V5, 303-316.

APPENDIX
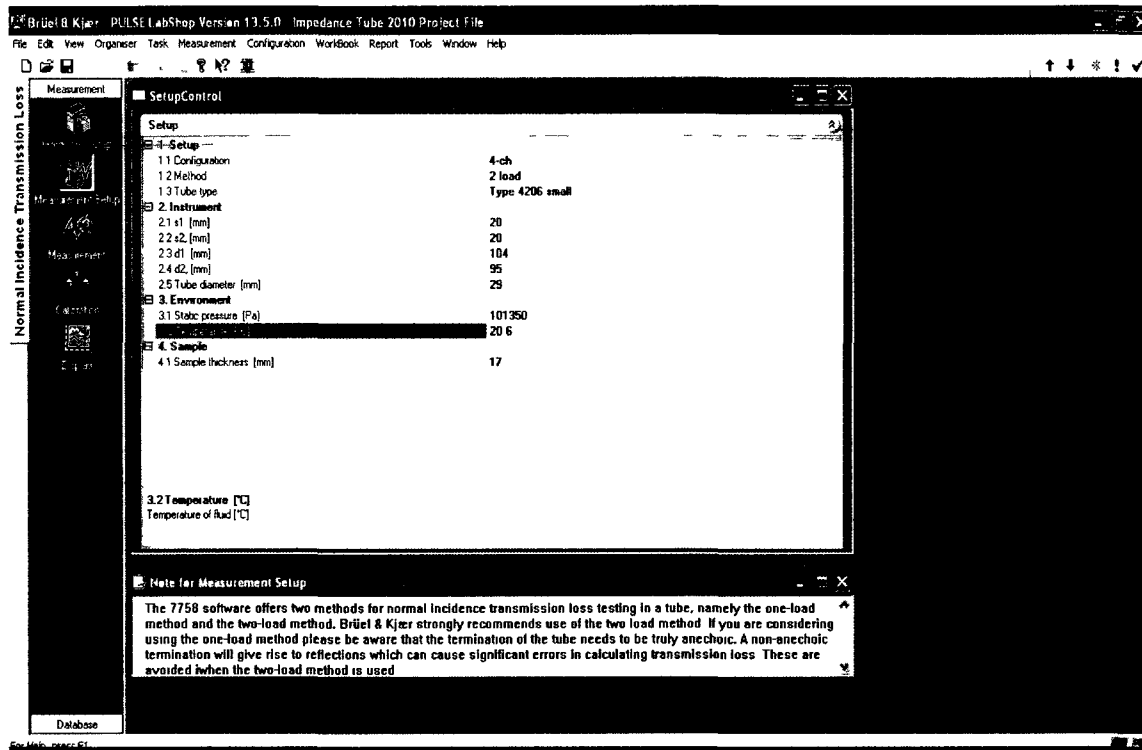
Figure 45: Print Screen of Acoustic Measurement Parameters within PULSE Version 13.5.0 for Impedance Tube TL$_n$ Testing
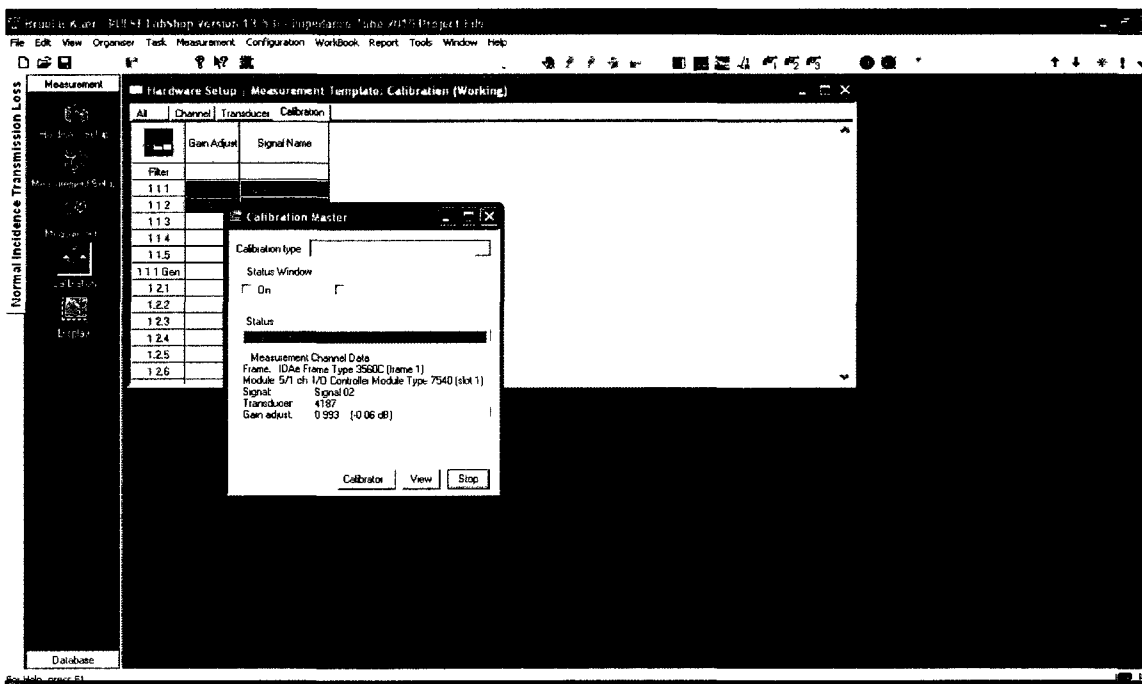
Figure 46: Print Screen of Calibration Verification Window for the Type 4187 Microphones
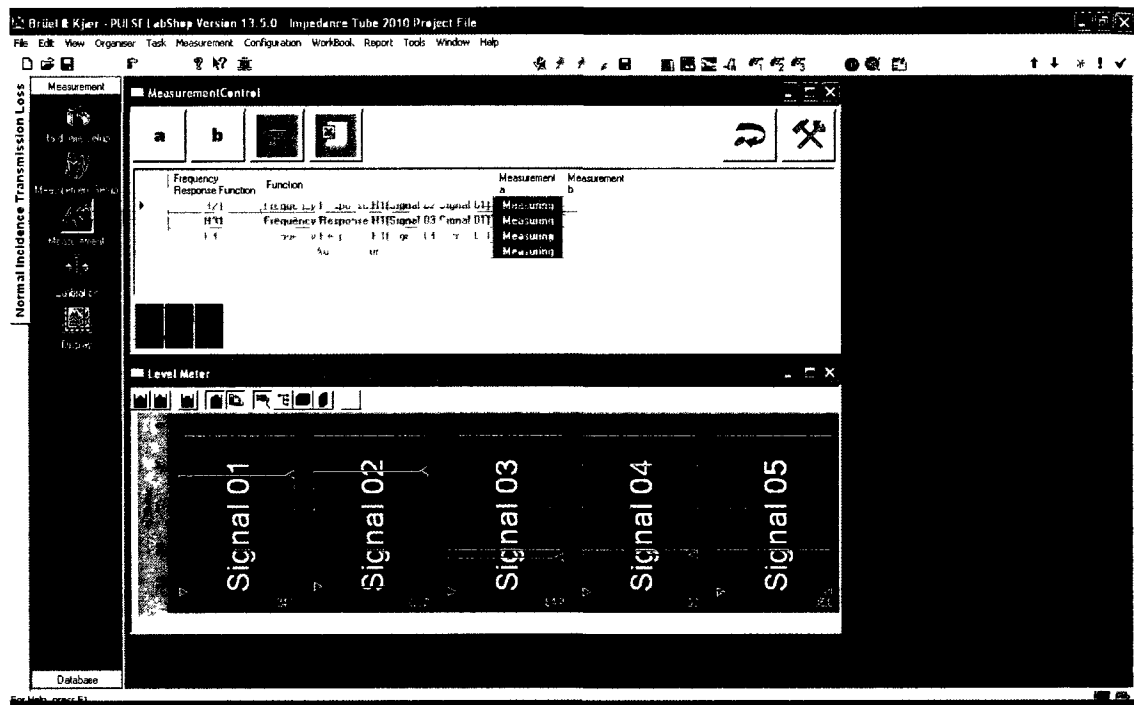
Figure 47: Print Screen of Measurement Windows inside PULSE Version 13.5.0 during TL_n Measurement
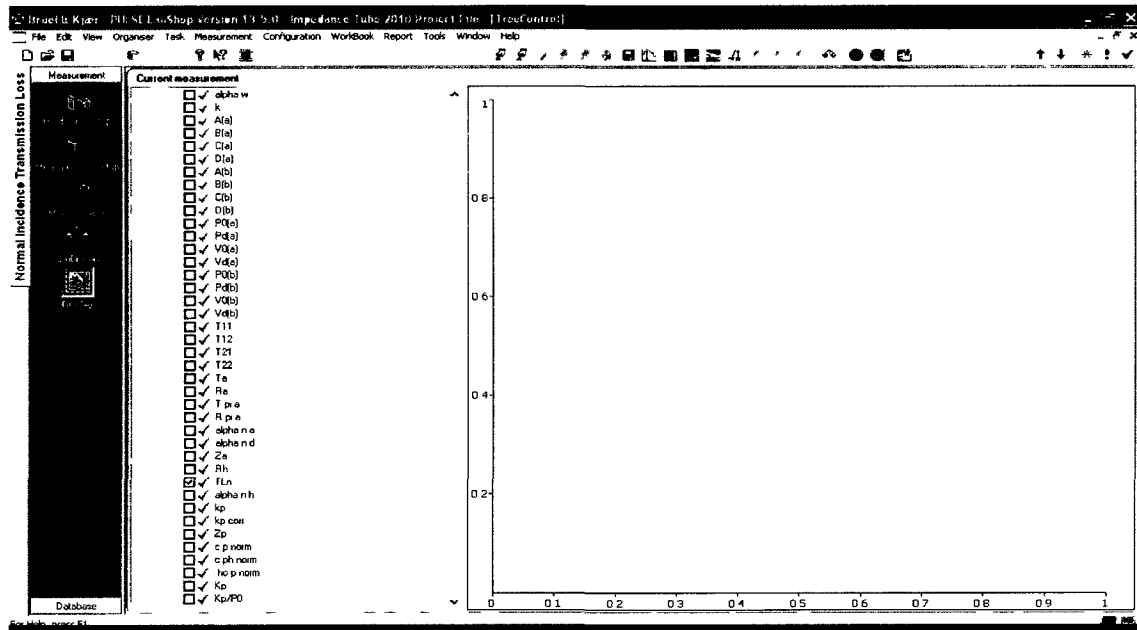
Figure 48: Print Screen of Measurement Results Window, focused on TL_n
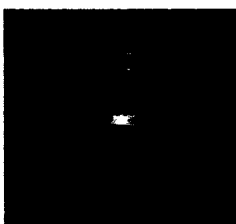
Figure 49: Picture of the High Frequency B&K Impedance Tube Sample Setup Example: 2 mm thick 6061-T6 Aluminum with a 19 mm thick RUL Sample with Clamping Acoustic Rings from B&K for Proper Setup
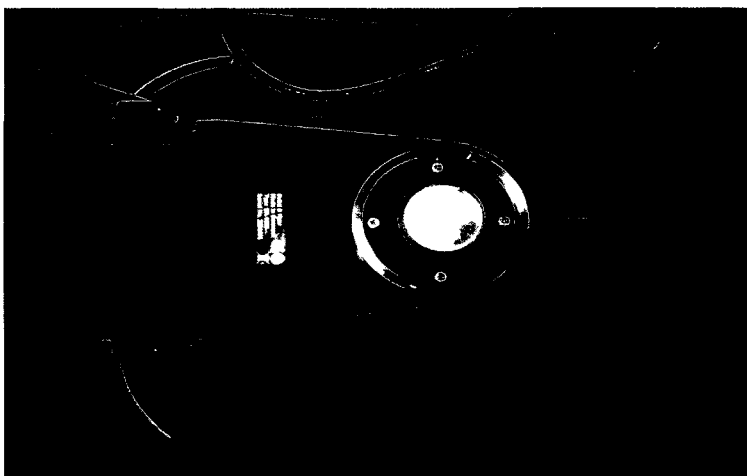
Figure 50: Picture of Side View of the High Frequency Impedance Tube Sample Holder with 2 mm thick 6061-T6 Aluminum Sample in Proper Position with B&K Acoustic Ring
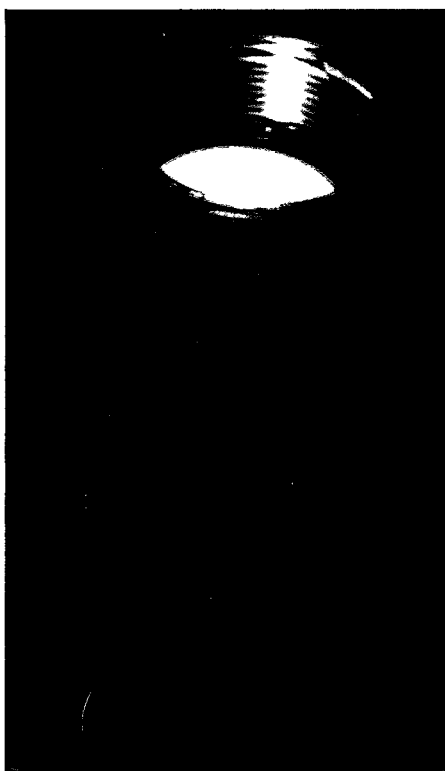
Figure 51: Picture of the High Frequency B&K Impedance Tube Extension with THL Material
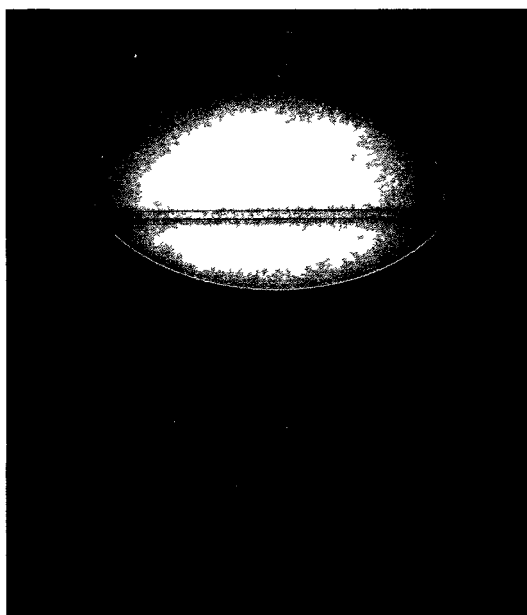
Figure 52: Picture of Low Frequency B&K Impedance Tube Extension with THL Material
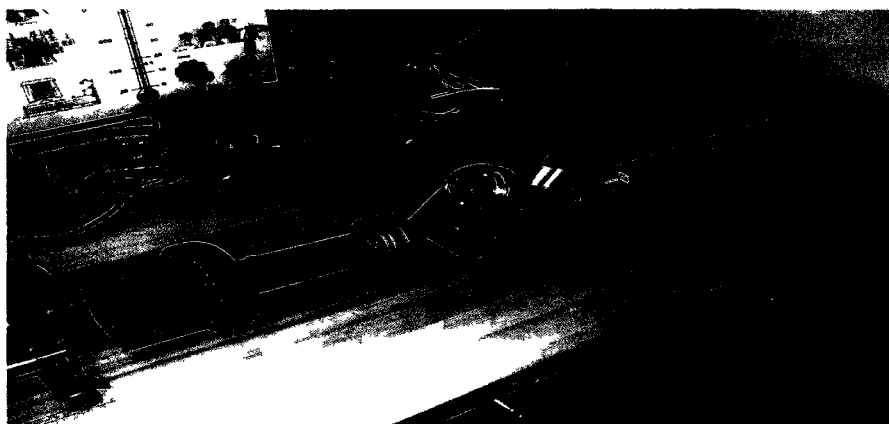
Figure 53: Picture of B&K Type 4206-T High Frequency Impedance Tube Assembly Setup

Figure 54: Picture of Loudspeaker of the Low Frequency B&K Type 4206-T Impedance Tube

108

Figure 55: Picture of the 2 mm thick 6061-T6 Aluminum Sample with a 19 mm thick RUL Automotive Underpad Material Sample with the B&K Specialised Acoustic Sealing Rings for Proper Setup in the Low Frequency B&K Type 4206-T Impedance Tube
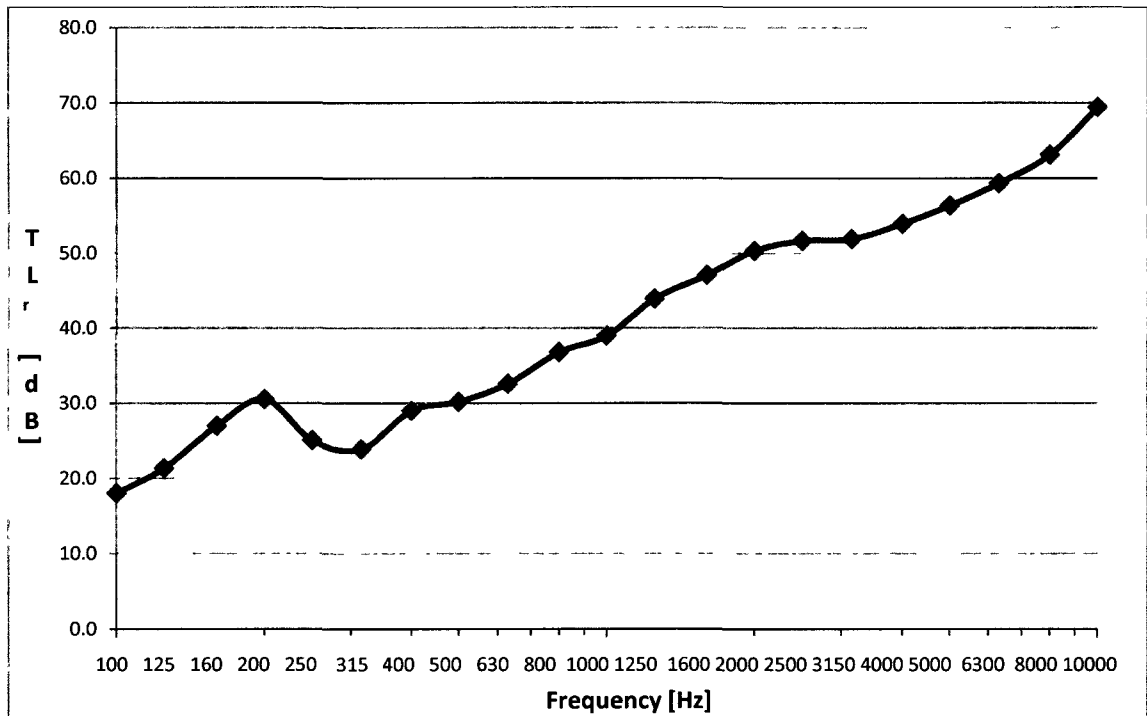
Figure 56: The 4.7 mm Thick, 60cmX60cm 6061-T6 Aluminum Sample with the 15 mm Thick, 60cmX60cm Sample of RUL Automotive Underpad TL Random Incidence from the J1400 Test in Canton, Michigan
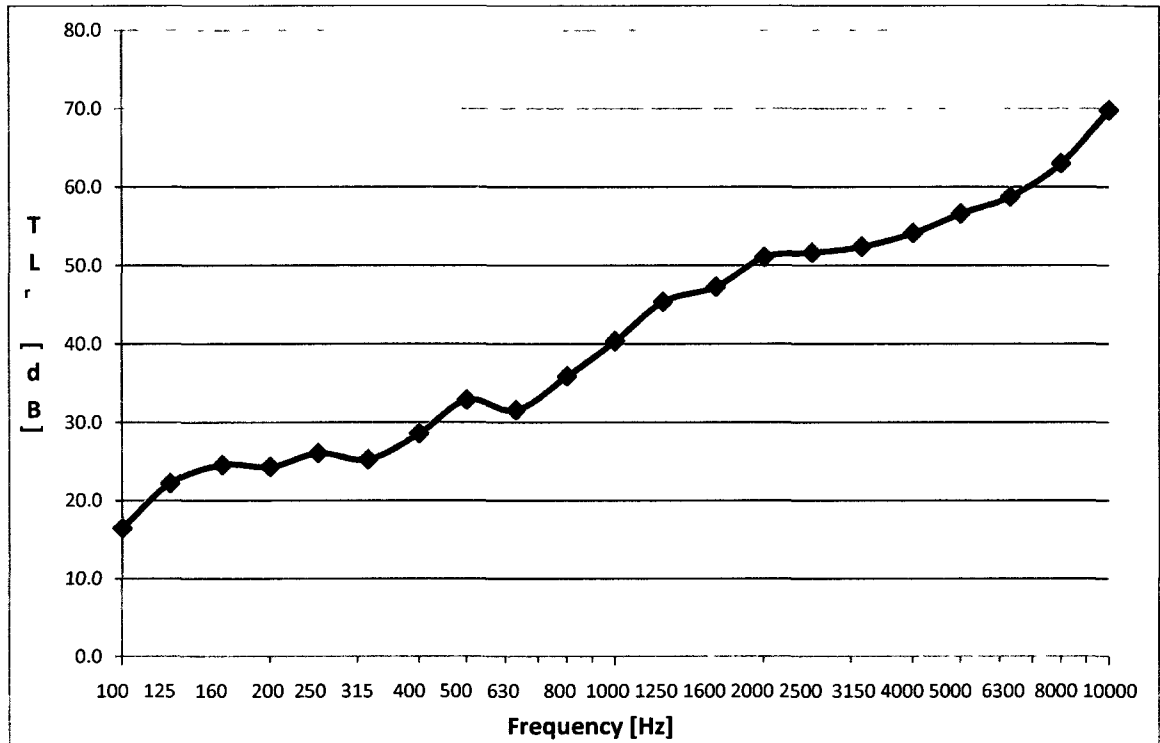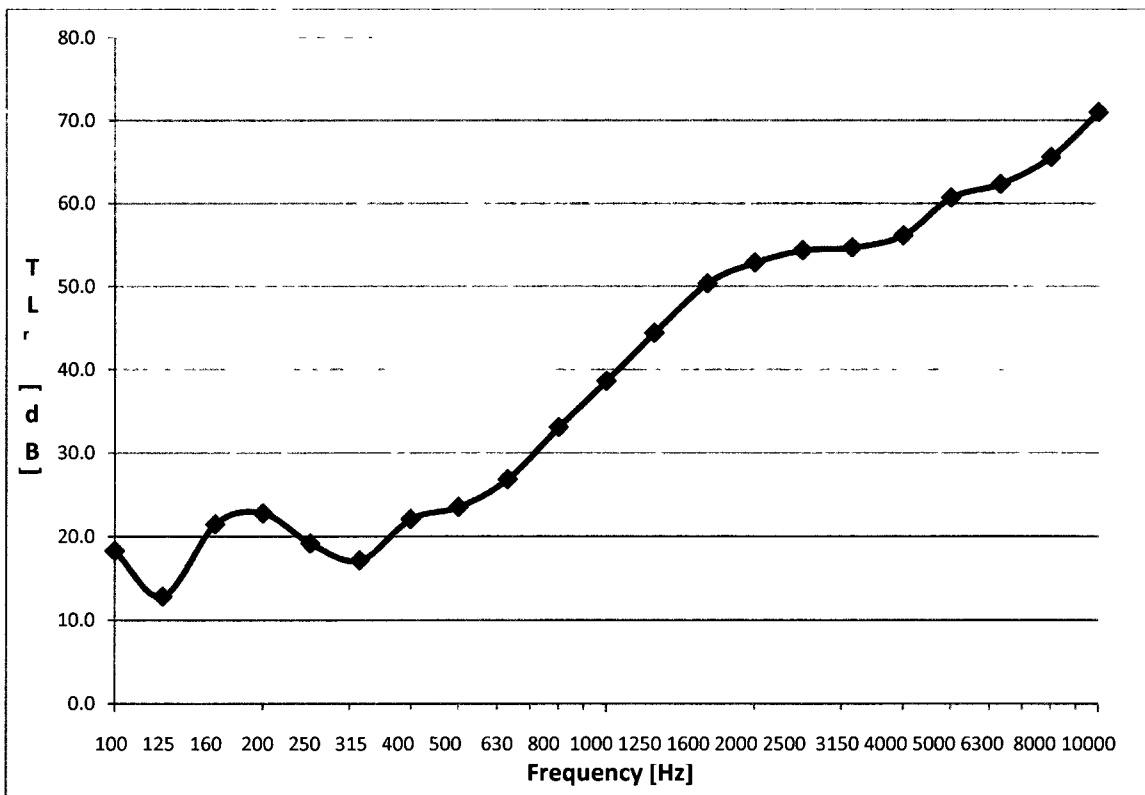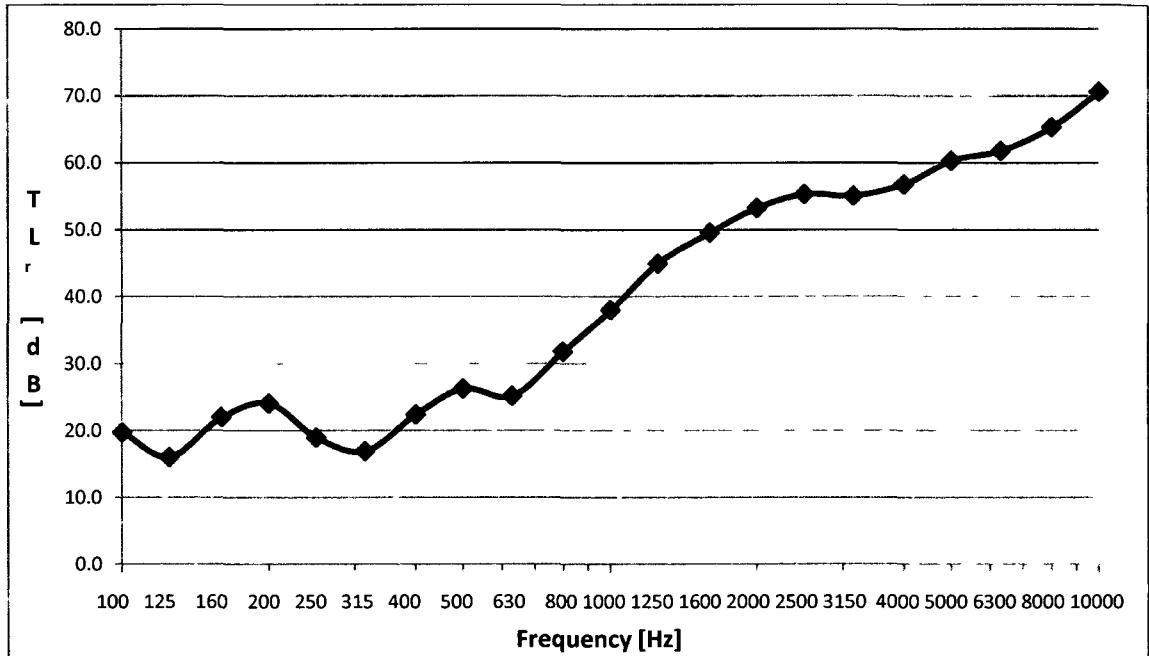
Figure 57: The 4.7 mm Thick, 60cmX60cm 6061-T6 Aluminum Sample with the 19 mm Thick, 60cmX60cm Sample of RUL Automotive Underpad TL Random Incidence from the J1400 Test in Canton, Michigan
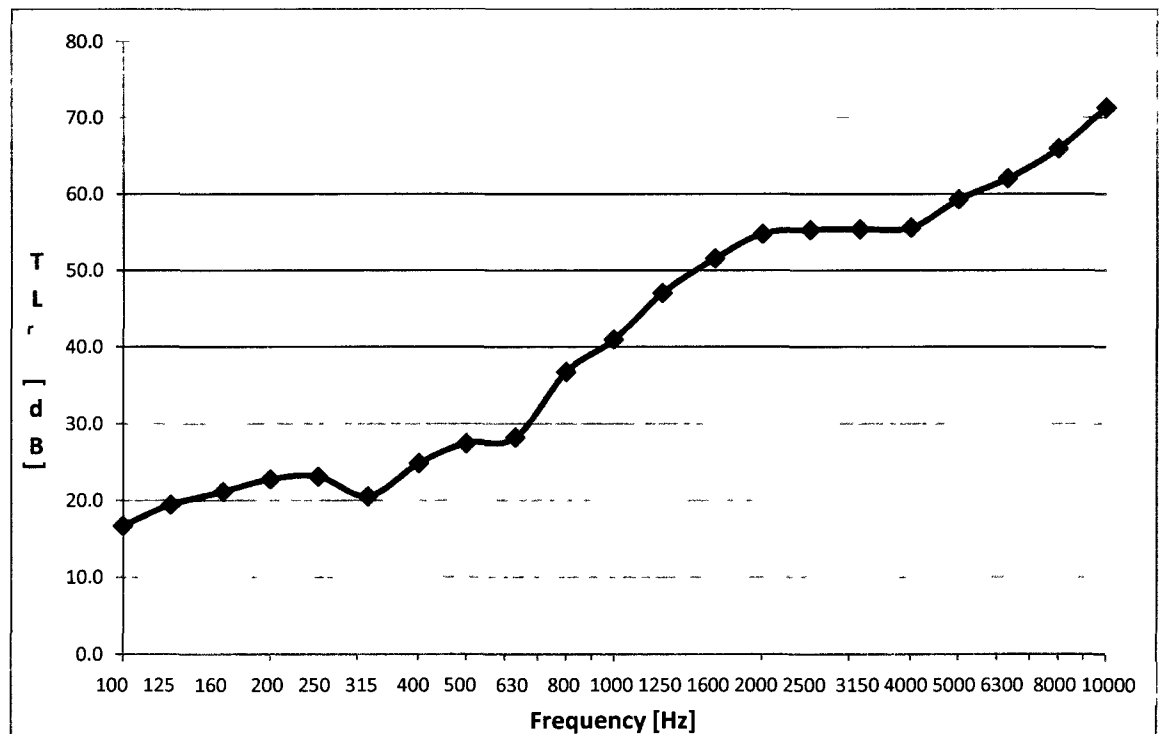
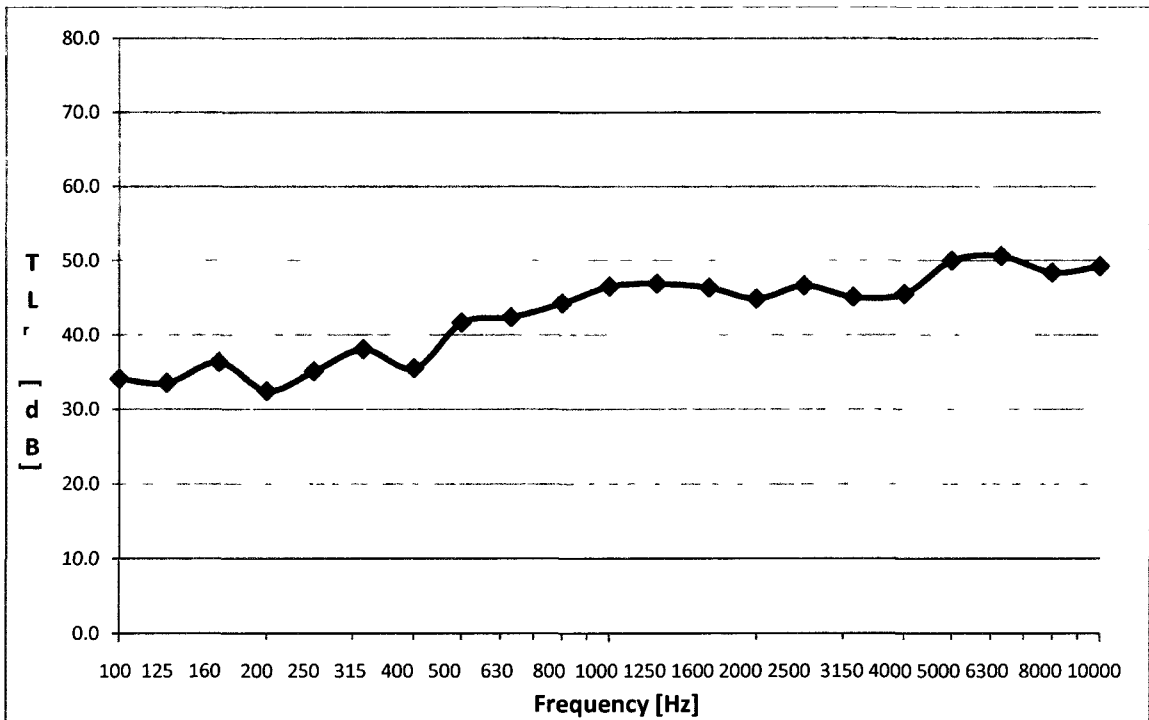Figure 58: The 2 mm Thick, 60cmX60cm 6061-T6 Aluminum Sample with the 15 mm Thick, 60cmX60cm Sample of RUL Automotive Underpad TL Random Incidence from the J1400 Test in Canton, Michigan
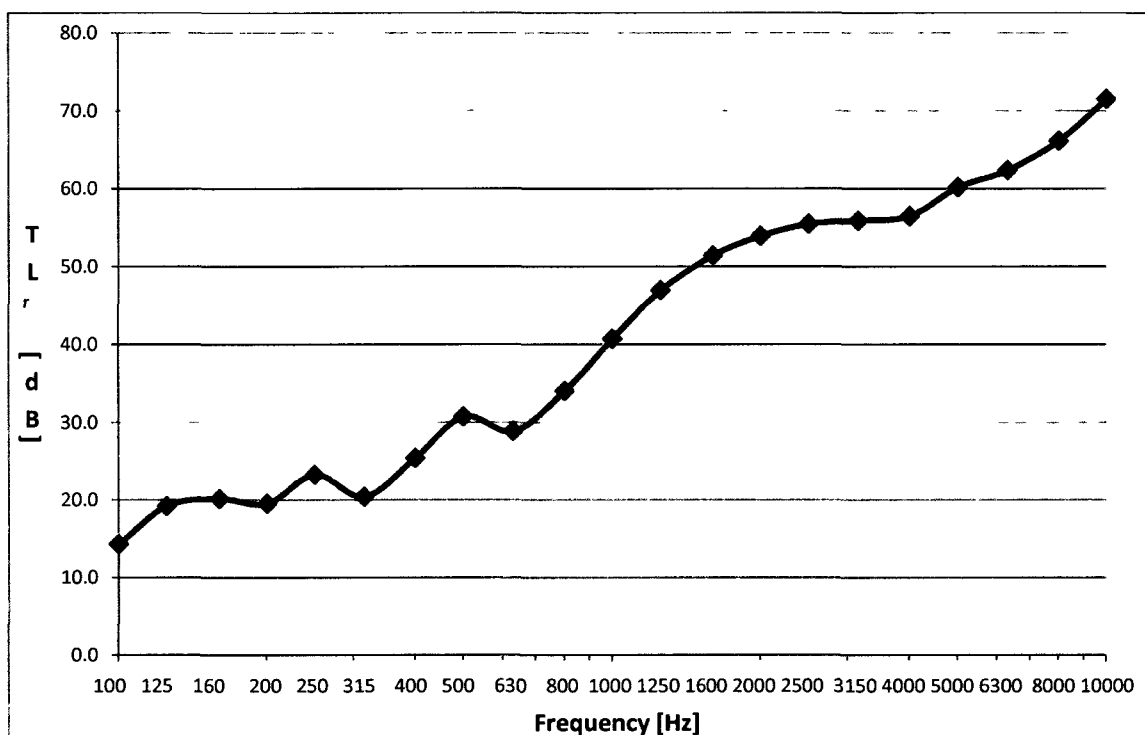
Figure 59: The 2 mm Thick, 60cmX60cm 6061-T6 Aluminum Sample with the 19 mm Thick, 60cmX60cm Sample of RUL Automotive Underpad TL Random Incidence from the J1400 Test in Canton, Michigan
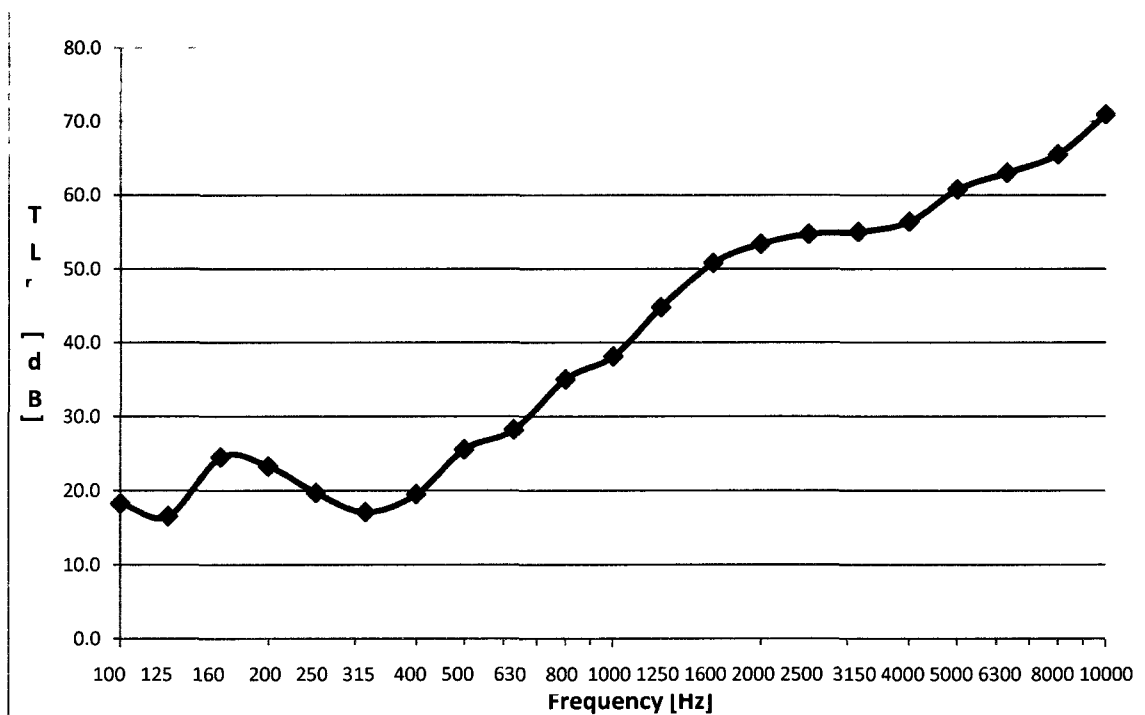
Figure 60: The 1.27 mm Thick, 60cmX60cm 6061-T6 Aluminum Sample with the 15 mm Thick, 60cmX60cm Sample of RUL Automotive Underpad TL Random Incidence from the J1400 Test in Canton, Michigan
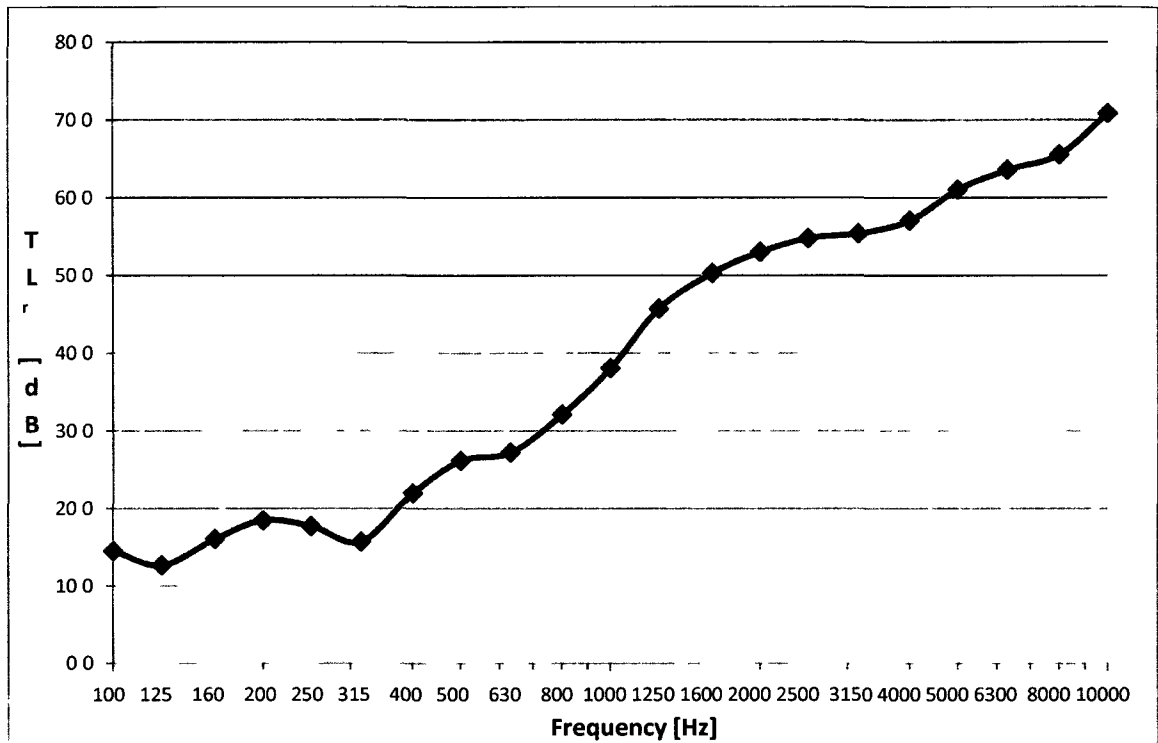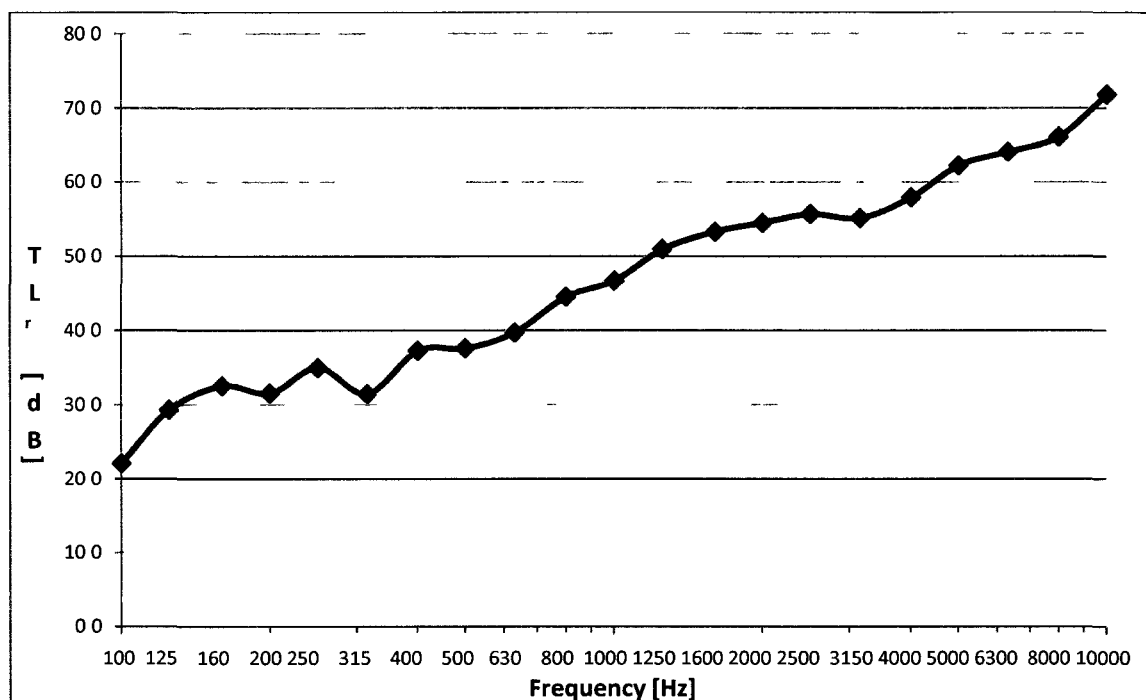
Figure 61: The 1.27 mm Thick, 60cmX60cm 6061-T6 Aluminum Sample with the 19 mm Thick, 60cmX60cm Sample of RUL Automotive Underpad TL Random Incidence from the J1400 Test in Canton, Michigan
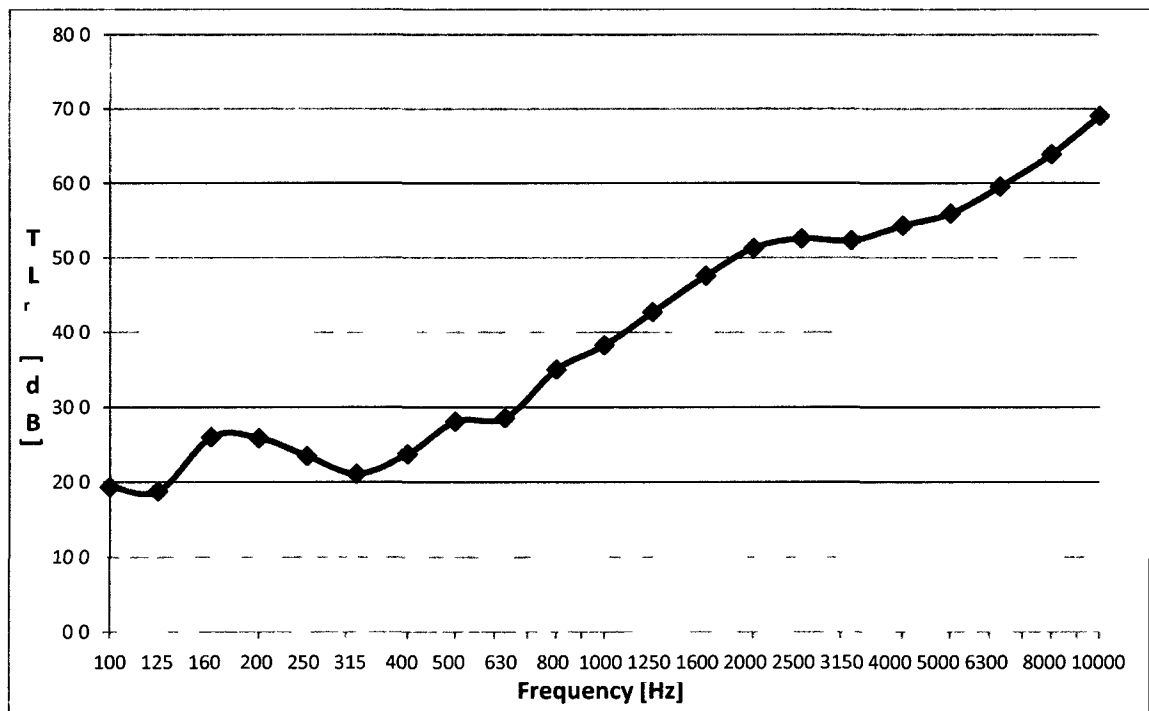
Figure 62: The 4 mm Thick, 60cmX60cm AZ31B Magnesium Sample with the 15 mm Thick, 60cmX60cm Sample of RUL Automotive Underpad TL Random Incidence from the J1400 Test in Canton, Michigan
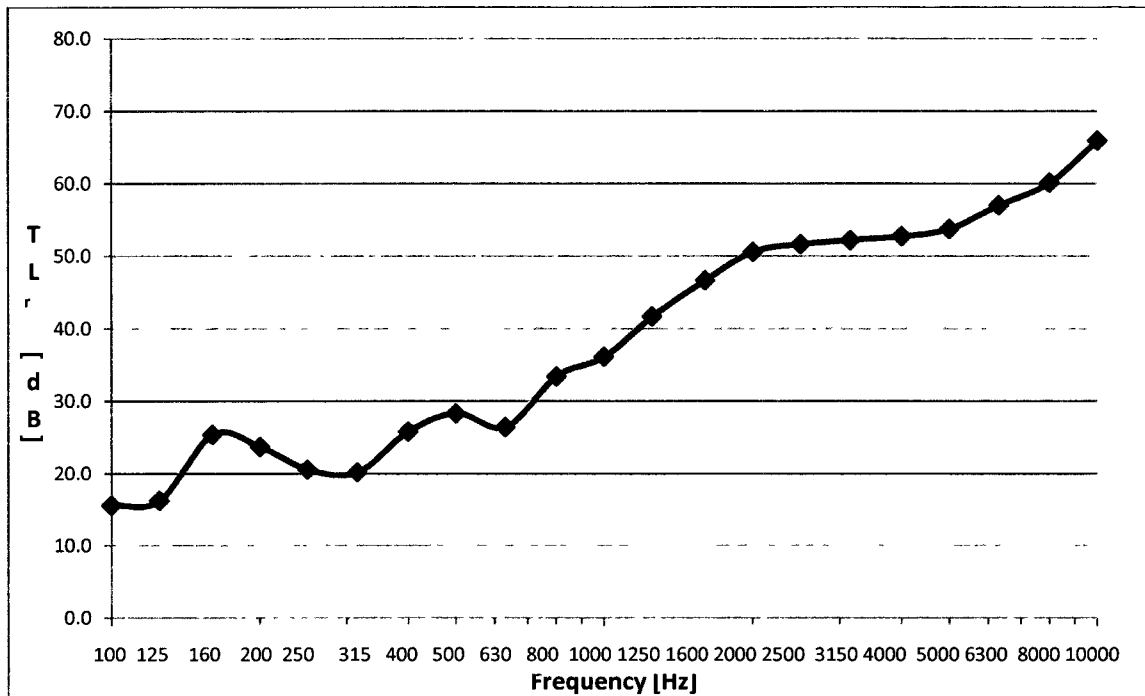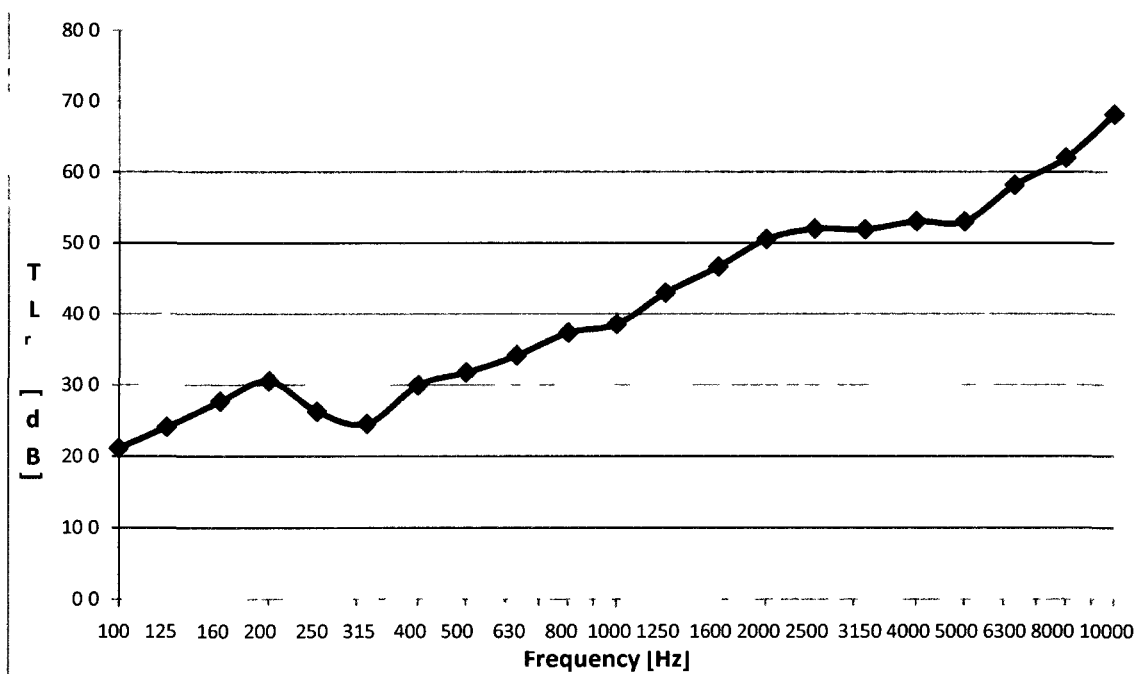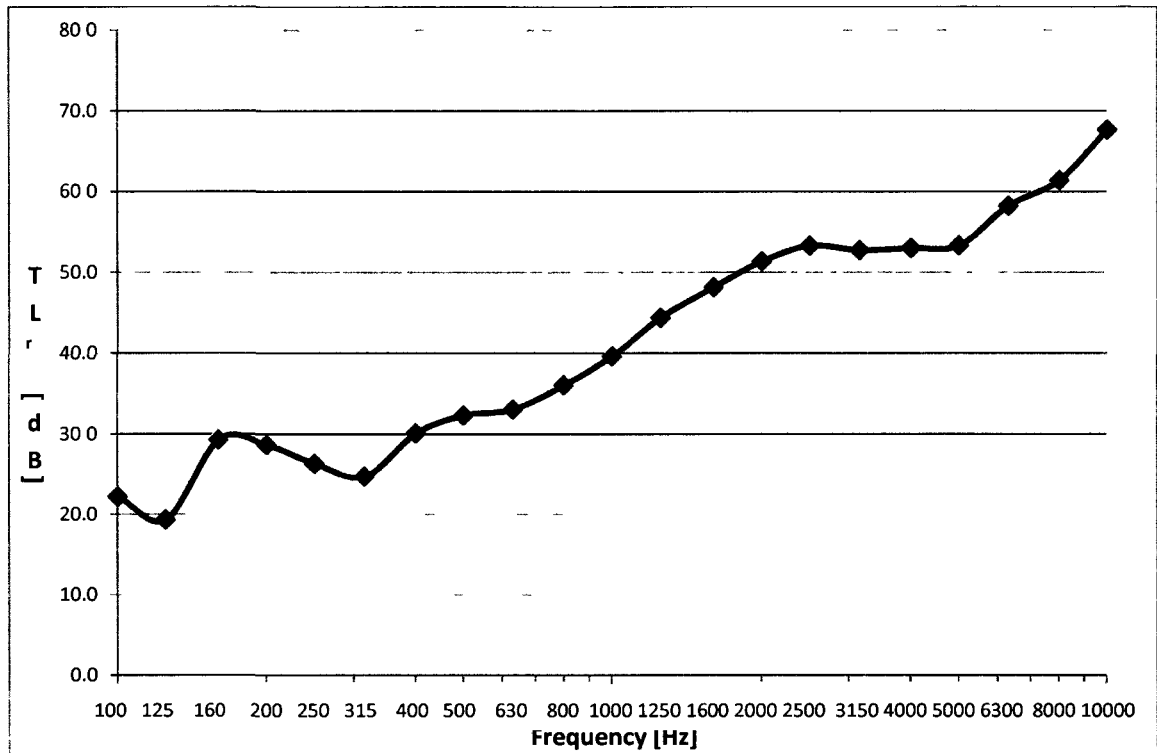
Figure 63: The 4 mm Thick, 60cmX60cm AZ31B Magnesium Sample with the 19 mm Thick, 60cmX60cm Sample of RUL Automotive Underpad TL Random Incidence from the J1400 Test in Canton, Michigan

Figure 64: The 2 mm Thick, 60cmX60cm AZ31B Magnesium Sample with the 15 mm Thick, 60cmX60cm Sample of RUL Automotive Underpad TL Random Incidence from the J1400 Test in Canton, Michigan

Figure 65: The 2 mm Thick, 60cmX60cm AZ31B Magnesium Sample with the 19 mm Thick, 60cmX60cm Sample of RUL Automotive Underpad TL Random Incidence from the J1400 Test in Canton, Michigan

Figure 66: The 4.9 mm Thick, 60cmX60cm 1018 Cold-Rolled Steel Sample with the 15 mm Thick, 60cmX60cm Sample of RUL Automotive Underpad TL Random Incidence from the J1400 Test in Canton, Michigan
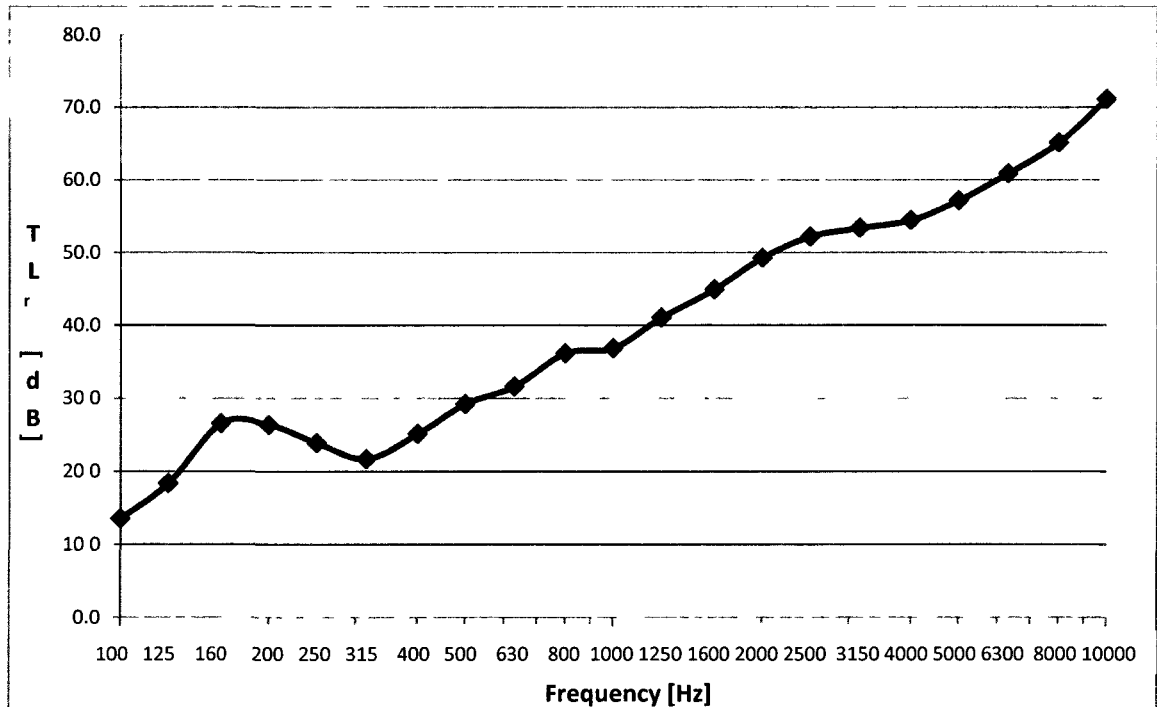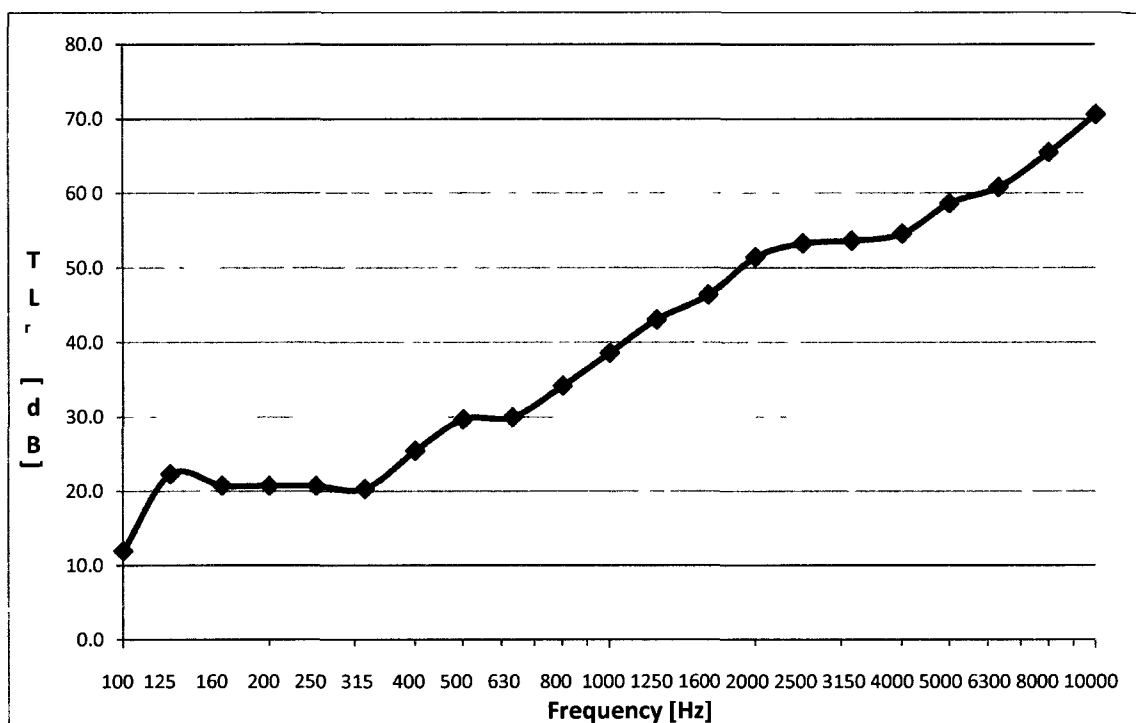
Figure 67: The 4.9 mm Thick, 60cmX60cm 1018 Cold-Rolled Steel Sample with the 19 mm Thick, 60cmX60cm Sample of RUL Automotive Underpad TL Random Incidence from the J1400 Test in Canton, Michigan


Figure 68: The 2 mm Thick, 60cmX60cm 1018 Cold-Rolled Steel Sample with the 15 mm Thick, 60cmX60cm Sample of RUL Automotive Underpad TL Random Incidence from the J1400 Test in Canton, Michigan

Figure 69: The 2 mm Thick, 60cmX60cm 1018 Cold-Rolled Steel Sample with the 19 mm Thick, 60cmX60cm Sample of RUL Automotive Underpad TL Random Incidence from the J1400 Test in Canton, Michigan

Figure 70: The 1 mm Thick, 60cmX60cm 1018 Cold-Rolled Steel Sample with the 15 mm Thick, 60cmX60cm Sample of RUL Automotive Underpad TL Random Incidence from the J1400 Test in Canton, Michigan

Figure 71: The 1 mm Thick, 60cmX60cm 1018 Cold-Rolled Steel Sample with the 19 mm Thick, 60cmX60cm Sample of RUL Automotive Underpad TL Random Incidence from the J1400 Test in Canton, Michigan
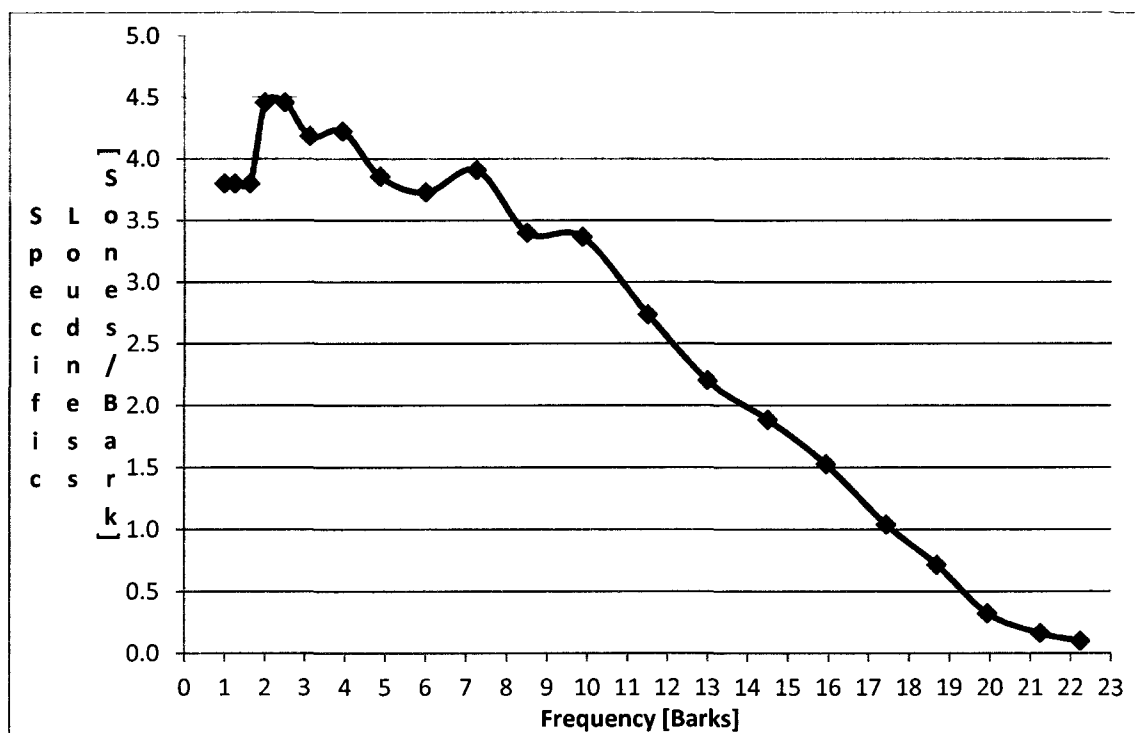
Figure 72: Averaged Specific Loudness for a Free Field Sound Field Condition from Microphones 6 and 10 for the 15 mm Thick, 60cmX60cm Sample of RUL Automotive Underpad with Random or Uniform White Noise 10 Seconds Signal Duration, 87.8 dB in the Semi-Anechoic Room
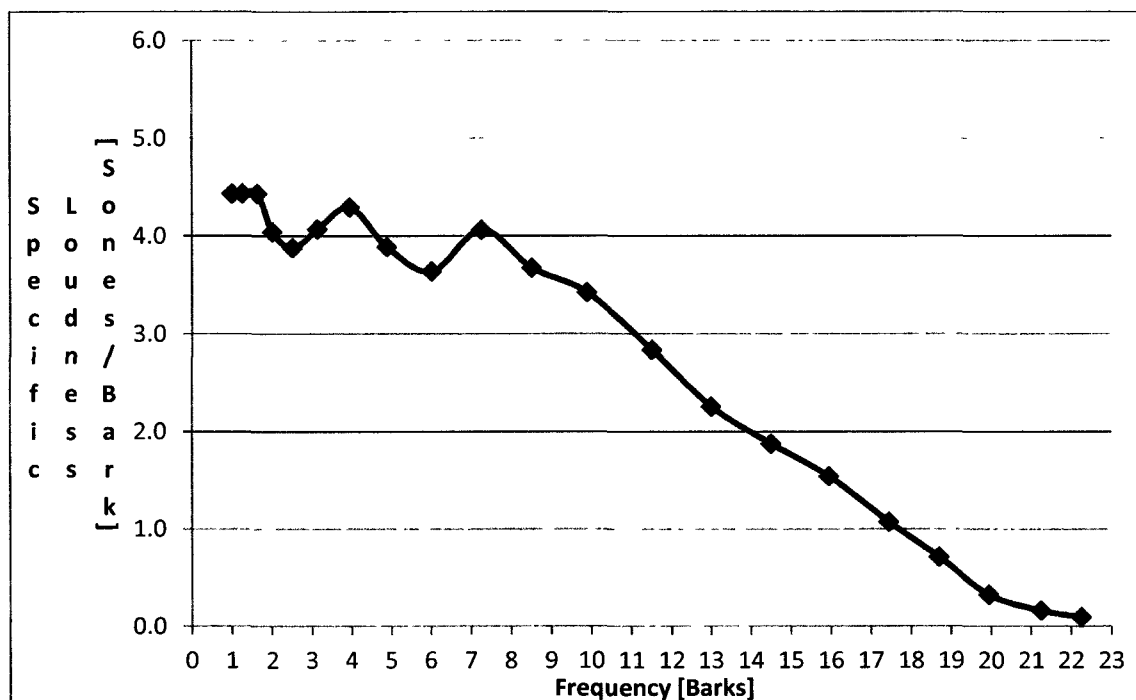
Figure 73: Averaged Specific Loudness for a Free Field Sound Field Condition from Microphones 6 and 10 for the 15 mm Thick, 60cmX60cm Sample of RUL Automotive Underpad with Periodic Random or Scattered White or Pseudorandom Noise 10 Seconds Signal Duration, 88.0 dB in the Semi-Anechoic Room
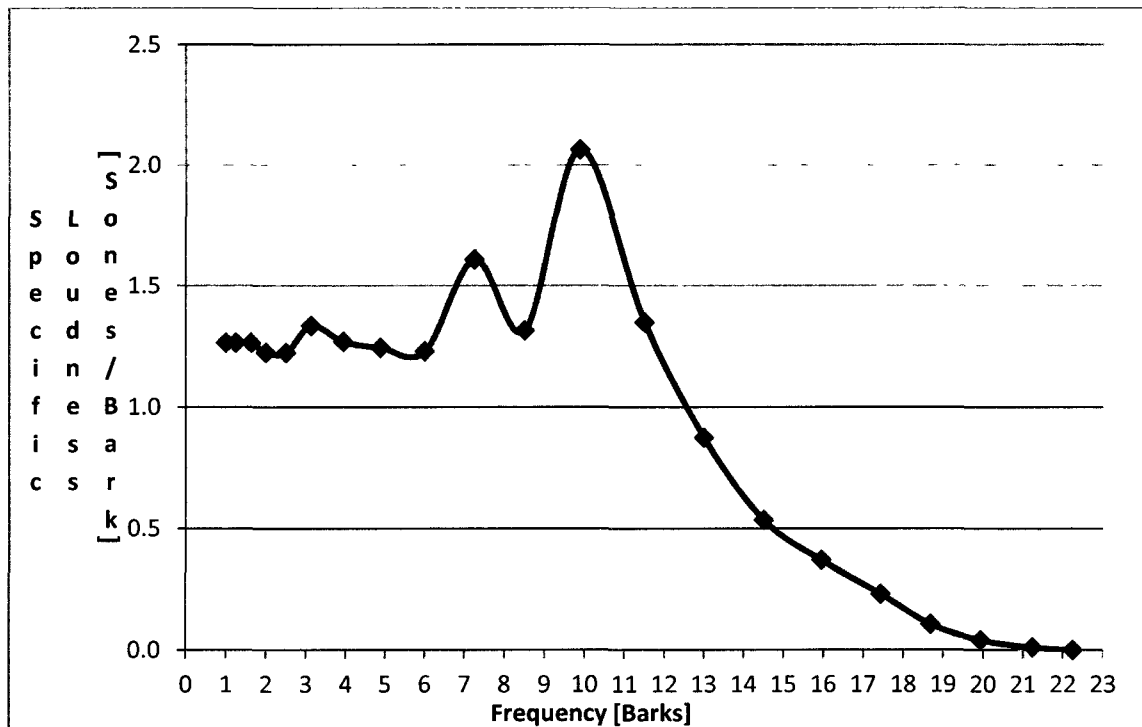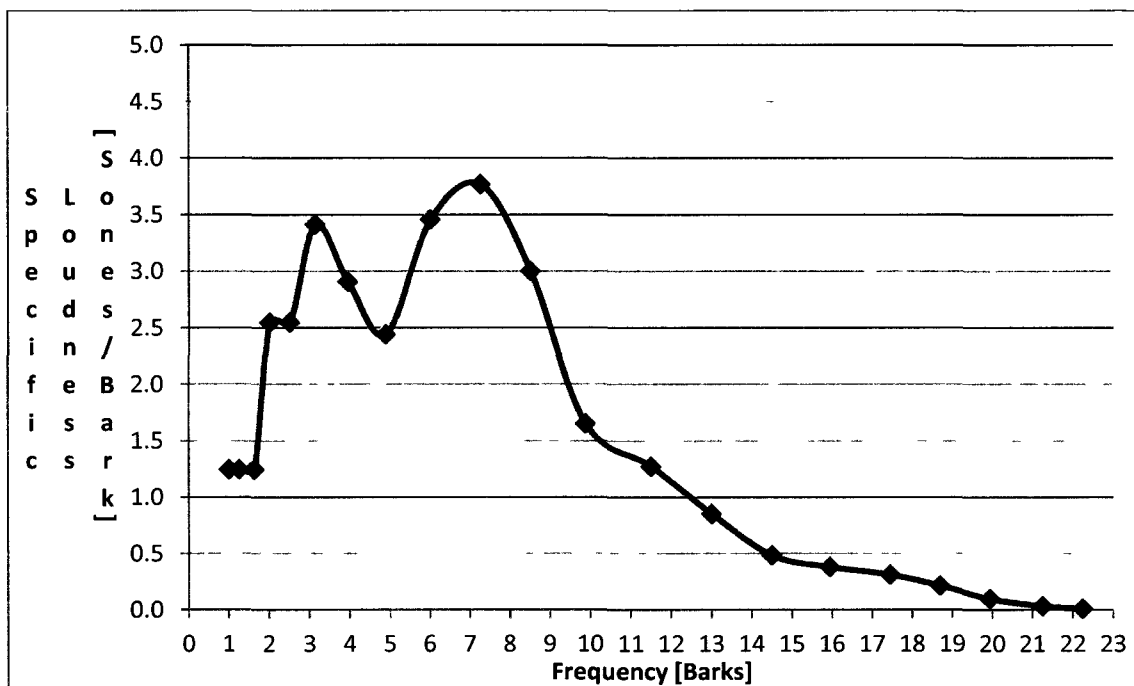

Figure 74: Averaged Specific Loudness for a Free Field Sound Field Condition from Microphones 6 and 10 for the 15 mm Thick, 60cmX60cm Sample of RUL Automotive Underpad with Diesel Generator Noise 10 Seconds Signal Duration, 71.5 dB in the Semi-Anechoic Room

Figure 75: Averaged Specific Loudness for a Free Field Sound Field Condition from Microphones 6 and 10 for the 15 mm Thick, 60cmX60cm Sample of RUL Automotive Underpad with Electric Motor Noise 10 Seconds Signal Duration, 83.0 dB in the Semi-Anechoic Room
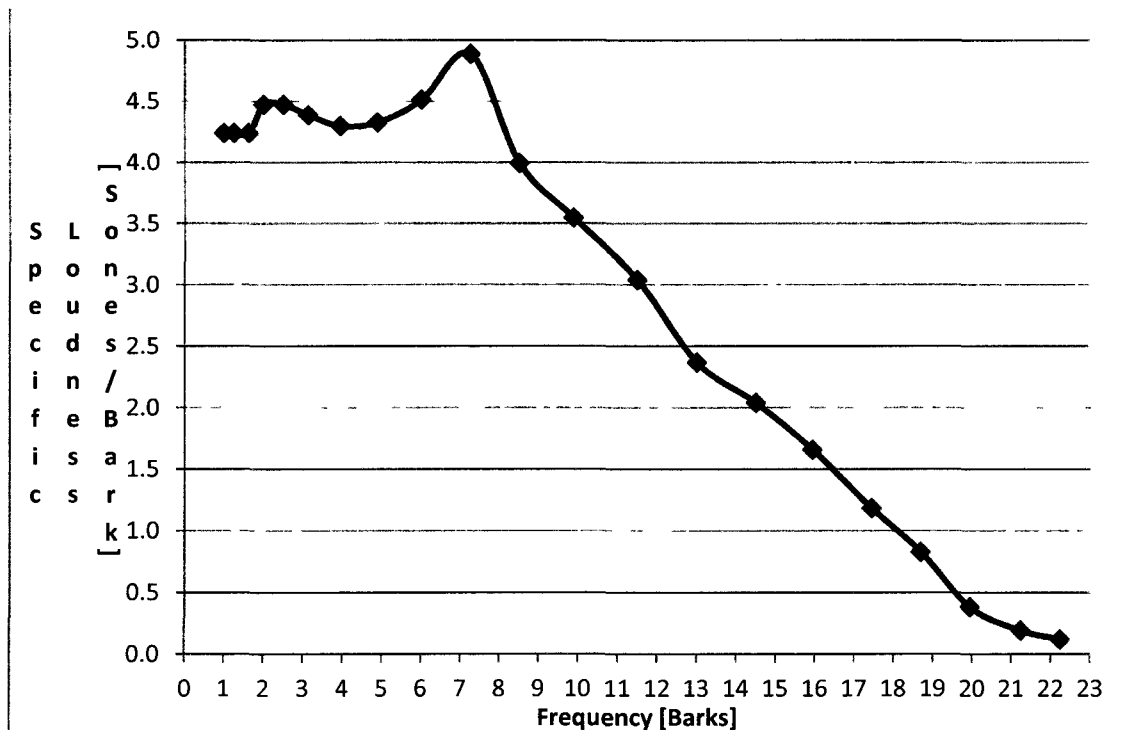

Figure 76: Averaged Specific Loudness for a Free Field Sound Field Condition from Microphones 6 and 10 for the 19 mm Thick, 60cmX60cm Sample of RUL Automotive Underpad with Random or Uniform White Noise 10 Seconds Signal Duration, 90.1 dB in the Semi-Anechoic Room
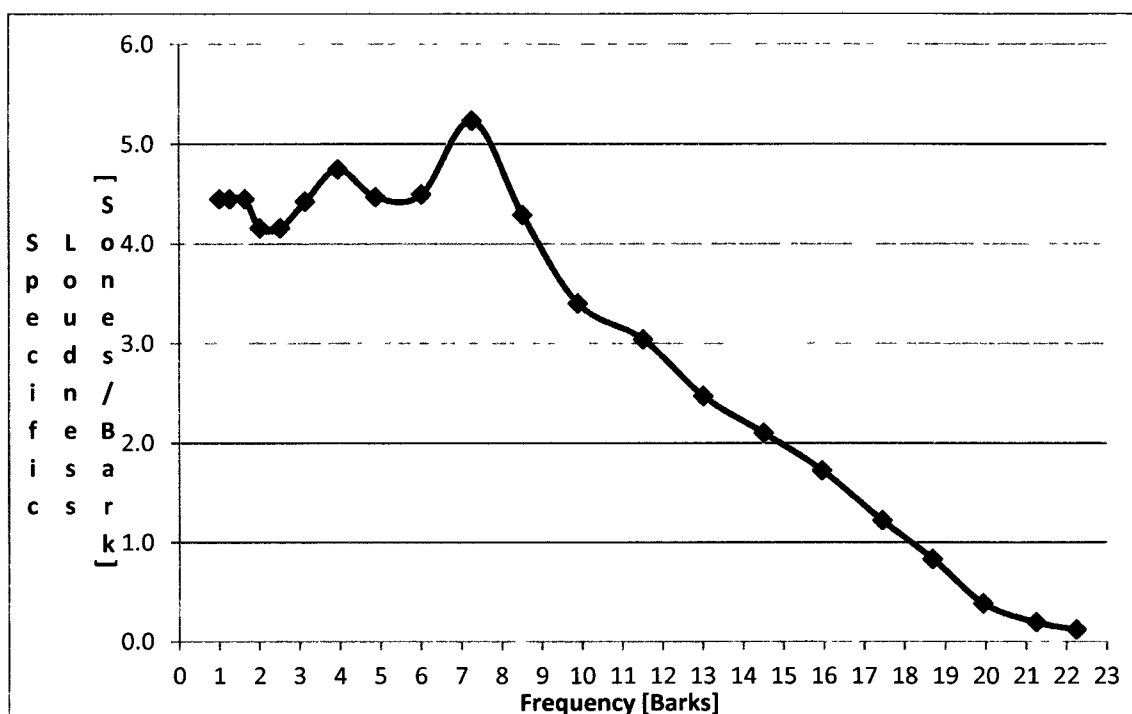
Figure 77: Averaged Specific Loudness for a Free Field Sound Field Condition from Microphones 6 and 10 for the 19 mm Thick, 60cmX60cm Sample of RUL Automotive Underpad with Periodic Random or Scattered White or Pseudorandom Noise 10 Seconds Signal Duration, 89.8 dB in the Semi-Anechoic Room
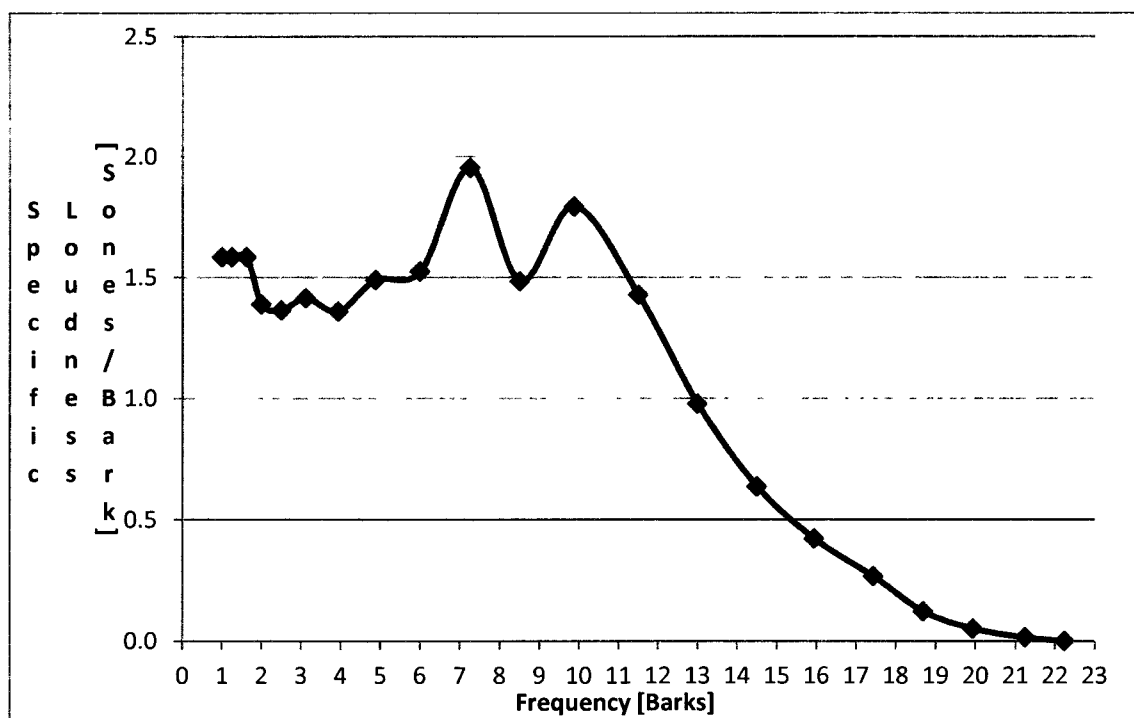

Figure 78: Averaged Specific Loudness for a Free Field Sound Field Condition from Microphones 6 and 10 for the 19 mm Thick, 60cmX60cm Sample of RUL Automotive Underpad with Diesel Generator Noise 10 Seconds Signal Duration, 74.2 dB in the Semi-Anechoic Room
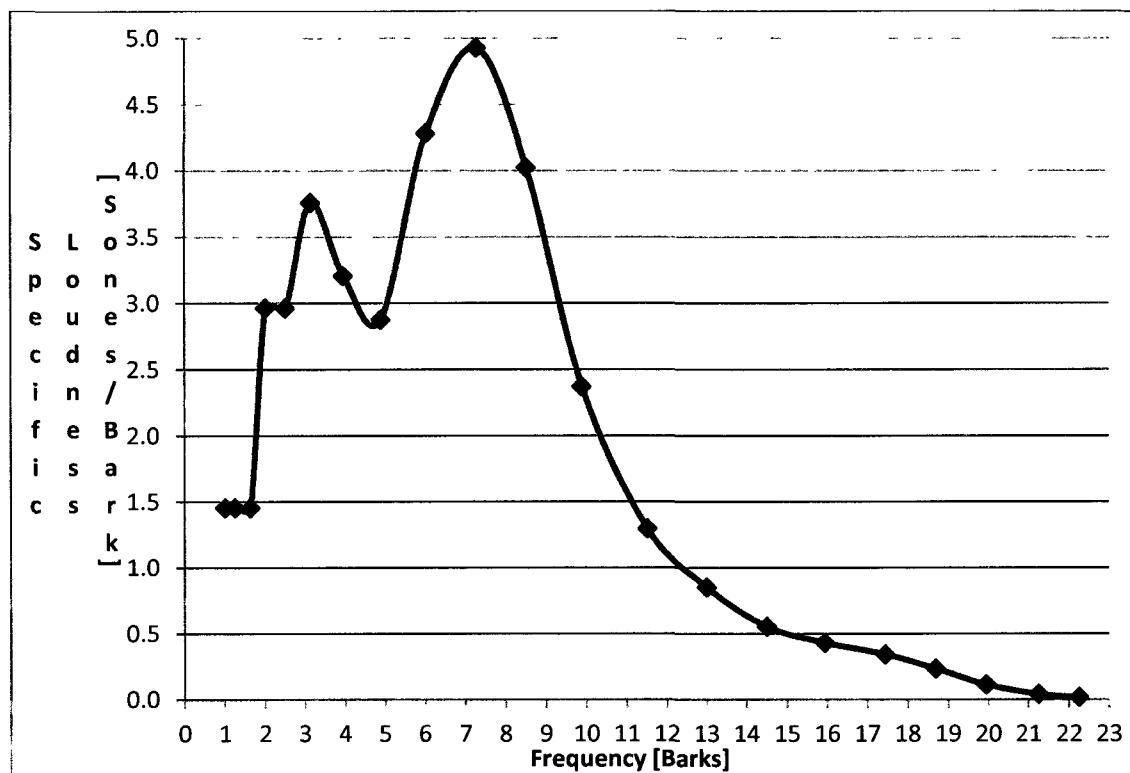
Figure 79: Averaged Specific Loudness for a Free Field Sound Field Condition from Microphones 6 and 10 for the 19 mm Thick, 60cmX60cm Sample of RUL Automotive Underpad with Electric Motor Noise 10 Seconds Signal Duration, 86.3 dB in the Semi-Anechoic Room
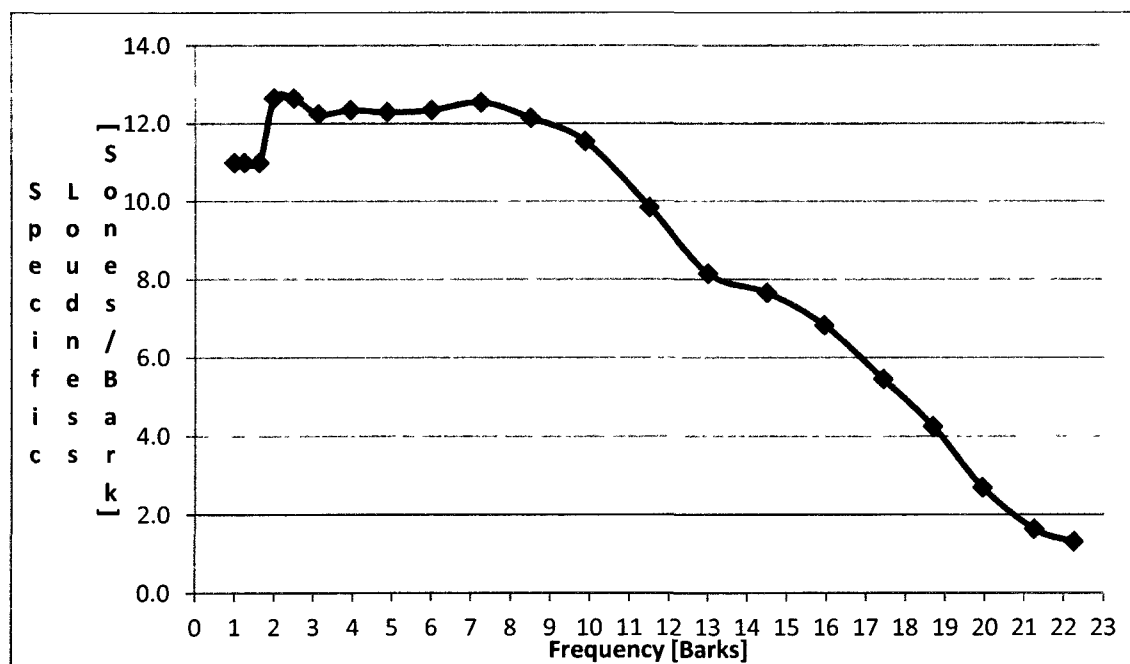

Figure 80: Averaged Specific Loudness for a Diffuse Field Sound Field Condition from Microphones 1 and 5 for the 4.7 mm Thick, 60cmX60cm Sample of 6061-T6 Aluminum, Demonstrating Irrelevancy, for Random or Uniform White Noise 10 Seconds Signal Duration, 106.6 dB in the Reverberation Pit
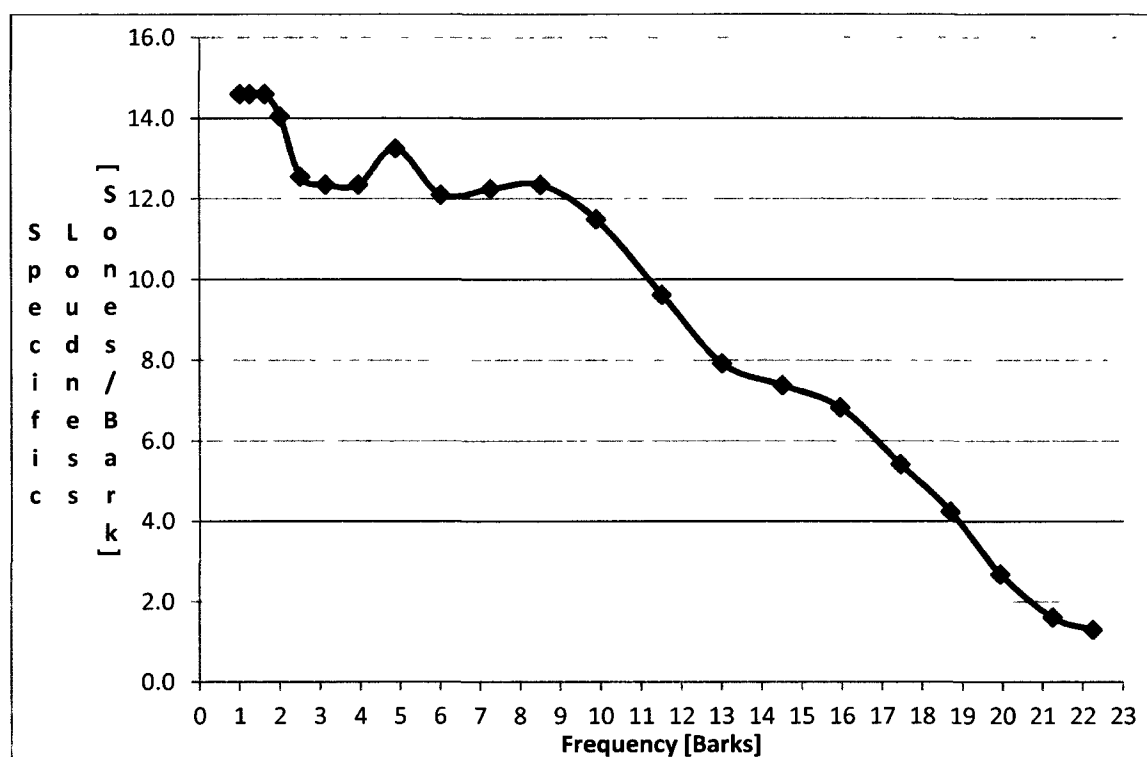
Figure 81: Averaged Specific Loudness for a Diffuse Field Sound Field Condition from Microphones 1 and 5 for the 4.7 mm Thick, 60cmX60cm Sample of 6061-T6 Aluminum, Demonstrating Irrelevancy, for Periodic Random or Scattered White or Pseudorandom Noise 10 Seconds Signal Duration, 106.9 dB in the Reverberation Pit
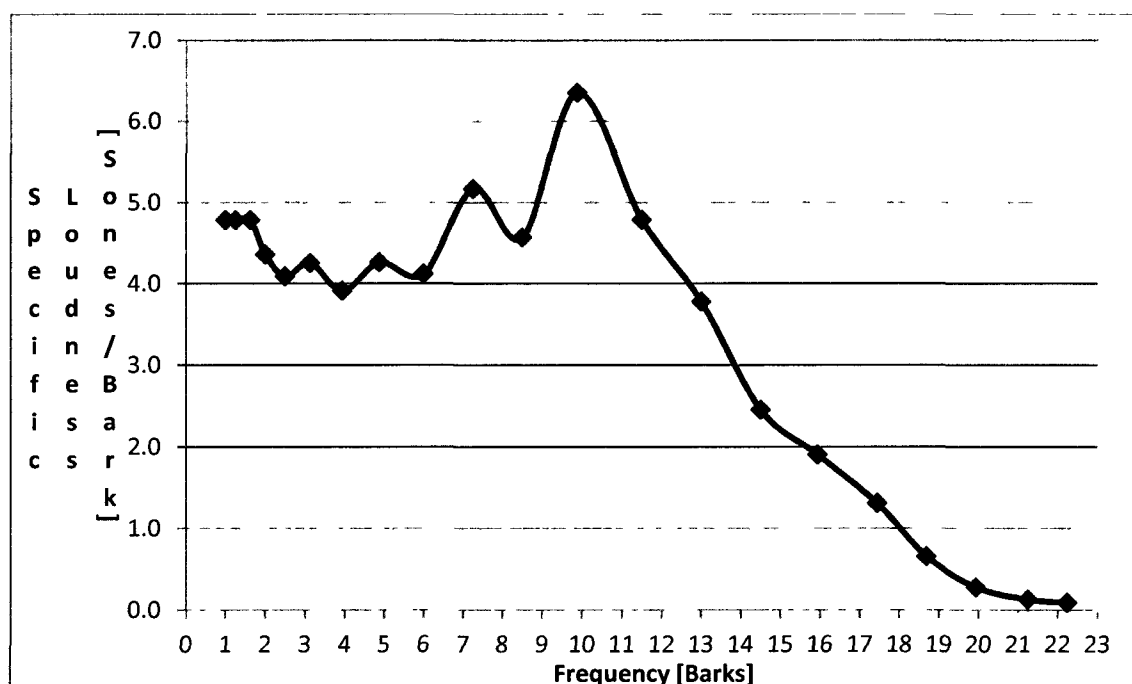

Figure 82: Averaged Specific Loudness for a Diffuse Field Sound Field Condition from Microphones 1 and 5 for the 4.7 mm Thick, 60cmX60cm Sample of 6061-T6 Aluminum, Demonstrating Irrelevancy, for Diesel Generator Noise 10 Seconds Signal Duration, 91.2 dB in the Reverberation Pit
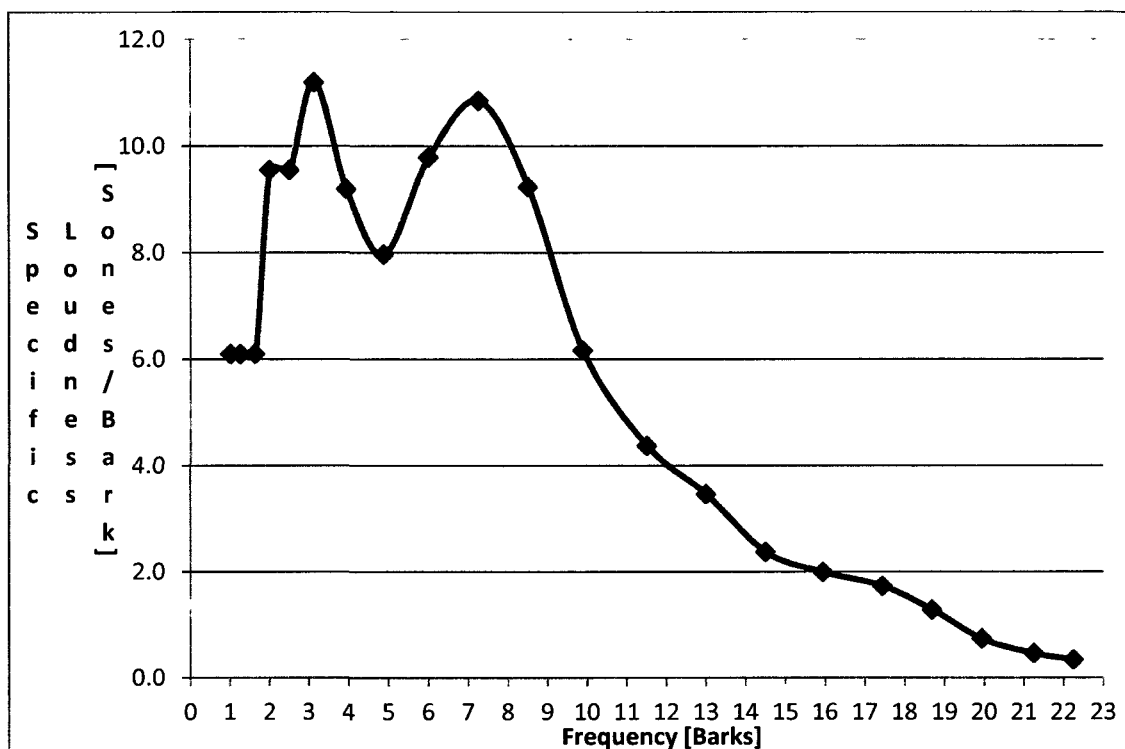
Figure 83: Averaged Specific Loudness for a Diffuse Field Sound Field Condition from Microphones 1 and 5 for the 4.7 mm Thick, 60cmX60cm Sample of 6061-T6 Aluminum, Demonstrating Irrelevancy, for Electric Motor Noise 10 Seconds Signal Duration, 101.8 dB in the Reverberation Pit

Table 8: Averaged Total Loudness in Sones for a Free Field Sound Field Condition from Microphones 6 and 10 in the Time Domain from 0.2 s to 1.18 s, representing each Second in the 10-Second Long Signals of Random or Uniform White Noise, Periodic Random or Scattered White or Pseudorandom Noise, Diesel Generator Noise, and Electric Motor Noise for the 19 mm Thick, and 15 mm Thick, 60cmX60cm Samples of RUL Automotive Underpad

Table 9: Averaged Total Loudness in Sones for a Diffuse Field Sound Field Condition from Microphones 1 and 5 in the Time Domain from 0.2 s to 1.18 s, representing each Second in the 10-Second Long Signals of Random or Uniform White Noise, Periodic Random or Scattered White or Pseudorandom Noise, Diesel Generator Noise, and Electric Motor Noise for the 4.7 mm Thick, 60cmX60cm Sample of 6061-T6 Aluminum, Demonstrating Irrelevancy

SIGNAL TYPE	RUL LAYER THICKNESS	
	15 mm RUL	19 mm RUL
Random	1.03	1.05
Periodic Random	1.03	1.06
Diesel Generator	0.95	0.93
Electric Motor	0.86	0.86

Table 10: Averaged Sharpness in Acum for a Free Field Sound Field Condition from Microphones 6 and 10 in the Time Domain from 0.2 s to 1.18 s, representing each Second in the 10-Second Long Signals of Random or Uniform White Noise, Periodic Random or Scattered White or Pseudorandom Noise, Diesel Generator Noise, and Electric Motor Noise for the 19 mm Thick, and 15 mm Thick, 60cmX60cm Samples of RUL Automotive Underpad

SIGNAL TYPE	SAMPLE TYPE & THICKNESS
	4.7 mm Al
Random	1.28
Periodic Random	1.25
Diesel Generator	1.03
Electric Motor	0.97

Table 11: Averaged Sharpness in Acum for a Diffuse Field Sound Field Condition from Microphones 1 and 5 in the Time Domain from 0.2 s to 1.18 s, representing each Second in the 10-Second Long Signals of Random or Uniform White Noise, Periodic Random or Scattered White or Pseudorandom Noise, Diesel Generator Noise, and Electric Motor Noise for the 4.7 mm Thick, 60cmX60cm Sample of 6061-T6 Aluminum, Demonstrating Irrelevancy

VITA AUCTORIS

Michael Bowie was born in 1985 in Windsor, Ontario. He graduated from Vincent Massey High School in 2003. From there he went on to the University of Windsor where he obtained a B.A.Sc. in Mechanical Engineering in 2007. He is currently a candidate for the Master's degree in Mechanical Engineering at the University of Windsor and plans to graduate in Fall 2011.